
Theses and Dissertations

Fall 2014

Optimal sensing matrices

Hema Kumari Achanta
University of Iowa

Follow this and additional works at: <https://ir.uiowa.edu/etd>



Part of the [Electrical and Computer Engineering Commons](#)

Copyright 2014 Hema Kumari Achanta

This dissertation is available at Iowa Research Online: <https://ir.uiowa.edu/etd/1421>

Recommended Citation

Achanta, Hema Kumari. "Optimal sensing matrices." PhD (Doctor of Philosophy) thesis, University of Iowa, 2014.

<https://doi.org/10.17077/etd.d0za6wct>

Follow this and additional works at: <https://ir.uiowa.edu/etd>



Part of the [Electrical and Computer Engineering Commons](#)

OPTIMAL SENSING MATRICES

by

Hema Kumari Achanta

A thesis submitted in partial fulfillment of the
requirements for the Doctor of Philosophy
degree in Electrical and Computer Engineering
in the Graduate College of
The University of Iowa

December 2014

Thesis Supervisors: Professor Soura Dasgupta
Assistant Professor Weiyu Xu

Copyright by
HEMA KUMARI ACHANTA
2014
All Rights Reserved

Graduate College
The University of Iowa
Iowa City, Iowa

CERTIFICATE OF APPROVAL

PH.D. THESIS

This is to certify that the Ph.D. thesis of

Hema Kumari Achanta

has been approved by the Examining Committee for the thesis requirement for the Doctor of Philosophy degree in Electrical and Computer Engineering at the December 2014 graduation.

Thesis Committee: _____

Soura Dasgupta, Thesis Supervisor

Weiyu Xu, Thesis Supervisor

Raghuraman Mudumbai

Er-Wei Bai

Paul Muhly

To my mother Srimati Durga Bhavani Achanta, my father Sri Dattatreya Sarma Achanta, my brother Prasanta Kumar Achanta and all my teachers.

ACKNOWLEDGEMENTS

I am overwhelmed to acknowledge the help, guidance and support extended by several people in the completion of this task. I offer my sincere gratitude to my research supervisor, Professor Soura Dasgupta, who has always been a source of inspiration and guiding force in the course of the Ph.D Program. His constant mentoring, timely advises have ensured consistent progress and completion of this thesis. I will always be grateful for his continuous guidance and encouragement, and consider it a blessing to have worked under such a researcher with commendable insight into mathematical analysis, control theory and signal processing.

I express my sincere gratitude toward Professor Weiyu Xu and Professor Raghuraman Mudumbai for their insightful discussions which were a milestone during the span of my Ph.D work. I also wish to express my sincere gratitude to Professor Er-Wei Bai, Chair, Department of Electrical and Computer Engineering, University of Iowa. I would like to thank Professor Sudhakar Reddy, Professor Paul Muhly and Professor Anton Kruger for their constant encouragement throughout the program. I would also like to thank Professor Vittal, Osmania University for his best wishes.

I would like to thank Dr. Ashish Pandheripande, Dr. Manish Vemulapalli, Dr. Chris Schwarz, Dr. Ryan Abel, Dr. Paul Kump and Dr. Andrew Berns for all the help, inspiration and motivation. I would like to place on record the support of all the faculty and staff of Department of Electrical and Computer Engineering and Department of Mathematics, University of Iowa. I would like to thank Ms. Cathy

Kern and Dina Blanc for the support and help with all the paper work through out the program.

I wish to express my gratitude to my fellow labmates Aneela Yasmeen, Mahboob Ur-Rahman, Henry Ernest Baidoo-Williams, Josiah McClurg. I wish to thank my friends Aruna Tumuluri, Sneha Rudravaram, Sudhamsa Golla, Farhat Sultana and well wishers for their constant support and encouragement. Finally I also would like to thank my friends Katha Sheth, Varsha Shrivastava, Rohini Ratarekar, Saranya Thirumoolan, Smriti Rai and Sharada Jha for all the help they extended in my first year of staying away from home.

ABSTRACT

Location information is of extreme importance in every walk of life ranging from commercial applications such as location based advertising and location aware next generation communication networks such as the 5G networks to security based applications like threat localization and E-911 calling. In indoor and dense urban environments plagued by multipath effects there is usually a Non Line of Sight (NLOS) scenario preventing GPS based localization. Wireless localization using sensor networks provides a cost effective and accurate solution to the wireless source localization problem. Certain sensor geometries show significantly poor performance even in low noise scenarios when triangulation based localization methods are used. This brings the need for the design of an optimum sensor placement scheme for better performance.

The optimum sensor placement optimizes the underlying Fisher Information Matrix(FIM) . This thesis will present a class of canonical optimum sensor placements that produce the optimum FIM for N dimensional source localization ($N \geq 2$) for a case where the source location has a radially symmetric probability density function within an N dimensional sphere and the sensors are all on or outside the surface of a concentric outer N dimensional sphere. While the canonical solution that we designed for the $2D$ problem represents optimum spherical codes, the study of 3 or higher dimensional design provides great insights into the design of measurement matrices with equal norm columns that have the smallest possible condition number.

Such matrices are of great importance in compressed sensing based applications.

This thesis also presents an optimum sensing matrix design for energy efficient source localization in $2D$. Specifically, the results relate to the worst case scenario when the minimum number of sensors are active in the sensor network. We also propose a distributed control law that guides the motion of the sensors on the circumference of the outer circle to achieve the optimum sensor placement with minimum communication overhead.

The design of equal norm column sensing matrices has a variety of other applications apart from the optimum sensor placement for N -dimensional source localization. One such application is fourier analysis in Magnetic Resonance Imaging (MRI). Depending on the method used to acquire the MR image, one can choose an appropriate transform domain that transforms the MR image into a sparse image that is compressible. Some such transform domains include Wavelet Transform and Fourier Transform. The inherent sparsity of the MR images in an appropriately chosen transform domain, motivates us to provide a method for designing a compressive sensing measurement matrix by choosing a subset of rows from the Discrete Fourier Transform (DFT) matrix. This thesis uses the spark of the matrix as the optimality criterion. The spark of a matrix is defined as the smallest number of linearly dependent columns of the matrix. The objective is to select a subset of rows from the DFT matrix in order to achieve maximum spark. The design procedure leads us to an interesting study of coprime conditions on the row indices chosen in relation to the size of the DFT matrix.

PUBLIC ABSTRACT

Location information is of extreme importance in every walk of life ranging from commercial applications such as location based advertising and location aware next generation communication networks such as the 5G networks to security based applications like threat localization and E-911 calling. Locating a source of threat or a missing person using wireless signals transmitted from the source are examples of daily life situations that critically rely on location information. In indoor and dense urban environments the wireless signals are reflected/scattered by the obstacles such as buildings and trees. This degrades the quality of the wireless signal from the source that we are looking for. This negatively impacts the accuracy of the localization process. Thus one needs to understand the wireless environment and smartly deploy the sensors at appropriate places in order to get an accurate location estimate. In this thesis, the design of the optimum sensor deployment is modeled as the design of matrices with the columns defined as the sensor locations such that these matrices have certain optimum matrix properties.

Another interesting application where these matrix design techniques can be used is Magnetic Resonance Imaging. The motivation to study matrix design techniques for MRI comes from the fact that we would like to make few acquisitions but yet be able to understand the missing portions of the data. We would like to design a matrix which has optimum properties such that the measurement process of the MRI modeled by this matrix retains all the important information required.

TABLE OF CONTENTS

LIST OF FIGURES	xi
LIST OF ALGORITHMS	xiii
CHAPTER	
1 INTRODUCTION	1
1.1 Optimum Sensor Placement for Source Localization	2
1.1.1 Distance Measurement Techniques in Wireless Sensor Networks	3
1.1.1.1 Received Signal Strength Based Distance Measurements	4
1.1.2 The Importance of Sensor Geometry in Source Localization	5
1.1.3 The Fisher Information Matrix	7
1.2 Measurement matrix design for Compressed Sensing in MRI	10
1.3 Aim	11
1.3.1 Optimum Sensor Placement for Source Localization	12
1.3.2 A Distributed Control Law for Optimum Sensor Placement for Source Localization	14
1.3.3 Optimum Sensor Placement for Energy Efficient Source Monitoring	14
1.3.4 Coprime Conditions for Fourier Analysis for Sparse Recovery	16
1.4 Outline of the thesis	17
2 OPTIMUM SENSOR PLACEMENT FOR SOURCE LOCALIZATION	18
2.1 Problem formulation	19
2.2 Properties of F	21
2.3 Characterizing Optimality	27
2.4 Canonical Solutions	30
2.4.1 Avoiding Coplanarity	33
2.4.2 Achieving the Optimum FIM	38
2.4.3 Geometric Interpretation of the solution	47
2.5 Simulation Results for the three dimensional case	48
2.6 Conclusion	53
3 A DISTRIBUTED CONTROL LAW FOR OPTIMUM SENSOR PLACEMENT FOR SOURCE LOCALIZATION	55

3.1	Introduction	55
3.2	The Cost Function	56
3.3	Analysis	66
3.4	Convergence Analysis	70
3.5	Simulation Results	72
3.5.1	Simulation Scenario 1: 3 Node Network	73
3.5.2	Simulation Scenario 2: 8 Node Network	73
3.6	Conclusions	74
4	OPTIMUM SENSOR PLACEMENT FOR ENERGY EFFICIENT SOURCE LOCALIZATION USING LEAST NUMBER OF ACTIVE SENSORS	77
4.1	Sensing Applications: Signal Estimation	78
4.2	Source Monitoring	79
4.3	$K = 3$, N is an even number	80
4.4	$K = 3$, $N = 3$ or 5	86
4.4.1	(At Least 2 adjacent-3-angle Sets Giving the Maximum Condition Number)	89
4.4.2	(At Least 3 adjacent-3-angle Sets Giving the Maximum Condition Number)	90
4.4.3	(At Least 4 adjacent-3-angle Sets Giving the Maximum Condition Number)	93
4.5	$K = 3$, $N = 7$	97
4.6	$K = 3$, $N \geq 9$ is an Odd Number	103
4.7	Simulation Results	107
4.7.1	Worst Case Condition Number vs N	107
4.7.2	Worst mean square signal estimation error vs N	107
4.7.3	Monitoring Error vs SNR	109
4.8	Conclusions	110
5	COPRIME CONDITIONS FOR FOURIER SAMPLING FOR SPARSE RECOVERY	112
5.1	Introduction	112
5.2	Related Work	114
5.3	Some General Results	116
5.4	Specialization to the case where N is a product of two primes	121
5.5	Conclusion	126
6	SUMMARY AND FUTURE WORK	127
6.1	Summary	127
6.2	Future Work	130

APPENDIX	132
REFERENCES	144

LIST OF FIGURES

Figure	
1.1 Top : Illustration of the problem Setup for the 3-D source localization. Bottom: Illustration of the problem setup for energy efficient sensor placement for source monitoring	15
2.1 Illustration of proposed sensor placement for $n = 4$ and $r_2 = 2$	48
2.2 Plot of GDOP Versus Number of sensors in the network.	50
2.3 Plot of determinant of FIM Versus Number of sensors in the network. . .	51
2.4 Plot of Minimum Eigenvalue of FIM Versus Number of sensors in the network.	52
2.5 Plot of $10\log(\text{Average Normalized Mean square error in the source location})$ Versus Signal to Noise Ratio (dB). Red dotted line represents the performance of the random placement. Blue line represents the performance of the proposed optimum sensor placement	53
3.1 The underlying communication graph	57
3.2 Initial Network Topology	64
3.3 Final Network Topology	65
3.4 Initial Network Topology	73
3.5 Final Network Topology	74
3.6 Initial Network Topology	75
3.7 Final Network Topology	75
3.8 Trajectory of the sensors. The X-axis indicates the time in terms of the iterations and the Y-axis represents the angular position of the sensors on the circle (scaled by π)	76

4.1	Top: Illustration of the $\sum_{i=1}^N (\tilde{\theta}_{(i+2) \bmod N} - \tilde{\theta}_i) \bmod (2\pi) = 2 \times (2\pi)$ for a 4 sensor network. Bottom: Illustration of the regions where $f'(t_2) \geq 0$ and $f'(t_2) \leq 0$	82
4.2	Illustration of angular separation between columns of the sensing matrix/sensors in the network. Top left and right figures represent the proposed angular separation for the columns of the sensing matrix (optimum sensor placement with 6 columns/sensors) and the doubled angles respectively. Middle figures represents design for the matrix with 7 columns while the bottom figures represent the optimum design for 5 columns/sensors. .	106
4.3	Illustration of the proposed solution for a 8 node network and a 7 node network angles in the range $[0, 2\pi)$	108
4.4	Worst case Condition Number Versus N	109
4.5	Worst case estimation error versus the number of columns in the sensing matrix.	110
4.6	Mean square error(dB) in the source location estimate when the worst performing subset of sensors are active versus the Signal to Noise Ratio(dB).111	

LIST OF ALGORITHMS

Algorithm

3.1 The Distributed Control Law in Discrete Time 72

CHAPTER 1 INTRODUCTION

The objective of this dissertation is to design sensing matrices for two broad applications.

1. Optimum sensor placement for source localization.
2. Measurement matrix for compressive sensing.

In the first part of the dissertation the primary focus is on designing an optimum sensor node geometry that optimizes the Fisher Information Matrix associated with the $N \geq 2$ dimensional source location estimate by using the Received Signal Strength (RSS) measurements. The canonical solutions that we provide for optimum sensor placement problem for N dimensional localization of a single source provide great insights into the design of sensing matrices with equal norm columns that have some interesting properties pertaining to the condition number. Section 1.1 gives an overview of the related literature and applications of the problem. Section 1.2 and 1.3 present the precise mathematical objectives of the optimum sensor placement design.

In the second part of the dissertation the focus is on the design of a compressive sensing measurement matrix for Magnetic Resonance Imaging (MRI). The inherent sparsity of the MR images in an appropriately chosen transform domain, motivates this objectives of the thesis which is to provide a method for designing a compressive sensing measurement matrix for MRI by choosing a subset of rows from the Discrete Fourier Transform (DFT) matrix. The objective is to choose a subset of rows of

the DFT matrix, such that the chosen submatrix has the maximum spark. Spark is defined the smallest number of linearly dependent columns in a matrix. Section 1.2 provides a brief introduction to Compressive Sensing and Section 1.3 presents the specific mathematical definition of the problem.

1.1 Optimum Sensor Placement for Source Localization

In the recent past, research in location based services has gained momentum with smart location aware devices. The next generation communication networks such 5G are being designed to derive benefits from location information [1]. Apart from an attractive commerce surrounding the location based services, there are several military applications that require highly accurate location information.

Though GPS offers good location estimates when there is Line of Sight communication with the GPS satellites, in indoor and dense urban environments filled with obstacles and multipath effects there is usually a Non-Line-of-Sight (NLOS) scenario. In such cases wireless localization using sensor networks provides a cost effective and accurate solution to the wireless source localization problem.

Specifically in applications where the source poses a threat to life, wireless sensor technology becomes almost indispensable. Literature in [2], [3], [4],[5], [6], [7] and [8], [9], [10] provide several applications of wireless source localization and the corresponding optimum sensor placement. Other applications include location based advertising, disaster management, indoor navigation and positioning, packet routing in mobile networks, chemical and biological source tracking, ubiquitous comput-

ing, wearable body area networks, habitat monitoring, presence sensing based lighting systems, animal tracking to list a few. Besides these commercial and security based applications, future wireless sensor technology promise easy and safe navigation to people with disabilities [11].

In source localization using wireless sensor networks, groups of sensors receive signals from the source and wirelessly communicate their relative position information either in a centralized or distributed fashion to spot the source [12], [13], [14], [15]. Using the sensed data from the sensors, the sensors collectively estimate the source location.

Section 1.1.1 provides answer to the question of how we acquire location information of the source.

1.1.1 Distance Measurement Techniques in Wireless Sensor Networks

Classical techniques used for acquiring the location information include the range-based techniques and range-free localization techniques. The range based techniques use signal strength or the time of arrival of the received signal to estimate the true node to node distance. Though range-free localization techniques require lesser hardware and are economical, in applications that are sensitive to the accuracy of the estimate of the location and require absolute geolocation, range based techniques offer higher accuracy [16], [17].

Range based distance measurement techniques include

1. Received Signal Strength Measurements

2. Time Difference of Arrival Measurements

This thesis focuses on the use of the received signal strength model to acquire the relative position information of the source.

1.1.1.1 Received Signal Strength Based Distance Measurements

Suppose A is the strength of the signal emitted by the wireless source at a unit distance from the source and d is the distance between the source and the receiver (sensor), then the received signal strength s at the receiver is modeled using an inverse relation given by

$$s = \frac{A}{d^\beta} \quad (1.1)$$

where β is the path loss co-efficient. Hence in a sensor network with n sensors receiving signals from a source, if $y \in \mathbb{R}^N$ where $N = 2$ or 3 is the source location and $x_i \in \mathbb{R}^N$ is the location of the i -th sensor node, then the received signal strength at this i -th sensor node is given by

$$s_i = \frac{A}{\|x_i - y\|^\beta}. \quad (1.2)$$

Throughout this work, the radio environment is assumed to be plagued by log normal shadowing [18]. Thus from (1.2),

$$\ln s_i = \ln A - \beta \ln \|x_i - y\| + w_i, \quad (1.3)$$

where w_i is a zero mean uncorrelated gaussian random variable with variance σ^2 . The

log normal shadowing model takes care of the uncertainty involved in the estimation of the path loss parameter β and the multipath effects in the environment.

Section 1.1.2 addresses the need for the design of an optimum sensor geometry in the context of source localization.

1.1.2 The Importance of Sensor Geometry in Source Localization

The sensor geometry plays a significant role in determining the accuracy of the source location estimate [19], [20], [21]. This brings the need to find an optimal configuration for the sensor placement relative to the source. The key question here is why not use triangulation methods to localize a source? In general, 3 non-collinear sensor nodes with known location can localize a source in two dimensions and 4 non-coplanar sensors can do the job in three dimensions. However in environments with multipath effects and obstacles, triangulation methods perform poorly i.e. produce high localization errors. Consider the following example in [22] which asserts that certain sensor geometries produce large localization errors even in the presence of very small noise when linear localization algorithms such as triangulation are used.

Suppose there are three sensor nodes at $[0, 0]^T$, $[43, 7]^T$ and $[47, 0]^T$. Suppose also that the source is at $y = [17.9719, -29.3227]^T$. The distances of the source at y from each sensor node are 34.392 from the first node, 44.1106 from the second node and 41.2608 from the third node. Now, let us suppose that the distance measurements are perturbed by noise. Let the distances of the source node from the sensor nodes after perturbation from noise be 35, 42 and 43 respectively. If these perturbed dis-

tance estimates are used to estimate the source location, then the linear algorithm i.e the triangulation algorithm estimates the source to be at $[16, 8617, -6.5076]^T$. This illustrates that triangulation shows a significantly poor performance even in low noise situations. This brings the need to find an optimal configuration for the sensor placement that takes into account the cluttered environment to produce the best possible accuracy in the location estimation process.

The sensor placement strategy varies with the

1. application [23] - [24],
2. environment in which the sensors are deployed and
3. method used for acquiring data from the source.

For example, in robotics the sensors should be placed such that the robot best perceives the physical world. Similarly, the sensor configuration for monitoring the health of structures needs to give best information of the overall health of the structure. The sensor placement algorithm however is significantly different when there is only probabilistic information of the source location and the optimum configuration is different for different distributions of the source location. In applications like finding a microphone in a conference room, mine sweeping, presence sensing based lighting control, the location of the source is known to be constrained in a particular geographic region. In certain applications, the source may be more likely to be present at a point in the region than the others. In such cases the source location distribution is modeled accordingly by assigning weights of importance to those locations to improve accuracy.

Specifically, the work in chapter 2 focuses on placing the sensors on or outside the surface of a N dimensional sphere in order to locate a single source given that the region where the source is expected to be present is known to be a concentric N dimensional sphere of a smaller radius. The sensor configuration is subject to the constraint that the sensors need to be placed at a certain distance from the source. This constraint is of interest in applications where the source poses a threat like in the case of localizing the source of fire or to locate a bomb or a terror threat in public places. It is also a topic of interest for applications like seamless wireless connectivity using high altitude long endurance drones and satellites.

1.1.3 The Fisher Information Matrix

It is well known that [25] the error variance of unbiased estimators is lower bounded by the Cramer Rao Lower Bound (CRLB) matrix. Further asymptotically the maximum likelihood estimator approaches this bound. Thus one measure of how good an estimate is, is provided by maximizing the inverse of the CRLB matrix also known as the Fisher Information Matrix (FIM).

Traditional optimal design experiments aim at

1. Minimization of the trace of the inverse of the FIM
2. Maximization of the determinant of the underlying FIM
3. Maximization of the minimum eigenvalue of the underlying FIM [26], [27].

To establish the problem statement, we first find the Fisher Information Matrix (FIM) corresponding to the received signals at the sensors in two cases.

1. The source location y is deterministic but unknown
2. The source location y is a random vector

Case (1) is the Source Monitoring problem [28] and case (2) corresponds to the Source Localization problem [29]. In the case of source monitoring, it is assumed that the source location has already been estimated and that the sensors are continuously estimating the location of the source from a safe distance.

Define $S = [s_1, s_2, \dots, s_n]$ and $W = [\ln s_1 - \ln A - \beta \ln \|x_1 - y\|, \dots, \ln s_n - \ln A - \beta \ln \|x_n - y\|]$. As the w_i 's are mutually orthogonal, the probability density function of $S|y$ is given by

$$p(S|y) = \frac{1}{(2\pi)^{\frac{n}{2}}} \frac{1}{|\Sigma|^{\frac{1}{2}}} \exp\left(-\frac{1}{2}W\Sigma^{-1}W^T\right) \quad (1.4)$$

where $\Sigma = E[W^TW]$. However, as the w_i 's are mutually uncorrelated and thus mutually orthogonal (since $E(w_i) = 0 \forall i \in \{1, 2, \dots, N\}$) we have

$$E[W^TW] = \sigma^2 I. \quad (1.5)$$

Thus

$$p(S|y) = \frac{1}{(2\pi)^{\frac{n}{2}}} \frac{1}{\sigma^n} \exp\left(-\frac{1}{2\sigma^2}WW^T\right) \quad (1.6)$$

$$\iff \ln p_{s|y}(S|y) = -\frac{n}{2} \ln(2\pi\sigma^2) - \frac{1}{2\sigma^2}WW^T. \quad (1.7)$$

Now,

$$\frac{\partial}{\partial y} \ln p_{s|y}(S|y) = 0 - \frac{1}{2\sigma^2} \frac{\partial}{\partial y} (WW^T) = \frac{1}{\sigma^2} \frac{\partial}{\partial y} (W), \quad (1.8)$$

$$\frac{1}{\sigma^2} \frac{\partial}{\partial y} (W) = \frac{1}{\sigma^2} BW, \quad (1.9)$$

where

$$B = \left[-\beta \frac{x_1 - y}{\|x_1 - y\|^2}, \dots, -\beta \frac{x_n - y}{\|x_n - y\|^2} \right]. \quad (1.10)$$

Now define F given by [30]

$$F = E\left[\left\{\frac{\partial}{\partial y} \ln p_{s|y}(S|y)\right\}\left\{\frac{\partial}{\partial y} \ln p_{s|y}(S|y)\right\}^T\right] = \frac{1}{\sigma^4} BE[W^T W]B^T \quad (1.11)$$

Thus (1.11) becomes

$$F = \frac{1}{\sigma^2} BB^T. \quad (1.12)$$

On simplification we get,

$$F = \frac{\beta^2}{\sigma^2} \sum_{i=1}^n \frac{(x_i - y)(x_i - y)^T}{\|x_i - y\|^4}. \quad (1.13)$$

Fisher Information Matrix in the Source Monitoring Problem

The FIM in the source monitoring case is given by

$$FIM = F = \frac{\beta^2}{\sigma^2} \sum_{i=1}^n \frac{(x_i - y)(x_i - y)^T}{\|x_i - y\|^4}. \quad (1.14)$$

Fisher Information Matrix in the Source Localization Problem

The FIM in this case is given by

$$FIM = E_y[F] = \frac{\beta^2}{\sigma^2} E_y \left[\sum_{i=1}^n \frac{(x_i - y)(x_i - y)^T}{\|x_i - y\|^4} \right]. \quad (1.15)$$

Thus the optimum sensing matrix design problem is that of design an optimum sensor placement that achieves the Optimal FIM. The specific mathematical problem formulation is presented in Section 1.3.

Section 1.2 discusses the optimum sensing matrix design in the context of compressive sensing for MRI.

1.2 Measurement matrix design for Compressed Sensing in MRI

Compressive sensing is a non-adaptive linear projection mechanism that samples signals at a lower rate than the Nyquist sampling rate. Recently, the compressive sensing problem has seen a wide variety of applications that include pattern recognition, machine learning, locality selective hashing, processing radar data, sensor networks, Magnetic Resonance Imaging (MRI), spectrum sensing in cognitive radio applications, channel estimation and error correcting codes [31], [32].

A signal $N \times 1$ is said to be “ k -sparse” if it can be written as a linear combination of $k \ll n$ basis vectors. In other words, a signal is k -sparse if $N - k$ elements of the signal are zero [32].

For the problem set up, consider a k -sparse $N \times 1$ vector x . Let A be a $M \times N$ ($M < N$) measurement or sensing matrix. Then the output of the measurement process defined by A is a $M \times 1$ vector y given by

$$y = Ax. \quad (1.16)$$

The measurement matrix A should be such that given k , every k -sparse $N \times 1$ vector x can be recovered from the observed $M \times 1$ vector y . The recovery of x is a constrained optimization problem, where the vector with the smallest support that satisfies the data consistency is estimated. The support of a sparse vector x denoted by $supp(x)$ is defined as the set of indices of the non-zero elements of the vector x i.e.

$$supp(x) = \{i | x_i \neq 0\} \quad (1.17)$$

where x_i is the i -th element of the vector x . This method of recovery is often referred to as ℓ_0 recovery. The necessary and sufficient conditions to recover an arbitrary k -sparse vector using ℓ_0 recovery is now well-known to be $\mathbf{spark}(A) > 2k$, [33, 34]. The spark of A is the smallest number of linearly dependent columns in A [33, 34]. The ℓ_0 recovery is a combinatorial search. Thus one would like design a measurement matrix with the largest spark i.e one would like to design a measurement matrix A such that $\mathbf{spark}(A) = M + 1$. The specific aim in this context is discussed in Section 1.3.

1.3 Aim

The aim of this thesis is four fold.

1. This dissertation develops a canonical solution to the optimum sensor placement problem for N-D source localization when the source location has a spherically

symmetric probability density function with finite support.

2. Given the optimum sensor placement for $2 - D$ source localization, this thesis develops a distributed control law that guides the motion of the sensors to achieve the optimum sensor placement.
3. The third objective of the dissertation is to develop a optimum sensor placement scheme when only a subset of sensors in the network are actively participating in the process of 2-D source location monitoring. Particularly, the design aims at the specific case when only 3 sensors in the network are active. The objective is to achieve the best worst case performance.
4. The fourth objective of the dissertation is to design a measurement matrix for compressed sensing in MRI. The measurement matrix is a submatrix formed by choosing $L < N$ rows of the $N \times N$ Discrete Fourier Transform (DFT) matrix such that the designed submatrix has the maximum possible spark of $L + 1$.

1.3.1 Optimum Sensor Placement for Source Localization

In this work, it is assumed that the source location is distributed in a ball of radius r_1 , centered at the origin,

$$B(r_1) = \{a \in \mathfrak{R}^N \mid \|a\|_2 \leq r_1\}, \quad (1.18)$$

and that the distribution is *radially symmetric*. Thus the prior probability density function (pdf) of y is given by, [35],

$$f_Y(y) = \begin{cases} g(\|y\|) & \text{for } y \in B(r_1) \\ 0 & \text{else} \end{cases}. \quad (1.19)$$

Given the probability density function of the source location of the form in the above equation, the specific problem that this thesis addresses is to achieve optimality on the FIM matrix in (1.20). For convenience, the FIM equation is

$$FIM = E_y[F] = \frac{\beta^2}{\sigma^2} E_y \left[\sum_{i=1}^n \frac{(x_i - y)(x_i - y)^T}{\|x_i - y\|^4} \right]. \quad (1.20)$$

As the source is hazardous, we assume that sensors cannot be too close to it. Specifically they must obey

$$\|x_i\|_2 \geq r_2 > r_1. \quad (1.21)$$

The problem statements thus assume the following mathematical definition.

Problem 1: For a given integers $n \geq N + 1$, $N > 1$, and $y \in \mathfrak{R}^N$ with pdf as in (1.19), find distinct $x_i \in \mathfrak{R}^N$ for $i \in \{1, 2, \dots, n\}$, that do not lie on an $N - 1$ dimensional hyperplane, such that $\lambda_{\min}(F)$ is maximized subject to (2.4).

Problem 2: For a given integers $n \geq N + 1$, $N > 1$, and $y \in \mathfrak{R}^N$ with pdf as in (1.19), find distinct $x_i \in \mathfrak{R}^N$ for $i \in \{1, 2, \dots, n\}$, that do not lie on an $N - 1$ dimensional hyperplane, such that $\det(F)$ is maximized subject to (2.4).

Problem 3: For a given integers $n \geq N + 1$, $N > 1$, and $y \in \mathfrak{R}^N$ with pdf as in

(1.19), find distinct $x_i \in \mathfrak{R}^N$ for $i \in \{1, 2, \dots, n\}$, that do not lie on an $N - 1$ dimensional hyperplane, such that $trace(F^{-1})$ is minimized subject to (2.4).

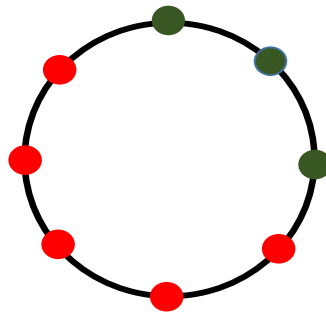
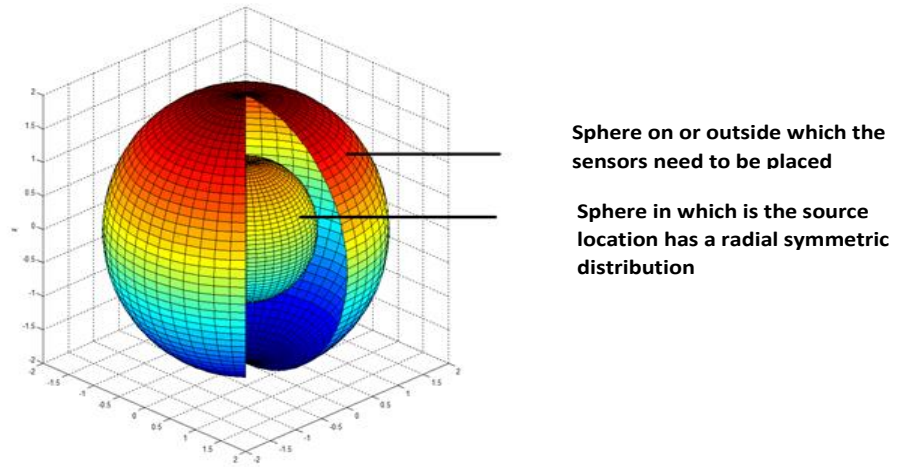
Chapter 2 holds a canonical result for these three problems.

1.3.2 A Distributed Control Law for Optimum Sensor Placement for Source Localization

In the wake of a growing need for autonomous sensor networks in search, localization and rescue operations, the concept of Self Organizing Networks (SON) has emerged as an energy efficient solution. The goal of this work is to develop a nonlinear distributed control law with the least communication overhead that guides the sensors to organize themselves to form the optimum sensor placement pattern required for minimum mean square error in localizing a source. The proposed nonlinear control law assumes that each sensor resides and moves on the prescribed circle, by accessing only the states of its two immediate clockwise and counterclockwise neighbors. Chapter 3 presents the theoretical proofs that guarantee convergence of the algorithm to the equispaced sensor placement scheme.

1.3.3 Optimum Sensor Placement for Energy Efficient Source Monitoring

In applications that require dense sensor deployment, the limited battery life of the sensors is a concern since replacing the battery on each sensor is an impractical and inefficient strategy in dense networks. Moreover, as discussed earlier, the geometry/topology of the sensor network heavily influences the accuracy with which the sensor network estimates the source location. Thus in applications that perform wire-



Green represents sensors in active mode

Red represents sensors in sleep mode

Figure 1.1: Top : Illustration of the problem Setup for the 3-D source localization. Bottom: Illustration of the problem setup for energy efficient sensor placement for source monitoring

less source localization using sensor networks, the objective of the sensor placement strategy is two fold.

- Improve the lifetime of the sensor network i.e improving the energy efficiency of the sensor network to avoid too frequent post deployment battery replacements.
- Optimize the FIM associated with the source location estimate.

Chapter 4 deals with the sensor placement for source localization in this context.

All the above aims relate to the design of an equal norm column matrix.

1.3.4 Coprime Conditions for Fourier Analysis for Sparse Recovery

The design of equal norm column sensing matrices has a variety of other applications apart from the optimum sensor placement for N-dimensional source localization. One such application is fourier analysis in Magnetic Resonance Imaging (MRI). Depending on the method used to acquire the MR image, one can choose an appropriate transform domain that transforms the MR image into a sparse image that is compressible. Some such transform domains include Wavelet Transform and Fourier Transform. The inherent sparsity of the MR images in an appropriately chosen transform domain, motivates one of the objectives of this thesis which is to provide a method for designing a compressive sensing measurement matrix by choosing a subset of rows from the Discrete Fourier Transform (DFT) matrix.

Chapter 5 considers the spark of $L \times N$ ($L < N$) submatrices of the $N \times N$ Discrete Fourier Transform (DFT) matrix. The $il - th$ element of the DFT matrix is given by $e^{\frac{2\pi il}{N}}$. A matrix has spark m if every collection of its $m - 1$ columns are

linearly independent. The motivation comes from applications of compressed sensing as MRI and synthetic aperture radar, where device physics dictates the measurements to be Fourier samples of the signal. Consequently the observation matrix comprises certain rows of the DFT matrix. To recover an arbitrary k -sparse signal, the spark of the observation matrix must exceed $2k + 1$. The technical question addressed in this work is how to choose the rows of the DFT matrix so that its spark equals the maximum possible value $L + 1$. This exposes certain coprimeness conditions that guarantee such a property. Specifically we propose methods to choose rows when the size of the matrix is a product of two primes.

1.4 Outline of the thesis

Chapter 2 holds the analysis and results for the optimum sensor placement problem for Source Localization in $N \geq 2$ dimensions. The distributed control law that guides the motion of sensors using only the relative position information of the nearest clockwise and counter clockwise neighbors is discussed in Chapter 2. The optimum sensor placement scheme for source monitoring in two dimensions when only a subset of 3 sensors are active in the sensor network is presented in Chapter 4. Chapter 5 presents the design of a measurement matrix as a submatrix of DFT (Discrete Fourier Transform) matrix for compressive sensing for MRI (Magnetic Resonance Imaging).

The work presented in Chapters 2-5 appear in the following papers [36], [37], [38], [39].

CHAPTER 2 OPTIMUM SENSOR PLACEMENT FOR SOURCE LOCALIZATION

The aim of this work is to find an optimal placement for the sensor nodes on or outside the surface of a $N \geq 2$ dimensional sphere in a non-coplanar (non-collinear in the case when $N = 2$) fashion in order to best localize a hazardous source whose location has a radially symmetric probability density function. The radius of the N dimensional sphere on or outside which the sensors are to be placed is chosen such that the sensors are at a safe distance from the hazards that the source may present.

We consider localization of the source using the Received Signal Strength (RSS) measurements under log-normal shadowing at various sensor nodes. The optimal placement of the sensor nodes is achieved through maximization of the smallest eigenvalue or the determinant of the expectation of the corresponding Fisher Information Matrix (FIM) or by minimizing the trace of the inverse of FIM. We show in Section 2.4 that the optimal solution is achieved if and only if the expectation of the FIM is a scaled identity.

We propose a canonical optimum sensor placement whose FIM produces a scaled identity. We define the Geometric Dilution of Precision for the sensor network in terms of the FIM and plot it with respect to the number of sensors in the network. We present simulations that confirm the superior performance of the proposed optimum sensor placement in terms of the least mean square error in comparison with instances of non-coplanar random sensor placement.

2.1 Problem formulation

As described in Chapter 1, we use the received signal strength (RSS) model to represent the method in which the sensors acquire the relative position information of the source and formalize the optimum sensor placement problem.

Throughout this chapter, the sensors $x_i \in \mathbb{R}^N$, $i \in \{1, \dots, n\}$ measure the RSS s_i emanated by a source located at $y \in \mathbb{R}^N$. Though the ambient space dimensions of interest are $N = 2$ or $N = 3$, for the sake of completeness the results will be derived for arbitrary $N > 1$.

The RSS is assumed to suffer from log-normal shadowing, [18]. In particular, with mutually uncorrelated $w_i \sim N(0, \sigma^2)$, β a path loss parameter and A the RSS at a unit distance, there holds:

$$\ln s_i = \ln A - \beta \ln \|x_i - y\| + w_i. \quad (2.1)$$

Throughout this work all norms refer to the 2-norm.

The source location itself is distributed in the ball of radius r_1 , centered at the origin,

$$B(r_1) = \{a \in \mathbb{R}^N \mid \|a\|_2 \leq r_1\}, \quad (2.2)$$

and that the distribution is *radially symmetric*. Thus the probability density function (pdf) of y is given by, [35],

$$f_Y(y) = \begin{cases} g(\|y\|) & \text{for } y \in B(r_1) \\ 0 & \text{else} \end{cases}. \quad (2.3)$$

As the source is hazardous, sensors cannot be too close to it. Specifically they must obey

$$\|x_i\|_2 \geq r_2 > r_1. \quad (2.4)$$

Our goal is to select x_i so that the s_i in (2.1), provide an optimum estimate of y , subject to (2.2)-(2.4). As the source location is random, a common optimality criterion is maximization, in an appropriate sense of the *Expectation of the Fisher Information Matrix (FIM)*. As shown in [25], for random parameter estimation, the inverse of the expectation of the FIM provides the Cramer-Rao Lower Bound (CRLB) matrix. Additionally, to assure unique localization, we also demand that the x_i not lie on an $N - 1$ dimensional hyperplane. For example, collinear sensor for $N = 2$, and coplanar sensors for $N = 3$, can only localize to within a flip ambiguity. This requirement also requires that $n > N$.

As shown in Chapter 1, for a nonrandom y the FIM for this problem is given to within a scaling factor, by

$$\sum_{i=1}^n \frac{(x_i - y)(x_i - y)^T}{\|x_i - y\|_2^4} \quad (2.5)$$

Consequently, we must “maximize”

$$F = E_y \left[\sum_{i=1}^n \frac{(x_i - y)(x_i - y)^T}{\|x_i - y\|_2^4} \right]. \quad (2.6)$$

What exactly does the maximization of F mean? Three standard criteria are

what we call E, D and T optimality. These respectively, refer to the maximization of the minimum eigenvalue of F , i.e. $\lambda_{\min}(F)$, the maximization of $\det(F)$ or the minimization of $\text{trace}(F^{-1})$. The last in particular, is the equivalent to minimizing the total mean square localization error, [25]. One of the facts demonstrated in this chapter is that the solutions to all three problems are identical.

Formally, the objective of this work is to solve the following three problems:

Problem 1: For a given integers $n \geq N + 1$, $N > 1$, and $y \in \mathfrak{R}^N$ with pdf as in (2.3), find distinct $x_i \in \mathfrak{R}^N$ for $i \in \{1, 2, \dots, n\}$, that do not lie on an $N - 1$ dimensional hyperplane, such that $\lambda_{\min}(F)$ is maximized subject to (2.4).

Problem 2: For a given integers $n \geq N + 1$, $N > 1$, and $y \in \mathfrak{R}^N$ with pdf as in (2.3), find distinct $x_i \in \mathfrak{R}^N$ for $i \in \{1, 2, \dots, n\}$, that do not lie on an $N - 1$ dimensional hyperplane, such that $\det(F)$ is maximized subject to (2.4).

Problem 3: For a given integers $n \geq N + 1$, $N > 1$, and $y \in \mathfrak{R}^N$ with pdf as in (2.3), find distinct $x_i \in \mathfrak{R}^N$ for $i \in \{1, 2, \dots, n\}$, that do not lie on an $N - 1$ dimensional hyperplane, such that $\text{trace}(F^{-1})$ is minimized subject to (2.4).

2.2 Properties of F

In this section, we examine some properties of (2.6). We first define a single summand in (2.6), namely,

$$H(x) = E \left[\frac{(x - y)(x - y)^T}{\|x - y\|^4} \right]. \quad (2.7)$$

With this F in (4.2) becomes:

$$F = \sum_{i=1}^n H(x_i). \quad (2.8)$$

The first Lemma discusses how $H(x)$ changes under an orthogonal transformation. Its importance comes from the fact that two x_i that have the same norm, are related through an orthogonal transformation.

Lemma 2.2.1 *Consider $H(x)$ as in (2.7), y distributed with pdf as in (2.3). Then with $P \in \mathbb{R}^{N \times N}$ an orthogonal matrix, there holds*

$$H(Px) = PH(x)P^T \quad (2.9)$$

Proof: Consider $z = P^T y$. As $\det(P) = \pm 1$, and $\|z\| = \|y\|$, because of (2.3), there holds,

$$f_Z(z) = f_Y(z) \quad (2.10)$$

$$= f_y(y). \quad (2.11)$$

$$\begin{aligned} H(Px) &= E \left[\frac{(Px-y)(Px-y)^T}{\|x-y\|^4} \right] \\ &= E \left[\frac{P(x-P^T y)(x-P^T y)^T P^T}{\|P(x-P^T y)\|^4} \right] \\ &= E \left[\frac{P(x-z)(x-z)^T P^T}{\|(x-z)\|^4} \right] \\ &= PE \left[\frac{(x-z)(x-z)^T}{\|(x-z)\|^4} \right] P^T \\ &= PH(x)P^T. \end{aligned}$$

The following lemma characterizes the eigenvalues of $H(x)$. To this end we present the following lemma that denotes $e_i \in \mathbb{R}^N$ to be the vector whose i -th element is one and the rest zero.

Lemma 2.2.2 *Consider $y \in \mathbb{R}^N$ with pdf (2.3) and $R > r_1$. Then for every $k \in \{1, \dots, N\}$, $H(Re_k)$ is a positive semidefinite diagonal matrix all but whose i -th diagonal elements equal each other, while the i -th diagonal element is distinct from the rest and positive. Further $H(Re_k)$ is positive definite unless*

$$\text{Prob}(\|y\| \neq 0) = 0. \quad (2.12)$$

Proof: Because of the radial symmetry of (2.3) it suffices to prove the result for $k = 1$. Denote y_i to be the i -th element of y . Then for $i \in \{2, \dots, n\}$

$$E \left[\frac{y_i}{\|y - Re_1\|^4} \right] = E \left[\frac{y_i}{((y_1 - R)^2 + \sum_{l=2}^n y_l^2)^2} \right]. \quad (2.13)$$

Fixing all elements of y except y_i , gives us

$$\frac{y_i}{((y_1 - R)^2 + \sum_{l=2}^n y_l^2)^2} \quad (2.14)$$

which is an odd function of y_i , while $g(\|y\|)$ is an even function. Thus,

$$E \left[\frac{y_i}{\|y - Re_1\|^4} \right] = 0. \quad (2.15)$$

Similarly, for the same i and any $l \neq i$,

$$E \left[\frac{y_i y_l}{\|y - Re_1\|^4} \right] = 0. \quad (2.16)$$

Now for any $i \neq 1$, the $(1, i)$ -th element of $H(Re_1)$ is given by:

$$[H(Re_1)]_{i1} = E \left[\frac{y_i (y_1 - R)}{\|y - Re_1\|^4} \right] \quad (2.17)$$

$$= E \left[\frac{y_i y_1}{\|y - Re_1\|^4} \right] - RE \left[\frac{y_i}{\|y - Re_1\|^4} \right]$$

$$= 0. \quad (2.18)$$

Similarly, for $i \in \{2, \dots, n\}$ and $m \in \{2, \dots, n\} \setminus \{i\}$,

$$[H(Re_1)]_{im} = E \left[\frac{y_i y_m}{\|y - Re_1\|^4} \right] \quad (2.19)$$

$$= 0. \quad (2.20)$$

Thus $H(Re_1)$ is diagonal. The rest of the theorem follows from the fact for all

$i \in \{2, \dots, n\}$:

$$\begin{aligned}
0 &\leq E \left[\frac{y_i^2}{((y_1 - R)^2 + \sum_{l=2}^n y_l^2)^2} \right] & (2.21) \\
&= [H(Re_1)]_{ii} \\
&\neq E \left[\frac{(y_1 - R)^2}{((y_1 - R)^2 + \sum_{l=2}^n y_l^2)^2} \right] \\
&= [H(Re_1)]_{11} \\
&> 0 \quad ,
\end{aligned}$$

that

$$E \left[\frac{y_i^2}{((y_1 - R)^2 + \sum_{l=2}^n y_l^2)^2} \right] = E \left[\frac{y_m^2}{((y_1 - R)^2 + \sum_{l=2}^n y_l^2)^2} \right] \quad (2.22)$$

for all $i, m \in \{2, \dots, n\}$ and that equality in (2.21) holds iff (2.12) holds.

As $f_Y(y)$ is radially symmetric, (2.12) implies that the source is almost surely at the origin. Thus unless there is no uncertainty in the location of the source $H(x)$ is positive definite. This is essentially the setting considered in [28]. As all vectors of the same norm are related by orthogonal transformation, Lemmas 2.2.1 and 2.2.2 lead to the following Theorem.

Theorem 2.2.1 *Consider $y \in \mathbb{R}^N$ distributed as in (2.3). Then for all $\|x\| > r_1$, $H(x)$ in (2.7) is positive semidefinite, with $N - 1$ eigenvalues that are equal to each other and another that is distinct from them and is positive. Further, $H(x)$ is positive definite unless (2.12) holds.*

In the sequel $\text{trace}(H(x))$ will play a critical role. Evidently, because of Lemma

2.2.1 it depends only on $\|x\|$. Consider the following notation:

$$T(R) = \text{trace}(H(x)); \forall \|x\| = R. \quad (2.23)$$

This brings us to a key difference between the development here and that in [29]-[36].

The development in that work relied on the fact that in those settings

$$H(R_1 e_i) > H(R_2 e_i) \quad (2.24)$$

for all $r_1 < R_1 < R_2$. For general radially symmetric distributions *this is in general false*. Suppose in particular $N = 3$, and y is uniformly distributed on the *surface* of the sphere of radius r_1 , i.e. in (2.3),

$$g(\|y\|) = \frac{\delta(\|y\| - r_1)}{4\pi r_1^2}. \quad (2.25)$$

Then it is shown in Appendix A that

$$\frac{d[H(Re_3)]_{33}}{dR} \quad (2.26)$$

is in fact *positive* when $R > r_1$ is sufficiently close to r_1 . As $[H(Re_3)]_{33}$ is an eigenvalue of $H(Re_3)$, this means that (2.24) will not hold. This counterintuitive result is in part a consequence of the fact that under (3.39), $H(Re_3)$ is *finite*.

In a significant technical departure from [29]-[36] this work will show that what

is instead sufficient for the development here is that for all $R > r_1$, $\mathcal{T}(R)$ in (2.23) be a decreasing function of R . This is proved below.

Theorem 2.2.2 *Consider (2.3) and (2.7). For $R > r_1$, $\mathcal{T}(R)$ in (2.23) is a decreasing function of R .*

Proof: As all vectors of the same norm are related by orthogonal transformations, for all $R > r_1$

$$\text{trace}(R) = \text{trace} \left(E \left[\frac{(Re_1 - y)(Re_1 - y)^T}{\|Re_1 - y\|^4} \right] \right) \quad (2.27)$$

$$= E \left[\frac{\|Re_1 - y\|^2}{\|Re_1 - y\|^4} \right] \quad (2.28)$$

$$= E \left[\frac{1}{\|Re_1 - y\|^2} \right] \quad (2.29)$$

$$= E \left[\frac{1}{((y_1 - R)^2 + \sum_{l=2}^n y_l^2)^2} \right]. \quad (2.30)$$

The result follows from the fact that whenever $\|y\| \leq r_1 < R_1 < R_2$

$$(y_1 - R_1)^2 + \sum_{l=2}^n y_l^2 < (y_1 - R_2)^2 + \sum_{l=2}^n y_l^2. \quad (2.31)$$

2.3 Characterizing Optimality

In this section we characterize x_i that achieve optimality for all three of the Problems 1 to 3. This requires the following Lemma.

Lemma 2.3.1 Consider a positive definite $A = A^T \in \mathbb{R}^{N \times N}$. Then

$$\lambda_{\min}(A) \leq \frac{\text{trace}(A)}{N}, \quad (2.32)$$

$$\det(A) \leq \left(\frac{\text{trace}(A)}{N} \right)^N \quad (2.33)$$

$$\text{trace}(A^{-1}) \geq \frac{N^2}{\text{trace}(A)}. \quad (2.34)$$

Further, the equality holds in each of (2.32-2.34) iff

$$A = \frac{\text{trace}(A)}{N} I \quad (2.35)$$

Proof: Observe that for all $i \in \{1, \dots, N\}$, every eigenvalue $\lambda_i(A)$ is positive. Then (2.32) follows from the fact that the trace is the sum of the eigenvalues. Further the equality requires that for all $i \in \{1, \dots, N\}$

$$\lambda_i(A) = \frac{\text{trace}(A)}{N}. \quad (2.36)$$

As A is symmetric this can happen iff (2.35) holds.

The AM-GM inequality states that the arithmetic mean of N numbers is greater than or equal to its geometric mean, with equality iff all the N numbers are equal.

Finally, also from the AM-GM inequality

$$\begin{aligned} \text{trace}(A^{-1}) &= N \sum_{i=1}^N \frac{1}{N\lambda_i(A)} \\ &\geq N \left(\prod_{i=1}^N \frac{1}{\lambda_i(A)} \right)^{\frac{1}{N}}. \end{aligned} \quad (2.37)$$

The result follows from the fact that equality in (2.37) holds iff (2.36) holds and that under it

$$N \left(\prod_{i=1}^N \frac{1}{\lambda_i(A)} \right)^{\frac{1}{N}} = N \left(\frac{N}{\text{trace}(A)} \right) \quad (2.38)$$

Theorem 2.3.1 *The $x_i \in \mathbb{R}^N$, do not lie on an $N - 1$ dimensional hyperplane, solve all three of Problems 1-3, iff (a) for all $i \in \{1, \dots, n\}$, $\|x_i\| = r_2$ and lead to*

$$F = \frac{nT(r_2)}{N}I. \quad (2.39)$$

Proof: The fact that such x_i exist is proved in Section 2.4. The fact they optimize follows from Lemma 2.3.1, which requires that the trace of F be as large as possible, and the fact that because of Theorem 2.2.2 and (2.4)

$$\text{trace}(F) \leq \sum_{i=1}^n \text{trace}(H(x_i)) \quad (2.40)$$

$$\leq nT(r_2), \quad (2.41)$$

with equality iff each x_i has norm r_2 .

Thus the optimum occurs when each sensor resides on a ball of radius r_2 . Observe, that the optimizing solution cannot be unique. To see this, observe because of Lemma 2.2.1, $H(-x_i) = H(x_i)$. Thus flipping the sign of any sensor location does not alter F . Similarly, suppose a set of x_i optimize. Then replacing each by Px_i , will also result in an F that equals (2.39). Further suppose, $n = N + 1$ sensors achieve optimality. Then optimality with $2N + 2$ sensors can be achieved with an infinite number of combinations. For example, one can choose the first $N + 1$ to lie at x_i and for arbitrary orthogonal P , the remaining at Px_i .

Because of this, rather than proposing an exhaustive list of optimal configurations, in Section 2.4 we propose a set of canonical solutions.

2.4 Canonical Solutions

Section 2.3 had proofs that the solution to all three problems involves $\|x_i\| = r_2$, and the satisfaction of (2.39). Also the solutions are nonunique in potentially nontrivial ways. This section provides a class of canonical solutions, and in the process proves the existence of x_i that do not lie on an $N - 1$ dimensional hyperplane and satisfy (2.39). Though the interest is for $N = 2$ or $N = 3$, for the sake of completeness this section provides these solutions for all $N > 1$. This section also exposes certain salient differences between the $N = 2$ and $N = 3$ cases.

Since a necessary condition for optimality is that all x_i have norm r_2 , and all such vectors are mutually related by orthogonal transformations, the canonical solutions we propose take the following form: For an orthogonal matrix $Q \in \mathbb{R}^{N \times N}$,

the $x_i \in \mathbb{R}^N$ obey:

$$x_{i+1} = Qx_i, \quad \|x_1\| = r_2, \quad \forall i \in \{1, \dots, n\}. \quad (2.42)$$

In view of Theorem 2.3.1, the goal is to characterize all orthogonal Q and x_1 pairs such that under (2.42), the x_i do not lie on an $N - 1$ dimensional hyperplane and result in (2.39). The first requirement necessitates that $n > N$.

Suppose under (2.42), (2.39) holds i.e.:

$$\begin{aligned} \sum_{i=1}^n H(x_i) &= \sum_{i=0}^{n-1} H(Q^i x_1) \\ &= \sum_{i=0}^{n-1} Q^i H(x_1) Q^i \\ &= \frac{n\mathcal{T}(r_2)}{N} I. \end{aligned} \quad (2.43)$$

Definition 2.4.1 *The orthogonal matrix $Q \in \mathbb{R}^{N \times N}$ and the vector $x_1 \in \mathbb{R}^N$, $\|x_1\| = r_2$ form an admissible pair if the x_i in (2.42) do not span an $N - 1$ dimensional hyperplane and obey (2.43).*

The rest of this section explores how Q changes with x_1 . Consider a $z_1 \in \mathbb{R}^N$, with $\|z_1\| = r_2$. Then there exists an orthogonal matrix P such that

$$z_1 = Px_1. \quad (2.44)$$

Then because of Lemma 2.2.1

$$\frac{nT(r_2)}{N} I = \frac{nT(r_2)}{N} P P^T \quad (2.45)$$

$$= P \left(\sum_{i=0}^{n-1} Q^i P^T P H(x_1) P^T P Q^i \right) P^T \quad (2.46)$$

$$= \sum_{i=0}^{n-1} (P Q^i P^T) H(P x_1) (P Q^i P^T) \quad (2.47)$$

$$= \sum_{i=0}^{n-1} (P Q P^T)^i H(z_1) (P Q P^T)^i \quad (2.48)$$

Thus under (2.44) the optimizing Q must be transformed to $P Q P^T$. This brings us to a distinction between $N = 2$ and $N = 3$ or for that matter any $N > 2$. For $N = 2$ all orthogonal matrices belong to one of two categories. The first known as *Givens Rotations* have the form for some $\theta \in \mathfrak{R}$

$$Q_1(\theta) = \begin{bmatrix} \cos \theta & \sin \theta \\ -\sin \theta & \cos \theta \end{bmatrix} \quad (2.49)$$

and

$$Q_2(\theta) = \begin{bmatrix} \cos \theta & \sin \theta \\ \sin \theta & -\cos \theta \end{bmatrix} \quad (2.50)$$

Among these (2.49) is a rotation matrix in that its determinant is one. In fact it rotates every vector counterclockwise by the angle θ . On the other hand, (2.50), having a determinant -1 , is not a rotation matrix. More compellingly $Q_2^2(\theta) = I$. Thus with $Q = Q_2(\theta)$ the set in (2.42) comprises precisely two elements, rendering the x_i collinear. Thus henceforth for $N = 2$ only Givens Rotations will be considered.

Observe:

$$Q_1(\theta_1)Q_1(\theta_2) = Q_1(\theta_1 + \theta_2) = Q_1(\theta_2)Q_1(\theta_1), \quad (2.51)$$

i.e. Givens Rotations commute.

Further, given any pair z_1, x_1 of the same norm, there exist $\theta_i \in \Re$ such that

$$z_1 = Q_i(\theta_i)x_1. \quad (2.52)$$

Should Q be a Givens Rotation then select $P = Q_1(\theta_1)$ in (2.44); and observe that:

$$PQP^T = QPP^T \quad (2.53)$$

$$= Q. \quad (2.54)$$

In other words, for $N = 2$, if a Givens Rotation Q leads to (2.43) with a particular x_1 , then the same Q also works with arbitrary z_1 of the same norm as x_1 . The commutativity in (2.51) does not extend to $N > 2$. Thus at least for $N > 2$ changing x_1 will cause Q to change.

2.4.1 Avoiding Coplanarity

A second point of departure between $N = 2$ and $N > 2$ comes from the fact that any three distinct points on a circle centered at the origin are necessarily

noncollinear. For $N > 2$, $N + 1$ distinct points on a hypersphere centered at the origin, can lie on an $N - 1$ dimensional hyperplane. The requirement of avoiding an $N - 1$ dimensional hyperplane imposes certain conditions on Q , which we now characterize in the theorem below. As background to this theorem we observe that a real orthogonal matrix Q is normal as $Q^T Q = Q Q^T = I$, [40]. Thus it is unitarily diagonalizable, i.e for some unitary $U \in C^{N \times N}$, with $U^H U = I$, and $\Omega \in C^{N \times N}$ a diagonal matrix comprising the eigenvalues of Q .

$$Q = U \Omega U^H. \quad (2.55)$$

Theorem 2.4.1 *Consider an orthogonal $Q \in \mathbb{R}^{N \times N}$ obeying (2.55), with diagonal $\Omega \in C^{N \times N}$ and unitary $U \in C^{N \times N}$, and x_i as in (2.42). Then with integer $n > N$, the set $\{x_i\}_{i=1}^n$ does not lie on an $N - 1$ dimensional hyperplane iff all of the following hold.*

- (i) *The eigenvalues of Q are distinct.*
- (ii) *One is not an eigenvalue of Q .*
- (iii) *All elements of $U^H x_1$ are nonzero.*

Proof: Observe that $\{x_i\}_{i=1}^n$ lie on an $N - 1$ dimensional hyperplane iff there is a nonzero $a \in \mathbb{R}^N$ and $b \in \mathbb{R}$ such that

$$a^T x_i = b \quad \forall i \in \{1, \dots, n\} \quad (2.56)$$

Define

$$\rho = U^H x_1, \quad (2.57)$$

and

$$\eta = U^H a. \quad (2.58)$$

Then (2.56) is equivalent to the existence of a nonzero $\eta \in C^N$ such that

$$\eta^H \Omega^i \rho = b \quad \forall i \in \{0, \dots, n-1\} \quad (2.59)$$

Denote $\Omega = \text{diag}\{\omega_1, \dots, \omega_N\}$. Suppose ρ_l , the l -th element of ρ is zero. Choose $\eta = \eta_l e_l$, for nonzero $\eta_l \in C$. Then

$$\eta^H \Omega^i \rho = \eta_l \omega_l^i \rho_l = 0 \quad \forall i \in \{0, \dots, n-1\} \quad (2.60)$$

i.e. $\{x_i\}_{i=1}^n$ lie on an $N-1$ dimensional hyperplane. Similarly suppose an eigenvalue of Q , i.e. a diagonal element of Ω is one. In particular suppose $\omega_l = 1$. Again choose $\eta = \eta_l e_l$, for nonzero $\eta_l \in C$ Then:

$$\eta^H \Omega^i \rho = \eta_l \omega_l^i \rho_l = \eta_l \rho_l \quad \forall i \in \{0, \dots, n-1\} \quad (2.61)$$

and again $\{x_i\}_{i=1}^n$ lie on an $N-1$ dimensional hyperplane. Suppose next (i) is violated.

Without loss of generality suppose $\omega_1 = \omega_2$. Choose η_1 and η_2 so that

$$[\eta_1^*, \eta_2^*] \begin{bmatrix} \rho_1 \\ \rho_2 \end{bmatrix} = 0 \quad (2.62)$$

and $\eta = [\eta_1^*, \eta_2^*, 0]^T$.

Then:

$$\eta^H \Omega^i \rho = \omega_1^i [\eta_1^*, \eta_2^*] \begin{bmatrix} \rho_1 \\ \rho_2 \end{bmatrix} = 0 \quad \forall i \in \{0, \dots, n-1\} \quad (2.63)$$

i.e. $\{x_i\}_{i=1}^n$ lie on an $N-1$ dimensional hyperplane. Thus (i-iii) are indeed necessary for $\{x_i\}_{i=1}^n$ to avoid an $N-1$ dimensional hyperplane.

Henceforth assume that (i-iii) hold. To establish a contradiction suppose $\{x_i\}_{i=1}^n$ lie on an $N-1$ dimensional hyperplane. Then (2.59) holds. Taking differences on both sides of (2.59) for successive value of i , as Ω is diagonal there holds for all $i \in \{0, \dots, n-2\}$ and $\eta \neq 0$,

$$0 = \eta^H \Omega^{i+1} \rho - \eta^H \Omega^i \rho \quad (2.64)$$

$$= \eta^H \text{diag}\{\omega_1 - 1, \dots, \omega_N - 1\} \Omega^i \rho. \quad (2.65)$$

$$0 = \eta^H \Omega^{i+1} \rho - \eta^H \Omega^i \rho \quad (2.66)$$

$$= \eta^H \text{diag}\{\omega_1 - 1, \dots, \omega_N - 1\} \Omega^i \rho. \quad (2.67)$$

As under (ii) all $\omega_i \neq 1$, $\tilde{\eta} = \mathbf{diag}\{\omega_1 - 1, \dots, \omega_N - 1\}^H \eta \neq 0$. Thus as $n > N$, for all $i \in \{0, \dots, N - 1\}$ and $\tilde{\eta} \neq 0$,

$$\tilde{\eta}^H \Omega^i \rho = 0. \quad (2.68)$$

Thus, [41], $[\Omega, \rho]$ is not a completely controllable pair. As Ω is a diagonal matrix with distinct diagonal elements, at least one element of ρ must be zero, [41]. This contradicts (iii) proving the result.

Since the eigenvalues of Q are on the unit circle, and complex eigenvalues appear in conjugate pairs, for even N this means that the eigenvalues of Q must be distinct, complex and of the form $e^{\pm j\theta_i}$. For $N = 2$ this necessitates the use of Given Rotations as the eigenvalues of (2.50) are ± 1 regardless of θ . On the other hand for odd N , $\lfloor \frac{N}{2} \rfloor$ eigenvalues are complex and of the form $e^{\pm j\theta_i}$. The remaining eigenvalue must be at -1 . Thus for odd N , $\det(Q) = -1$, preventing Q from being a rotation matrix. This also brings into sharp relief a contrast between $N = 2$ and $N = 3$. While for the former admissible Q matrices are rotation matrices, for $N = 3$ they cannot be.

Only the necessity of (i) and (ii) was noted in [36], making the argument there incomplete. The role of (iii) is quite crucial. Thus, while

$$Q = \begin{pmatrix} \cos \theta & \sin \theta & 0 \\ -\sin \theta & \cos \theta & 0 \\ 0 & 0 & -1 \end{pmatrix} \quad (2.69)$$

satisfies (i) and (ii), and can be paired with $x_1 = [1, 1, 1]^T$, it cannot be paired with e_3 or $[1, 1, 0]^T$. This further underscores the quirks induced by the noncommutativity of orthogonal matrices for $N > 2$.

2.4.2 Achieving the Optimum FIM

This subsection presents work on designing Q , x_1 pairs that ensure (2.43).

Suppose $W \in \mathfrak{R}^{N \times N}$ is an orthogonal matrix for which

$$x_1 = r_2 W e_1. \quad (2.70)$$

Then because of lemmas 2.2.1 and 2.2.2 one obtains

$$H(x_1) = W \Lambda W^T \quad (2.71)$$

where for $\lambda_1 > 0$, $\lambda_2 \geq 0$ and $\lambda_1 \neq \lambda_2$,

$$\Lambda = \mathbf{diag} \{ \lambda_1, \lambda_2 I_{N-1} \}. \quad (2.72)$$

Define

$$T = U^H W \quad (2.73)$$

with U defined in (2.55). Then (2.43) is equivalent to:

$$\begin{aligned} \frac{nT(r_2)}{N} I &= \frac{nT(r_2)}{N} U^H U \\ &= U^H \left(\sum_{i=0}^{n-1} Q^i H(x_1) Q^i \right) U \\ &= U^H \left(\sum_{i=0}^{n-1} (U \Omega U^H)^i W \Lambda W^T (U \Omega^* U^H)^i \right) U \\ &= U^H \left(\sum_{i=0}^{n-1} U \Omega^i U^H W \Lambda W^T U \Omega^{*i} U^H \right) U \\ &= \sum_{i=0}^{n-1} \Omega^i T \Lambda T^H \Omega^{*i} \end{aligned} \quad (2.74)$$

Observe (iii) of Theorem 2.4.1 is equivalent to the requirement that all elements of

$$U^H x_1 = U^H W e_1 \quad (2.75)$$

be nonzero. In other words the first column of T is nonzero. It will be evident in the sequel that to satisfy (2.43) it is necessary for all diagonal elements of $T \Lambda T^H$ to be the same. The work that follows shows that this requirement is equivalent to the requirement that all elements in the first column of T are equal. As T is unitary this automatically means that all elements in its first column are nonzero.

Lemma 2.4.1 *Suppose $T \in C^{N \times N}$ is unitary. With Λ as in (2.72) and $\lambda_1 \neq \lambda_2$, all diagonal elements of $T \Lambda T^H$ are equal iff all elements in the first column of T are*

equal and nonzero. Further, all elements of $T\Lambda T^H$ are nonzero.

Proof: Observe that for some $\alpha \neq 0$

$$\Lambda = \lambda_2 I + \alpha e_1 e_1^T. \quad (2.76)$$

Thus:

$$\begin{aligned} T\Lambda T^H &= T(\lambda_2 I + \alpha e_1 e_1^T)T^H \\ &= \lambda_2 I + \alpha T e_1 e_1^T T^H \end{aligned} \quad (2.77)$$

Thus the i -th diagonal element of $T\Lambda T^H$ is $\lambda_2 + \alpha \mu_i$ where μ_i is the magnitude square of the i -th element of $T e_1$. Thus all elements of $T e_1$ have the same magnitude. As T is nonsingular no element of $T e_1$ can be zero. Also from (2.77) the off-diagonal elements of $T\Lambda T^H$ are α times the product of the elements of $T e_1$ and must be nonzero.

The following theorem characterizes Q, x_1 pairs that are admissible when N is even.

Theorem 2.4.2 *Suppose for integer $M \geq 1$, $n > N = 2M$. Consider orthogonal $Q \in \mathbb{R}^{N \times N}$ obeying (2.55) with unitary $U \in \mathbb{C}^{N \times N}$ and diagonal $\Omega \in \mathbb{C}^{N \times N}$, and with orthogonal $W \in \mathbb{R}^{N \times N}$, $0 < \lambda_1 \neq \lambda_2 \geq 0$, (2.70-2.73). Then the Q and x_1 , form an admissible pair iff all of the following hold.*

(a) *All elements of $T e_1$ have the same magnitude.*

(b) *There exist real $\theta_1, \dots, \theta_M$, such that the diagonal elements of Ω are $e^{\pm j\theta_i}$ and*

distinct.

(c) For all $i \in \{1, \dots, M\}$, $e^{\pm j\theta_i} \neq \pm 1$.

(d) For all $\{i, l\} \subset \{1, \dots, M\}$, including $i = l$, $\theta_i \pm \theta_l$ are integer multiples of $2\pi/n$.

Proof:

Necessity:

The necessity of (b) and (c) follows from Theorem 2.4.1. Call v_{il} the il -th element of $T\Lambda T^H$. As the i -th diagonal of the summation in (2.74) is nv_{ii} , all diagonal elements of $T\Lambda T^H$ are equal. Then from Lemma 2.4.1, (a) must hold. Further also from Lemma 2.4.1, every $v_{il} \neq 0$.

The off-diagonal elements on the left hand side of (2.74) are two types. First for suitable $\{k, l\} \subset \{1, \dots, N\}$, $k \neq l$, and $\{r, s\} \subset \{1, \dots, M\}$, $r \neq s$,

$$v_{kl} \sum_{i=0}^{n-1} e^{\pm j i (\theta_r \pm \theta_s)} = v_{kl} \frac{1 - e^{\pm j n (\theta_r \pm \theta_s)}}{1 - e^{\pm j (\theta_r \pm \theta_s)}}. \quad (2.78)$$

Because of (b) and (c) the denominators are non-zero. Thus as (a) holds, for $r \neq s$, $n(\theta_r \pm \theta_s)$ is a multiple of 2π , i.e. $\theta_r \pm \theta_s$ is a multiple of $2\pi/n$.

The second type of off-diagonal elements on the left hand side of (2.74) are: for suitable $\{k, l\} \subset \{1, \dots, N\}$, $k \neq l$, and $r \in \{1, \dots, M\}$,

$$v_{kl} \sum_{i=0}^{n-1} e^{\pm 2j i \theta_r} = v_{kl} \frac{1 - e^{\pm j 2n \theta_r}}{1 - e^{\pm 2j \theta_r}}. \quad (2.79)$$

Because of (c) the denominators are again non-zero. Thus as (a) holds, $2n\theta_r$ is a multiple of 2π . Thus (d) is also necessary.

Sufficiency

To prove sufficiency we first note that as remarked before Lemma 2.4.1, (a-c) together with Theorem 2.4.1 assure that the x_i in (2.42) do not inhabit an $N - 1$ dimensional hyperplane. That the off-diagonal elements of the summation in (2.74) also zero follows by reversing the arguments proving the necessity of (d). That the diagonal elements in the sum are equal follows from (a) and Lemma 2.4.1.

The foregoing represents a complete characterization of Q when $N = 2M$, and $n > N$. It is interesting that the noncollinearity requirement mandates the use of Givens rotations for $N = 2$, in stark contrast to the $N = 3$ case where rotation matrices preclude noncoplanarity.

The work that follows shows that for every $M \geq 1$, a Q conforming to this characterization can be found. Recall that for $N = 2$ if a Q , x_1 with $\|x_1\| = r_2$ pair is admissible, then so is Q , x for all $x \in \mathfrak{R}^2$ with norm r_2 . Call $u_2 \in \mathfrak{R}^2$ the vector of all ones. It is readily verified that $H(\frac{1}{\sqrt{2}}r_2u_2)$ has equal diagonal elements. Thus, with $x_1 = \frac{r_2}{\sqrt{2}}u_2$, from Lemma 2.4.1, with W as in (2.70) We_1 has both elements of equal magnitude. Consider $U = T_e$ below,

$$T_e = \frac{1}{\sqrt{2}} \begin{bmatrix} 1 & 1 \\ j & -j \end{bmatrix}. \quad (2.80)$$

Then U^HWe_1 also has both elements of the same magnitude. Then the Q below

satisfies all requirements of the Theorem 2.4.2 and forms an admissible pair with any $x \in \mathfrak{R}^2$ with magnitude r_2 .

$$Q = U \text{diag} \left\{ e^{j\frac{2\pi}{n}}, e^{-j\frac{2\pi}{n}} \right\} U^H \quad (2.81)$$

$$= \frac{1}{2} \begin{bmatrix} e^{j\frac{2\pi}{n}} & e^{-j\frac{2\pi}{n}} \\ j e^{j\frac{2\pi}{n}} & -j e^{-j\frac{2\pi}{n}} \end{bmatrix} \begin{bmatrix} 1 & -j \\ 1 & j \end{bmatrix} \quad (2.82)$$

$$= \begin{bmatrix} \cos \frac{2\pi}{n} & \sin \frac{2\pi}{n} \\ -\sin \frac{2\pi}{n} & \cos \frac{2\pi}{n} \end{bmatrix} \quad (2.83)$$

This is thus the Givens rotation by $2\pi/n$. Thus n -sensors are distributed equispaced on the circle centered at origin with radius r_2 . These are *optimum spherical codes* in \mathfrak{R}^2 in that these are collection of n -points on a circle such that the minimum distance between them is the maximum possible.

As replacing any x_i by $-x_i$ does not impair optimality, sensors equispaced on a semicircle are also optimum. On the other hand:

$$Q = U \text{diag} \left\{ e^{j\frac{2\pi}{n}+\pi}, e^{-j\frac{2\pi}{n}+\pi} \right\} U^H \quad (2.84)$$

$$= \begin{bmatrix} \cos \frac{2\pi}{n} & \sin \frac{2\pi}{n} \\ \sin \frac{2\pi}{n} & -\cos \frac{2\pi}{n} \end{bmatrix} \quad (2.85)$$

also meets the requirement of Theorem 2.4.2 and constitutes a matrix of the form in (2.50).

Then for $M > 1$, the $N \times N$ matrix

$$T = \mathbf{diag} \{ T_e, T_e, \dots, T_e \} \quad (2.86)$$

obeys (a) if $x_1 = [1, \dots, 1]^T / \sqrt{N}$.

Indeed in this case with:

$$Q_i = \begin{bmatrix} \cos(\theta_i) & \sin(\theta_i) \\ -\sin(\theta_i) & \cos(\theta_i) \end{bmatrix} \quad (2.87)$$

one obtains:

$$Q = \text{diag}\{Q_1, Q_2, \dots, Q_M\}. \quad (2.88)$$

The θ_i chosen to be odd multiples of π/n will satisfy (d). For example one could choose for $k \in \{1, \dots, M\}$

$$\theta_k = \frac{(2k-1)\pi}{n}. \quad (2.89)$$

Given that there are M of these with $n > 2M$, one has for all $k \in \{1, \dots, M\}$ that

$$0 < \theta_k \leq \frac{(2M-1)\pi}{n} < \pi, \quad (2.90)$$

i.e. these satisfy (b-c) as well.

The following theorem characterizes the design of Q x_1 pair for odd values of $N > 1$.

Theorem 2.4.3 *Suppose for integer $M \geq 1$, $n > N = 2M + 1$. Consider orthogonal $Q \in \mathbb{R}^{n \times n}$ obeying (2.55) with unitary $U \in \mathbb{C}^{n \times n}$ and diagonal $\Omega \in \mathbb{C}^{n \times n}$, and with orthogonal $W \in \mathbb{R}^{n \times n}$, $0 < \lambda_1 \neq \lambda_2 \geq 0$, (2.70-2.73). Then Q and x_1 form an*

admissible pair iff all of the following hold.

- (a) All elements of Te_1 have the same magnitude.
- (b) There exist real $\theta_1, \dots, \theta_M$, such that $2M$ of the $2M + 1$ diagonal elements of Ω are $e^{\pm j\theta_i}$, are distinct and appear in conjugate pairs. The remaining diagonal element of Ω is -1 .
- (c) For all $i \in \{1, \dots, M\}$, $e^{\pm j\theta_i} \neq \pm 1$.
- (d) For all $\{i, l\} \subset \{1, \dots, M\}$, including $i = l$, $\theta_i \pm \theta_l$ are integer multiples of $2\pi/n$.
- (e) For all $i \in \{1, \dots, M\}$, $(\pm\theta_i - \pi)$ are integer multiples of $2\pi/n$.

Proof:

Necessity:

The necessity of (a-c) follows as in the proof of Theorem 2.4.2. The off diagonal elements on the left hand side of (2.74) are now of three types. First for suitable $\{k, l\} \subset \{1, \dots, N\}$, $k \neq l$, and $\{r, s\} \subset \{1, \dots, M\}$, $r \neq s$, obey (2.78). The second for suitable suitable $\{k, l\} \subset \{1, \dots, N\}$, $k \neq l$, and $r \in \{1, \dots, M\}$, obey (2.79). Thus as in the proof of Theorem 2.4.2 (2.74) implies (d).

The third type of off diagonal element is for suitable suitable $\{k, l\} \subset \{1, \dots, N\}$, $k \neq l$, and $r \in \{1, \dots, M\}$, obey:

$$v_{kl} \sum_{i=0}^{n-1} e^{ji(\pm\theta_r - \pi)} = v_{kl} \frac{1 - e^{jn(\pm\theta_r - \pi)}}{1 - e^{j(\pm\theta_r - \pi)}}. \quad (2.91)$$

Again because of (c) the denominator is non-zero, and thus for this element to be

zero (e) must hold.

Sufficiency:

Proof of sufficiency follows as in the proof of Theorem 2.4.2.

The work that follows shows the design of a Q , x_1 admissible pair for $N = 3$. Suppose $u_3 \in \mathfrak{R}^3$ is a vector with all ones. Consider $x_1 = \frac{1}{\sqrt{3}}r_2u_3$. Then with W as in (2.70), all elements of We_1 have the same magnitude. Choose $U = T_o$ where

$$T_o = \begin{bmatrix} \frac{1}{\sqrt{2}} & \frac{1}{\sqrt{2}} & 0 \\ \frac{j}{\sqrt{2}} & \frac{-j}{\sqrt{2}} & 0 \\ 0 & 0 & -1 \end{bmatrix}. \quad (2.92)$$

Thus the vector U^HWe_1 has all elements of the same magnitude satisfying the condition in Theorem 2.4.3. Thus Q below satisfies all the conditions in Theorem 2.4.3 and hence Q , $x_1 = \frac{1}{\sqrt{3}}r_2u_3$ form an admissible pair.

$$Q = U \text{diag} \left\{ e^{j\frac{2\pi}{n}+\pi}, e^{-j\frac{2\pi}{n}+\pi}, -1 \right\} U^H \quad (2.93)$$

$$= \begin{bmatrix} -\cos \frac{2\pi}{n} & -\sin \frac{2\pi}{n} & 0 \\ \sin \frac{2\pi}{n} & -\cos \frac{2\pi}{n} & 0 \\ 0 & 0 & -1 \end{bmatrix} \quad (2.94)$$

Then for $M > 1$, the $N \times N$ matrix

$$T = \mathbf{diag} \{T_e, T_e, \dots, T_e, -1\} \quad (2.95)$$

obeys (a) if $x_1 = [1, \dots, 1]^T / \sqrt{N}$.

In this case with:

$$Q_i = \begin{bmatrix} \cos(\theta_i) & \sin(\theta_i) \\ -\sin(\theta_i) & \cos(\theta_i) \end{bmatrix} \quad (2.96)$$

one obtains:

$$Q = \text{diag}\{Q_1, Q_2, \dots, Q_M, -1\}. \quad (2.97)$$

The θ_i chosen to be odd multiples of π/n will satisfy (d). For example one could choose for $k \in \{1, \dots, M\}$

$$\theta_k = \frac{(2k-1)\pi}{n}. \quad (2.98)$$

Given that there are M of these with $n > 2M$, one has for all $k \in \{1, \dots, M\}$ that

$$0 < \theta_k \leq \frac{(2M-1)\pi}{n} < \pi, \quad (2.99)$$

i.e. these satisfy (b-c) as well.

2.4.3 Geometric Interpretation of the solution

The proposed canonical solution has the following attractive feature when $N = 3$. All x_i lie on the base of two inverted cones with axes parallel to the z-axis, and vertices at the origin. All the points on the base of the first cone have a z-coordinate that is the negative of those on the base of the second cone. The rims of the bases lie on the sphere of radius r_2 . The x_i 's alternate between the two bases. Each

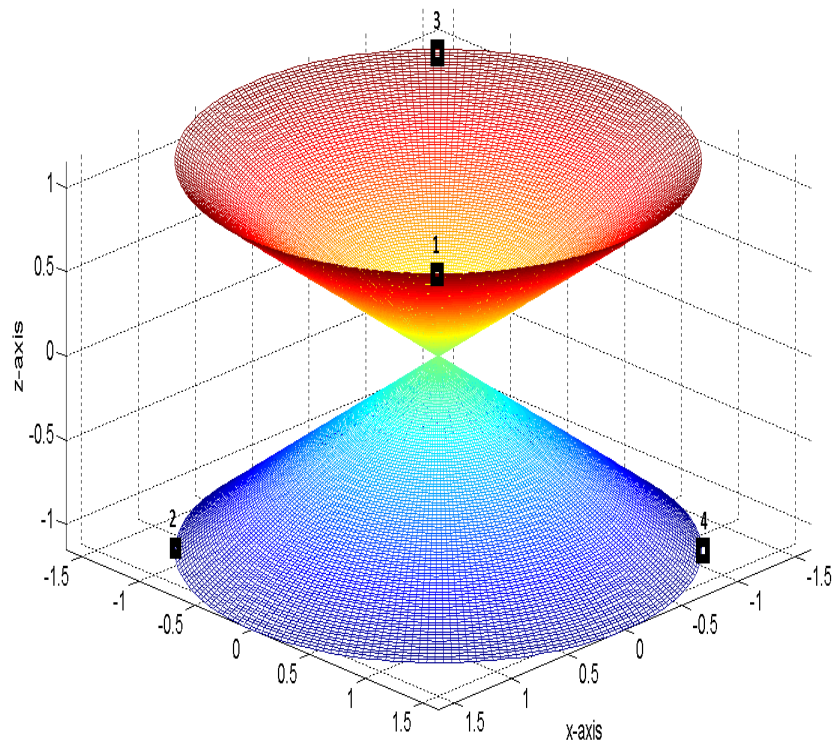


Figure 2.1: Illustration of proposed sensor placement for $n = 4$ and $r_2 = 2$

x_i is further rotated by an angle of $2\pi/n - \phi$ parallel to the $x - y$ plane, from the previous x_i as shown in Figure 2.1.

2.5 Simulation Results for the three dimensional case

We compare the performance of the proposed optimum solution with that of the performance of a non-coplanar random sensor placement in the following simulations.

1. Geometric Dilution of Precision of the network versus the number of nodes in the network.

2. $\det(FIM)$ versus the number of nodes in the network.
3. $\lambda_{min}(FIM)$ versus the number of nodes in the network.
4. Average mean square error in the source location estimate versus the standard deviation of the gaussian term in the log-normal shadowing.

We perform all the simulations with the following simulation parameters.

1. The signal strength at unit distance from the source $A = 1$.
2. The path loss co-efficient $\beta = 2$.
3. Number of source locations selected from the uniform distribution=100.
4. Radius of the sphere in which the source locations were uniformly distributed = 0.1.
5. Radius of the outer sphere on which the sensors were placed = 1.
6. The localization error for each of the 100 source locations is averaged over 10,000 iterations.

For gaussian noise, the Geometric Dilution of Precision is related to the Cramer Rao Lower Bound (CRLB) through the following relation (2.100) [42], [43], [44].

$$GDOP = \frac{\sqrt{CRB}}{\sigma}. \quad (2.100)$$

where $CRB = \text{trace}(FIM^{-1})$ is the corresponding Cramer Rao bound obtained from the Fisher Information Matrix (FIM) and σ is the standard deviation of the gaussian term in the log-normal shadowing. Given that the distribution of the source location

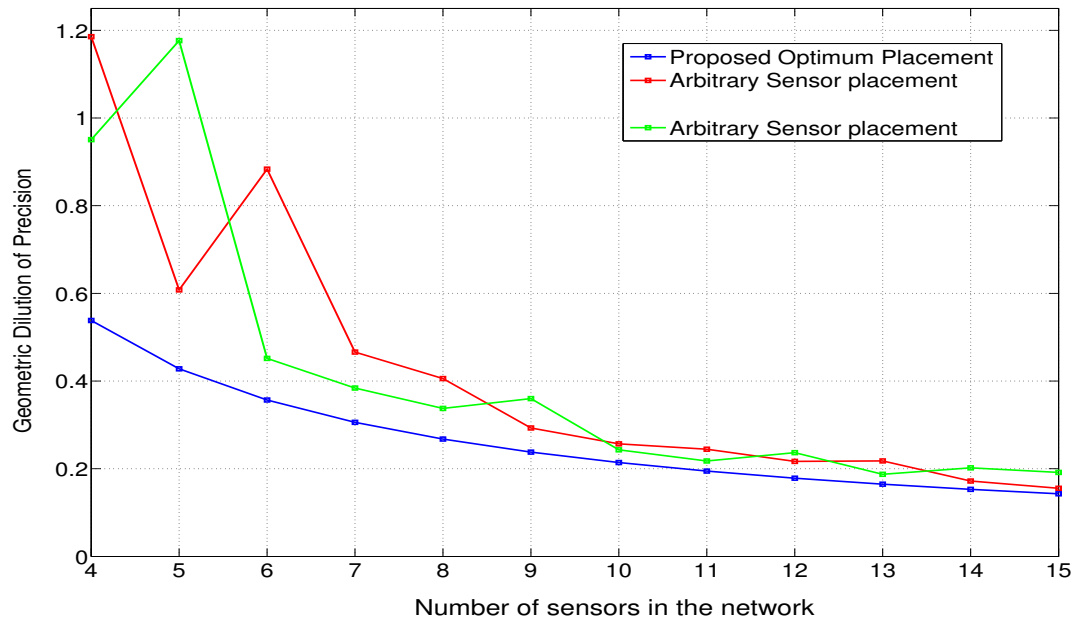


Figure 2.2: Plot of GDOP Versus Number of sensors in the network.

is known, we define the GDOP to be

$$GDOP = \frac{\sqrt{(average(trace(FIM^{-1})))}}{\sigma}. \quad (2.101)$$

Figure 2.2 compares the GDOP for the proposed optimum sensor placement with that of the random placements in the case where the source location has a uniform distribution within a sphere. Clearly, the proposed optimum sensor placement shows better performance when compared to non-coplanar random sensor placement.

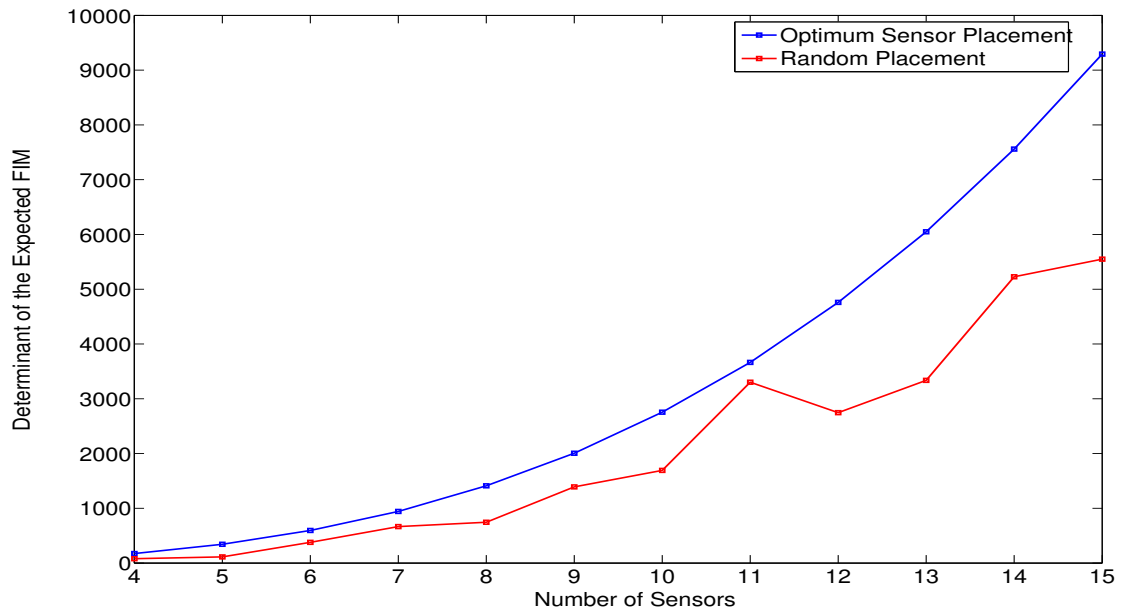


Figure 2.3: Plot of determinant of FIM Versus Number of sensors in the network.

Figure. 2.3 shows that the $\det(FIM)$ is lower for the proposed optimum sensor placement in contrast to the $\det(FIM)$ for random sensor placement.

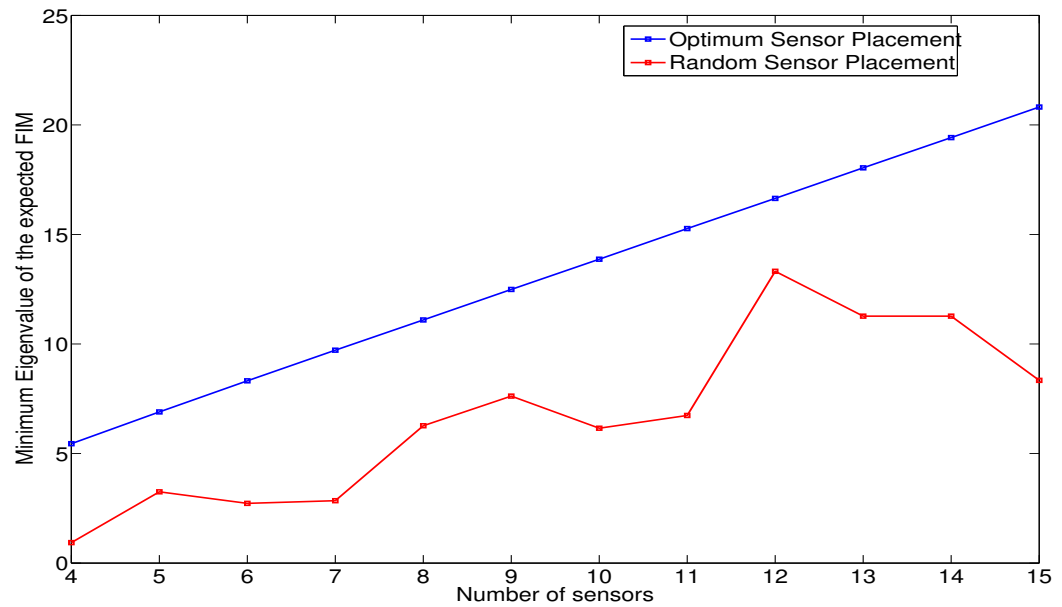


Figure 2.4: Plot of Minimum Eigenvalue of FIM Versus Number of sensors in the network.

Figure. 2.4 shows that the $\lambda_{min}(FIM)$ is larger for the proposed optimum sensor placement in contrast to the $\lambda_{min}(FIM)$ for random sensor placement.

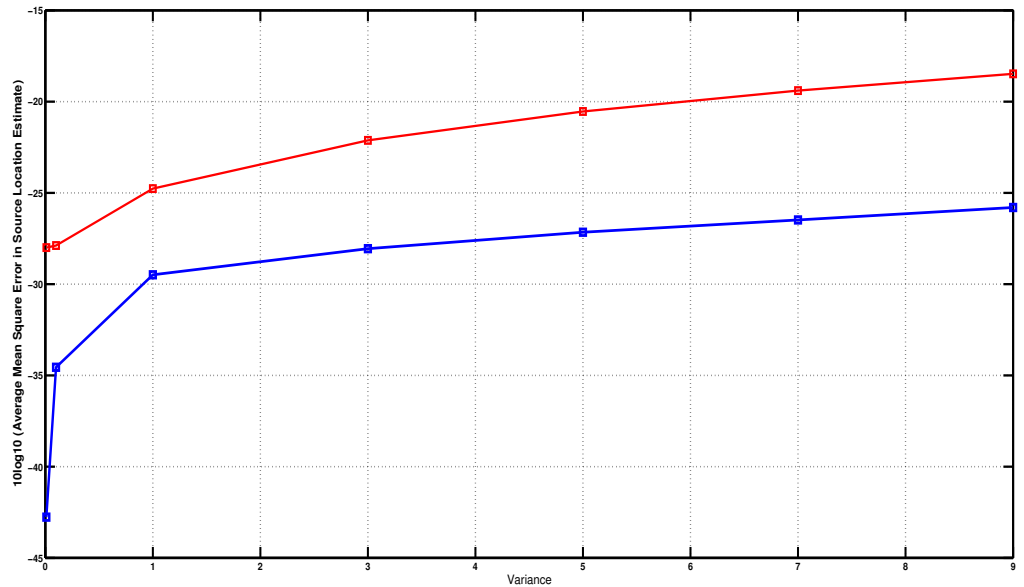


Figure 2.5: Plot of $10\log_{10}(\text{Average Normalized Mean square error in the source location})$ Versus Signal to Noise Ratio (dB). Red dotted line represents the performance of the random placement. Blue line represents the performance of the proposed optimum sensor placement

Figure. 2.5 compares the average mean square error performance of the optimum sensor placement to the performance of the random placement. The variance of the log-normal shadowing varies between 0.01 and 9 in steps of 2. We use the improved Linear Least Squares Estimation method proposed in [45]. The simulations were performed using MATLAB.

2.6 Conclusion

This chapter presented a class of optimum solutions to the sensor placement problem to localize a hazardous source whose location has a radially symmetric dis-

tribution in a $N \geq 2$ dimensional sphere under the constraint that the sensors are at a particular distance from the source. The optimality criterion was the maximization of the smallest eigenvalue or the determinant of the underlying FIM or the minimization of the trace of the inverse of the expectation of the FIM. Through rigorous mathematical analysis we have shown that the optimality is achieved if and only if the expectation of the corresponding FIM is a scaled identity. The simulation results validate the theory developed.

CHAPTER 3

A DISTRIBUTED CONTROL LAW FOR OPTIMUM SENSOR PLACEMENT FOR SOURCE LOCALIZATION

The objective of this chapter is to design a nonlinear distributed control law that guides the motion a group of sensors to achieve a configuration that permits them to optimally localize a hazardous source they must keep a prescribed distance from. Chapter 2 shows that such a configuration involves the sensors being placed in an equispaced manner on a prescribed circle. The proposed nonlinear control law assumes that each sensor resides and moves on the prescribed circle while avoiding collisions, by accessing only the states of its two immediate clockwise and counter-clockwise neighbors.

3.1 Introduction

In the wake of a growing need for autonomous sensor networks in search, localization and rescue operations, the concept of Self Organizing Networks (SON) has emerged as an energy efficient solution. The goal of this work is to develop a nonlinear distributed control law with the least communication overhead that guides the sensors to organize themselves to form the optimum sensor placement pattern required for minimum mean square error in localizing a source.

Sensor networks must reorganize for various reasons including collecting multiple measurements for a better perspective on the communication environment, tracking a mobile source, repairing the network with dead nodes or simply saving energy

[46]- [51]. The interest here is to organize a group of sensors in a manner that permits them to optimally localize a source.

The specific setting considered in this chapter assumes that the source being localized is hazardous and the sensors must maintain a safe distance from the source. The sensors can measure the signal strength from the source and use that to localize the source that emits the signal. The signal strength itself experiences log normal shadowing, [18]. Optimality involves the maximization of an underlying Fisher Information Matrix. As explained in Section 3.2, earlier work in [28] and [29], under the above assumptions on the source location, shows that optimal sensor configuration involves sensors that lie in an equispaced manner on a specific circle.

The goal is thus to formulate a nonlinear distributed control law that permits the sensors to achieve such a configuration with minimum communication overhead, in the tradition of [52]-[55]. Specifically, we assume that the sensors lie on the prescribed circle and can measure the location of their immediate clock and counterclockwise neighbors. Using this information alone they achieve the desired configuration, while avoiding collisions.

3.2 The Cost Function

Consider a source at $y \in \mathbb{R}^2$ at the origin or uniformly distributed in a disk of radius r_1 , centered at the origin. A group of N sensors must collectively localize the source using received signal strength (RSS). The i -th sensor located at $x_i \in \mathbb{R}^2$ measures the RSS s_i that undergoes log-normal shadowing [18], i.e. for mutually

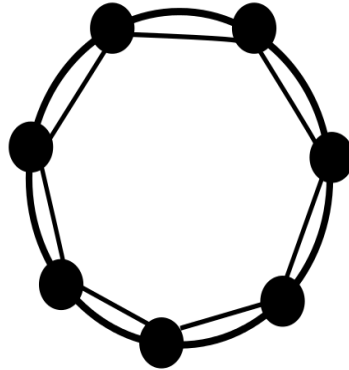


Figure 3.1: The underlying communication graph

uncorrelated $w_i \sim N(0, \sigma^2)$, obeys

$$\ln s_i = \ln A + \beta \ln \|x_i - y\| + w_i, \quad (3.1)$$

with known A and β . As the source is hazardous the sensors must be placed at a safe distance. Specifically, they must obey:

$$\|x_i\| \geq r \quad (3.2)$$

where in the setting of Chapter 2, $r > r_1$.

Based on the calculations presented in Chapter 1, the Fisher Information Matrix (FIM) associated with the estimation of the nonrandom source location y is given

by

$$F = \sum_{i=1}^N \frac{(x_i - y)(x_i - y)^T}{\|x_i - y\|^4} \quad (3.3)$$

For random y as in [29], the corresponding matrix is $E(F)$, [25].

As is standard, one criterion for optimality is the optimization of the FIM or $E(F)$ in a suitable sense. Chapter 2 shows that in both cases optimality is obtained if the x_i are equispaced on the circle of radius r centered at the origin.

Without loss of generality we assume that $r = 1$, and that all sensors reside and move on the unit circle. Thus the location of the i -th sensor can be parameterized as

$$x_i = \begin{bmatrix} \cos \theta_i \\ \sin \theta_i \end{bmatrix}. \quad (3.4)$$

Call

$$\theta = [\theta_1, \dots, \theta_N]^T. \quad (3.5)$$

By exchanging θ_i the sensors must achieve the following configuration: For arbitray $\theta_1^* \in [0, 2\pi]$ there should hold

$$\theta_i = \theta_i^* = \theta_1^* + \frac{2\pi(i-1)}{N}, \quad i \in \{1, \dots, N\}. \quad (3.6)$$

In the sequel, assume that

$$0 \leq \theta_1(0) < \theta_2(0) < \dots < \theta_N(0) < 2\pi. \quad (3.7)$$

For notational simplicity, assume also that

$$\theta_0 = \theta_N \text{ and } \theta_{N+1} = \theta_1. \quad (3.8)$$

The optimum sensor placement for source localization is the same as the optimum sensor placement for source monitoring. Thus the proposed algorithm uses the minimum eigenvalue of the FIM in the source monitoring case for the design of the appropriate cost function for the non-linear algorithm.

In the case of source monitoring, it is assumed that the source location has already been estimated and that the sensors are continuously estimating the location of the source from a safe distance. Since the location of the source is known, without loss of generality, it can be assumed that the source is at the origin. Thus the FIM is of the form

$$F = \sum_{i=1}^N x_i x_i^T \quad (3.9)$$

To evaluate the minimum eigenvalue of F consider a unit norm vector of the form $\eta = (\cos \alpha \quad \sin \alpha)^T$. The minimum eigenvalue of F is given by minimizing $\eta^T F \eta$ over α . Consider

$$\eta^T F \eta = \sum_{j=1}^K \eta^T x_j x_j^T \eta. \quad (3.10)$$

Since $\|\eta\|_2 = 1$ we can choose $\eta = \begin{pmatrix} \cos \alpha & \sin \alpha \end{pmatrix}^T$. Thus

$$\begin{aligned} \eta^T x_i x_i^T \eta &= \begin{bmatrix} \cos \alpha & \sin \alpha \end{bmatrix} \begin{bmatrix} \cos^2 \theta_i & \cos \theta_i \sin \theta_i \\ \cos \theta_i \sin \theta_i & \sin^2 \theta_i \end{bmatrix} \begin{bmatrix} \cos \alpha \\ \sin \alpha \end{bmatrix} \\ &= (\cos(\alpha) \cos(\theta_i) + \sin(\alpha) \sin(\theta_i))^2 \\ &= \cos^2(\alpha - \theta_i) \end{aligned}$$

After simplification, (3.10) becomes

$$\eta^T F \eta = \sum_{j=1}^N \cos^2(\alpha - \theta_{i_j}) = \frac{N}{2} + \frac{1}{2} \sum_{j=1}^N \cos(2(\alpha - \theta_{i_j})). \quad (3.11)$$

Define

$$J(\alpha) = \frac{N}{2} + \frac{1}{2} \sum_{j=1}^N \cos(2(\alpha - \theta_{i_j})). \quad (3.12)$$

Then the minimum or maximum eigenvalue of F is achieved when

$$J'(\alpha) = -2 \sum_{j=1}^N \sin(2(\alpha - \theta_{i_j})) = 0. \quad (3.13)$$

We also have

$$J''(\alpha) = -4 \sum_{j=1}^N \cos(2(\alpha - \theta_{i_j})) \geq 0 \quad (3.14)$$

at the minimum eigenvalue and the inequality is reversed at the maximum eigenvalue.

From (3.13),

$$\sin(2\alpha) \sum_{i=1}^N \cos(2\theta_i) = \cos(2\alpha) \sum_{i=1}^N \sin(2\theta_i) \quad (3.15)$$

The minimizing α is given by

$$\tan(2\alpha) = \frac{\sum_{i=1}^N \sin(2\theta_i)}{\sum_{i=1}^N \cos(2\theta_i)} \quad (3.16)$$

Thus when $(\sum_{j=1}^K \sin(2\theta_{i_j}))^2 + (\sum_{j=1}^K \cos(2\theta_{i_j}))^2 \neq 0$, from (3.13), the minimizing α satisfies

$$\cos(2\alpha) = \frac{\sum_{j=1}^N \cos(2\theta_j)}{\sqrt{(\sum_{j=1}^K \sin(2\theta_{i_j}))^2 + (\sum_{j=1}^N \cos(2\theta_j))^2}} \quad (3.17)$$

and

$$\sin(2\alpha) = \frac{\sum_{j=1}^N \sin(2\theta_j)}{\sqrt{(\sum_{j=1}^N \sin(2\theta_j))^2 + (\sum_{j=1}^N \cos(2\theta_j))^2}}. \quad (3.18)$$

From expansion of (3.12), we get

$$J(\alpha) = \frac{N}{2} + \frac{1}{2} \sum_{j=1}^N \cos(2\alpha) \cos(2\theta_j) + \frac{1}{2} \sum_{j=1}^N \sin(2\alpha) \sin(2\theta_j). \quad (3.19)$$

Substituting the minimizing α in (3.19) we have

$$J_{min} = \frac{N}{2} + \frac{1}{2} \frac{\sum_{j=1}^N \sum_{i=1}^N (\cos(2\theta_i) \cos(2\theta_j) + \sin(2\theta_i) \sin(2\theta_j))}{\sqrt{(\sum_{i=1}^N \sin(2\theta_i))^2 + (\sum_{i=1}^N \cos(2\theta_j))^2}}.$$

Define

$$\mathcal{D}^2 = \left(\sum_{I=1}^N \sin 2\theta_i \right)^2 + \left(\sum_{I=1}^N \cos 2\theta_i \right)^2. \quad (3.20)$$

Then

$$\begin{aligned}
\mathcal{D}^2 &= \sum_{i=1}^N \left(\sin^2 2\theta_i + \cos^2 2\theta_i \right) \\
&+ \sum_{i=1}^N \sum_{j=1, j \neq i}^N \cos 2\theta_i \cos 2\theta_j + \sum_{i=1}^N \sum_{j=1, j \neq i}^N \sin 2\theta_i \sin 2\theta_j \\
&= N + 2 \sum_{i=1}^N \sum_{j=i+1}^N \cos 2(\theta_i - \theta_j)
\end{aligned}$$

Similarly, we define

$$\mathcal{N} = \sum_{i=1}^N \sum_{j=1}^N \cos(2\theta_i) \cos(2\theta_j) + \sum_{i=1}^N \sum_{j=1}^N \sin(2\theta_i) \sin(2\theta_j). \quad (3.21)$$

It can be expanded as

$$\begin{aligned}
\mathcal{N} &= \sum_{i=1}^N (\sin^2 2\theta_i + \cos^2 2\theta_i) + \sum_{i=1}^N \sum_{j=1, j \neq i}^N \cos 2\theta_i \cos 2\theta_j \\
&+ \sum_{i=1}^N \sum_{j=1, j \neq i}^N \sin 2\theta_i \sin 2\theta_j \\
&= N + 2 \sum_{i=1}^N \sum_{j=i+1}^N \cos 2(\theta_i - \theta_j)
\end{aligned}$$

From (3.14), we know that $\mathcal{N} < 0$. Thus J_{min} can be expressed as

$$J_{min} = \frac{N}{2} - \frac{1}{2} \frac{|\mathcal{N}|}{\mathcal{D}}. \quad (3.22)$$

i.e.

$$J(\alpha_{min}) = \frac{N}{2} - \frac{1}{2} \sqrt{\frac{N}{2} + \sum_{i=1}^N \sum_{j=i+1}^K \cos 2(\theta_i - \theta_j)}. \quad (3.23)$$

Thus the optimum sensor placement is given by the set of angles $\{\theta_0, \theta_1, \dots, \theta_{N-1}\}$ that solve the following optimization problem.

$$C_1 = \min_{\theta_0, \dots, \theta_{N-1}} \sum_{i=1}^N \sum_{j=i+1}^N \cos 2(\theta_i - \theta_j). \quad (3.24)$$

A possible candidate control law could of course be the gradient descent minimization of $C_1(\theta)$, i.e.

$$\dot{\theta}(t) = - \left. \frac{\partial C_1(\theta)}{\partial \theta} \right|_{\theta=\theta(t)} \quad (3.25)$$

The difficulty is that this law requires each sensor to know every other sensors angle thus violating the goal of minimizing the communication overhead.

An alternative cost function could be:

$$C_2(\theta) = \sum_{i=1}^N (\cos 2(\theta_{i+1} - \theta_i) + \cos 2(\theta_{i-1} - \theta_i)). \quad (3.26)$$

The resulting gradient descent control law would be:

$$\dot{\theta}_i(t) = 2 \sin(2(\theta_i(t) - \theta_{i+1}(t))) + 2 \sin(2(\theta_i(t) - \theta_{i-1}(t))). \quad (3.27)$$

There are several difficulties with this law as well. Suppose $\theta_2(0) - \theta_1(0)$ is small but $\theta_3(0) - \theta_2(0)$ is not. Then $\dot{\theta}_2(0)$ will decrease and θ_2 and θ_1 will cross, failing to meet

our collision avoidance goal. Evidently, the problem rests on the fact that around zero $\sin(\cdot)$ is a decreasing function.

For example in the case of a network with 4 sensor nodes, consider the initial example network topology shown in Figure. 3.2. The gradient descent algorithm produces the topology in Figure 3.3 which corresponds to the stationary point $\{0, \frac{\pi}{2}, \frac{3\pi}{2}, 2\pi\}$ leading to a collision between the sensor nodes at angular positions 0 and 2π . Thus this algorithm can evidently converge to a steady state configuration that does not conform to (3.6).

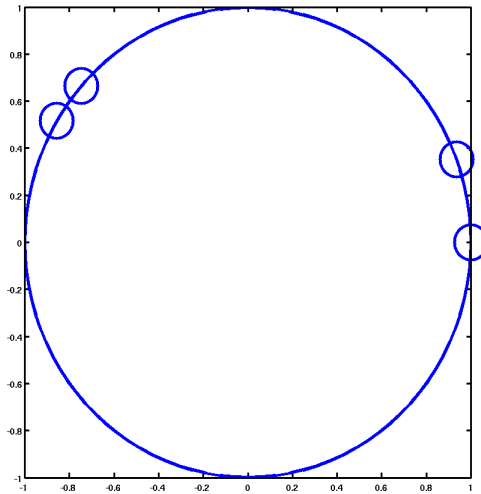


Figure 3.2: Initial Network Topology

Instead consider an alternative law that avoids these difficulties. The rest of

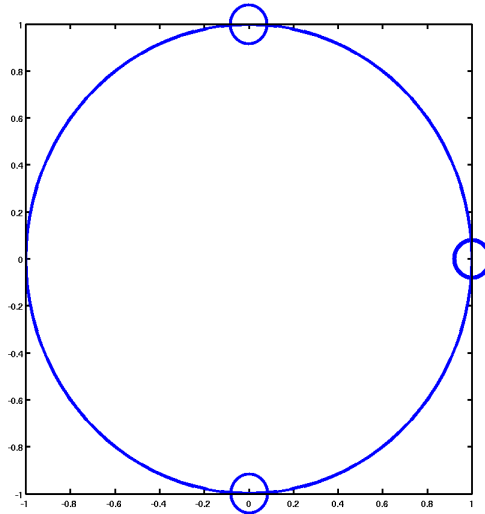


Figure 3.3: Final Network Topology

this chapter uses the following definitions

$$\text{sinc}(x) = \frac{\sin x}{x}, \quad (3.28)$$

and

$$f(\theta) = \begin{cases} \text{sinc}(\theta \bmod 2\pi) & \text{if } (|\theta| \bmod 2\pi) \leq \pi \\ \text{sinc}(2\pi - (\theta \bmod 2\pi)) & \text{else} \end{cases} \quad (3.29)$$

In particular if $\theta \in [0, \pi]$ then $f(\theta) = \text{sinc}(\theta)$. If on the other hand, $\theta \in (\pi, 2\pi)$ then $f(\theta) = \text{sinc}(2\pi - \theta)$. Observe that $f(\cdot)$ is an even function.

Then the algorithm is as follows: For all $i \in \{1, \dots, N\}$

$$\dot{\theta}_i(t) = f(\theta_i(t) - \theta_{i-1}(t)) - f(\theta_i(t) - \theta_{i+1}(t)). \quad (3.30)$$

Clearly it meets our requirement that each sensor executes its control law using only communication from two other sensors. It will be shown in the sections that follow that under (3.7) the clockwise and counterclockwise neighbors of a given sensor do not change. Thus this law will in fact only require communication from the two immediate neighbors on either side of a sensor.

3.3 Analysis

This section presents the discussion and analysis on the algorithm represented by (3.30). Whenever, $|\theta_i - \theta_{i-1}|$ and $|\theta_i - \theta_{i+1}|$ are less than or equal to π the first bullet of (3.29) applies. The first term in (3.30) tends to increase θ_i , while the second term decreases it. As for $|\alpha| \leq \pi$, $\text{sinc}(\alpha)$ is decreasing in $|\alpha|$, the i -th sensor moves away from the neighbor it is closer to.

Now suppose (3.7) holds and for some i , $|\theta_i - \theta_{i-1}| > \pi$. Because of (3.7) unless sensors cross this must mean that for all $j \neq i$, $|\theta_j - \theta_{j-1}| \leq \pi$. Also observe that

$$\text{sinc}(2\pi - (\theta_i - \theta_{i-1})) > \text{sinc}(\theta_i - \theta_{i-1}). \quad (3.31)$$

Effectively, the second bullet of (3.29) ensures that the contribution of θ_{i-1} to the motion of θ_i is governed by the smaller of the two possible angular difference between the angles of x_i and x_{i-1} . And again the i -th sensor moves away from the neighbor it is closer to. For precisely the same reason, and continuity of motion, under (3.7) sensors cannot cross, and we have the following Theorem.

Theorem 3.3.1 *Consider (3.30) under (3.29) and (3.7) the following holds for all*

$t \geq 0$:

$$\theta_1(t) < \theta_2(t) < \cdots < \theta_N(t). \quad (3.32)$$

Thus the neighbors of a sensor never change. Further for all $i \neq j$

$$0 < |\theta_i(t) - \theta_j(t)| < 2\pi. \quad (3.33)$$

The following theorem shows that under (3.7), all stationary points of (3.30) obey (3.6).

Theorem 3.3.2 *Consider (3.30) for $N > 2$, under (3.29) and (3.7). Then $\dot{\theta}(t) = 0$ iff for some θ_1^* each $\theta_i(t)$ equals the corresponding θ_i given in (3.6).*

Proof: First of all suppose each $\theta_i(t)$ equals the corresponding θ_i given in (3.6).

Then for all $i \in \{2, \dots, N\}$,

$$\theta_i - \theta_{i-1} = \frac{2\pi}{N} < \pi, \quad (3.34)$$

and

$$f(\theta_i - \theta_{i-1}) = \text{sinc}\left(\frac{2\pi}{N}\right). \quad (3.35)$$

Thus, for all $i \in \{2, \dots, N-1\}$, $\dot{\theta}_i(t) = 0$. That $\dot{\theta}_1(t)$ and $\dot{\theta}_N(t)$ are also zero follows

from the fact that as

$$\frac{2(N-1)\pi}{N} > \pi \quad (3.36)$$

$$\begin{aligned}
f(\theta_1 - \theta_N) &= f\left(\frac{2(N-1)\pi}{N}\right) \\
&= \text{sinc}\left(\frac{2\pi}{N}\right).
\end{aligned}$$

Suppose now $\dot{\theta}(t) = 0$. Then for all i

$$f(\theta_i - \theta_{i-1}) = f(\theta_i - \theta_{i+1}). \quad (3.37)$$

Under (3.7) from Theorem 3.3.1), (3.32) and (3.33) hold. Because of (3.33)

$$|\theta_i - \theta_{i-1}| > \pi \quad (3.38)$$

can hold for at most one i , and for this i

$$f(\theta_i - \theta_{i-1}) = \text{sinc}(2\pi - (\theta_i - \theta_{i-1})). \quad (3.39)$$

Observe that if for some $0 \leq \alpha \leq \beta < 2\pi$, $\text{sinc}(\alpha) = \text{sinc}(\beta)$ then either $\alpha = \beta$ or $\pi < \alpha < \beta < 2\pi$. In the latter case $0 < 2\pi - \beta < 2\pi - \alpha < \pi$. or

$$\alpha = 2\pi - \beta \quad (3.40)$$

Thus because of (3.37) for each i either

$$\theta_i - \theta_{i-1} = \theta_{i+1} - \theta_i \quad (3.41)$$

or

$$\theta_i - \theta_{i-1} = 2\pi - (\theta_{i+1} - \theta_i). \quad (3.42)$$

Further (3.42) can happen for at most one i . Suppose now (3.42) fails to hold for any i . Then for all i

$$|\theta_i - \theta_{i-1}| \leq \pi. \quad (3.43)$$

In particular this means that

$$\theta_N \leq \theta_1 + \pi. \quad (3.44)$$

Thus, as (3.41) holds for all i ,

$$\theta_i - \theta_{i-1} = \frac{\theta_N - \theta_1}{N - 1}, \quad (3.45)$$

resulting in

$$\theta_N - \theta_1 = \frac{\theta_N - \theta_1}{N - 1}$$

establishing a contradiction as $N > 2$. Thus there is precisely one i , namely $i = 1$ for which (3.38) holds. From (3.45) one must have:

$$2\pi - (\theta_N - \theta_1) = \frac{\theta_N - \theta_1}{N - 1}. \quad (3.46)$$

Thus

$$\theta_N - \theta_1 = \frac{2\pi(N - 1)}{N}. \quad (3.47)$$

Because of (3.45) for all $i \in \{2, \dots, N\}$

$$\theta_i - \theta_{i-1} = \frac{2\pi}{N} \quad (3.48)$$

proving the result.

3.4 Convergence Analysis

This section focuses on the convergence of the proposed algorithm to a stationary point of the form in (3.48). Observe under (3.7), (3.32) and (3.33) holds for all t . Now consider the function

$$V(\theta) = - \sum_{i=1}^N W(\theta_i, \theta_{i+1}) \quad (3.49)$$

where

$$W(\theta_i, \theta_{i+1}) = \begin{cases} \int_0^{\theta_{i+1}-\theta_i} \text{sinc}(z) dz & \text{if } |\theta_{i+1} - \theta_i| \leq \pi \\ \int_{2\pi-(\theta_{i+1}-\theta_i)}^0 \text{sinc}(z) dz & \text{else} \end{cases} . \quad (3.50)$$

When $|\theta_{i+1} - \theta_i| \leq \pi$ along the trajectories of (3.30)

$$\dot{W}(\theta_i(t), \theta_{i+1}(t)) = \left(\dot{\theta}_{i+1}(t) - \dot{\theta}_i(t) \right) \text{sinc}(\theta_{i+1}(t) - \theta_i(t)) \quad (3.51)$$

$$= \left(\dot{\theta}_{i+1}(t) - \dot{\theta}_i(t) \right) f(\theta_{i+1}(t) - \theta_i(t)). \quad (3.52)$$

Otherwise

$$\dot{W}(\theta_i(t), \theta_{i+1}(t)) = \left(\dot{\theta}_{i+1}(t) - \dot{\theta}_i(t) \right) \text{sinc}(2\pi - (\theta_{i+1}(t) - \theta_i(t))) \quad (3.53)$$

$$= \left(\dot{\theta}_{i+1}(t) - \dot{\theta}_i(t) \right) f(\theta_{i+1}(t) - \theta_i(t)). \quad (3.54)$$

Because of (3.33) $V(\theta)$ is bounded from above and below. Further as $f(\cdot)$ is an even function, and (3.8) holds

$$-\dot{V}(\theta(t)) = \sum_{i=1}^N \dot{W}(\theta_i(t), \theta_{i+1}(t)) \quad (3.55)$$

$$= \sum_{i=1}^N \left(\dot{\theta}_{i+1}(t) - \dot{\theta}_i(t) \right) f(\theta_{i+1}(t) - \theta_i(t)) \quad (3.56)$$

$$= \sum_{i=0}^{N-1} \dot{\theta}_i(t) f(\theta_i(t) - \theta_{i-1}(t)) \quad (3.57)$$

$$- \sum_{i=1}^N \dot{\theta}_i(t) f(\theta_i(t) - \theta_{i+1}(t)) \quad (3.58)$$

$$= \sum_{i=2}^{N-1} \dot{\theta}_i(t) (f(\theta_i(t) - \theta_{i-1}(t)) - f(\theta_i(t) - \theta_{i+1}(t))) \quad (3.59)$$

$$+ \dot{\theta}_N(t) (f(\theta_N(t) - \theta_{N-1}(t)) - f(\theta_N(t) - \theta_1(t))) \quad (3.60)$$

$$+ \dot{\theta}_1(t) (f(\theta_1(t) - \theta_N(t)) - f(\theta_1(t) - \theta_2(t))) \quad (3.61)$$

$$= \sum_{i=2}^{N-1} \dot{\theta}_i^2(t) + \dot{\theta}_N^2(t) + \dot{\theta}_1^2(t) \quad (3.62)$$

$$= \|\dot{\theta}(t)\|^2. \quad (3.63)$$

Thus along the trajectories of (3.30) one has

$$\dot{V}(\theta(t)) = -\|\dot{\theta}(t)\|^2. \quad (3.64)$$

Thus from Lasalle's invariance principle $\theta(t)$ converges uniformly asymptotically to a trajectory where $\dot{\theta} \equiv 0$. In view of Theorem 3.3.2 we thus have the following Theorem.

Theorem 3.4.1 *Under the conditions of Theorem 3.3.2, $\theta(t)$ converges uniformly to a point obeying (3.6).*

Algorithm 3.1 The Distributed Control Law in Discrete Time

- 1: N is the number of sensors in the network.
 - 2: k represents the time instant or the iteration counter.
 - 3: Θ is the vector of size N holding the angular position of the sensors.
 - 4: $F(\Theta)$ is a vector of size N whose i -th element is given by $f(\theta_i - \theta_{i-1}) - f(\theta_i - \theta_{i+1})$ where f is defined in (3.29)
 - 5: Initialize $\Theta[0] = 2\pi \cdot \text{rand}(N, 1)$
 - 6: Set the step size to be $\mu <$ minimum angular separation between any two neighbors.
 - 7: $k = 0$
 - 8: **while** ($\|F(\Theta)\|_2 < 10^{-7}$ or $k < 10^6$) **do**
 - 9: **for** ($i = 1, i \leq N, i = i + 1$) **do**
 - 10: $\theta_i = \theta_i + \mu f(\theta_i - \theta_{i-1}) - f(\theta_i - \theta_{i+1})$
 - 11: $k = k + 1$
 - 12: **end for**
 - 13: **end while**
 - 14: Plot results.
-

3.5 Simulation Results

Algorithm 3.1 presents the algorithm with the discrete time system that was used for the simulations.

3.5.1 Simulation Scenario 1: 3 Node Network

Figure. 3.4 represents the initial network topology with angular positions at $\{0; 1.1801; 1.5191; \}$ (all in radians). The step size μ was chosen to be 10^{-3} which is smaller than the minimum angular separation. Figure. 3.5 presents the final network topology produced by the algorithm with angular separation between neighboring nodes given by $\frac{2\pi}{3}$.

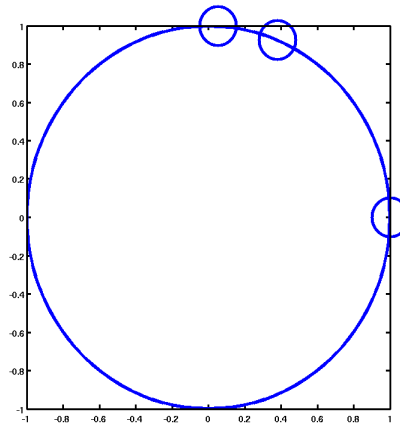


Figure 3.4: Initial Network Topology

3.5.2 Simulation Scenario 2: 8 Node Network

The algorithm is initialized with sensor angles $\{0, 0.2304, 0.4536, 1.0996, 1.8434, 3.2385, 5.5435, 5.6320\}$, (all in radians) presented in Figure. 3.6 . The minimum sensor separation is 0.0885. As shown in Figure. 3.6, sensors 7 and 8 have this minimum

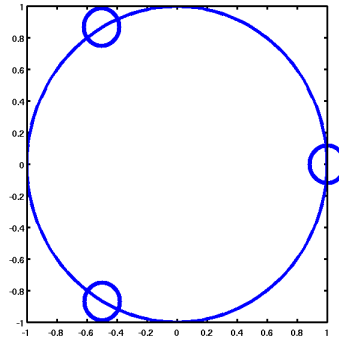


Figure 3.5: Final Network Topology

separation. The step size μ was chosen to be $10^{-3} < 0.0885$. The algorithm converges to the final topology shown in Figure. 3.7 with uniform angular separation of $\frac{2\pi}{8}$ between every pair of neighboring sensors. The trajectory of the sensors with respect to time in Figure 3.8 shows that there are no sensor cross-overs or collisions.

3.6 Conclusions

This chapter presents the design a distributed control law that guides the motion of the sensors on the circumference of a circle. The speciality of this control law comes from the fact that this produces the least communication overhead since each sensor communicates with only two neighboring nodes (one of which is a counter-clockwise neighbor and the other is a clockwise neighbor). The algorithm is globally convergent and avoids inter-sensor collisions. The simulation results that demonstrate the performance of the algorithm.

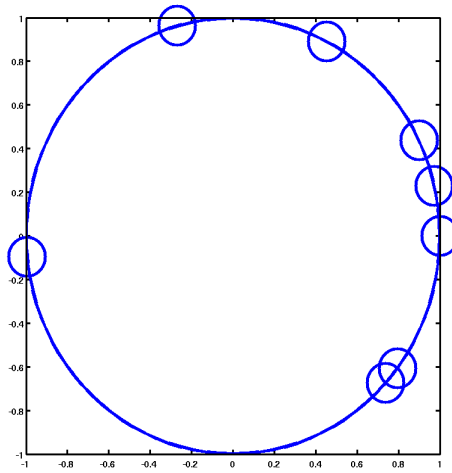


Figure 3.6: Initial Network Topology

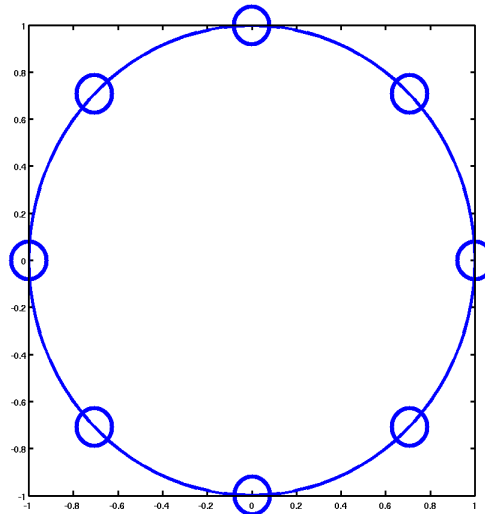


Figure 3.7: Final Network Topology

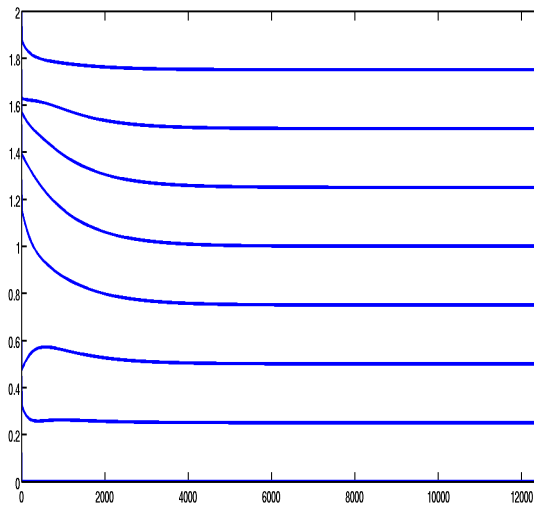


Figure 3.8: Trajectory of the sensors. The X-axis indicates the time in terms of the iterations and the Y-axis represents the angular position of the sensors on the circle (scaled by π)

CHAPTER 4

OPTIMUM SENSOR PLACEMENT FOR ENERGY EFFICIENT SOURCE LOCALIZATION USING LEAST NUMBER OF ACTIVE SENSORS

This chapter deals with the problem of designing sensing schemes to optimize the worst-case estimation performance when only a subset of sensors are operational in sensor networks. Consider a set of N sensors which are used to estimate an M -dimensional signal, where $N \geq M$. In this problem, only K sensors out of these N sensors are allowed to operate at a single time instant. This can happen in several applications scenarios in sensor networks. For example, to maximize the lifetime of a sensor network, at any single time instant, only K sensors are turned on to monitor the M -dimensional signal. If we assume each time these K sensors are uniformly selected from the $\binom{N}{K}$ possible subsets, so on average the lifetime of the sensor network is extended by a factor of $\frac{N}{K}$.

As another application example, in hostile environments such as battlefields, it is very common that only a limited number of sensors are able to survive and operate as designed. In this application, we assume that K sensors out of the N sensors are able to survive the hostile environment and are functional in sensing the M -dimensional signal. While we only have a limited sensing resources at hand, we however do not want to sacrifice the estimation performance from a limited number of observations. It is thus helpful to maximize the worst-case performance of the sensing system, regardless of what set of sensors are used or are able to survive. In this chapter, we consider the problem of designing optimal sensing in two contexts.

The first is described in Section 4.1 and the second is described in Section 4.2.

4.1 Sensing Applications: Signal Estimation

With $y \in \mathbb{R}^M$ representing the signal, consider a sensing matrix $A \in \mathbb{R}^{M \times N}$. Each of the N sensors generates a real observation represented by an inner product between y and a column of A . Let $KS \subseteq \{1, 2, \dots, N\}$, with cardinality $|KS| = K$, be the subset of sensors that are active at a given time. The measurement matrix of the active sensors is then $A_{KS} \in \mathbb{R}^{M \times K}$ consisting of the K columns of A indexed by KS . With noise w , the measurement $z \in \mathbb{R}^K$ is

$$z = A_{KS}^T y + w, \quad (4.1)$$

Suppose the singular values of A_{KS} are σ_i . Then as long as A_{KS} has full row rank, the estimation error satisfies

$$\|\hat{y} - y\|_2 = \|(A_{KS} A_{KS}^T)^{-1} A_{KS}(w)\|_2 \leq \frac{\|w\|_2}{\sigma_{min}}.$$

To optimize the worst-case performance, we must design A to maximize the smallest singular value among all the $\binom{N}{K}$ possible submatrices A_{KS} . We assume that each column of A has unit ℓ_2 norm. When $M = 2$, this is equivalent to minimizing the maximum condition number among all $\binom{N}{K}$ submatrices A_{KS} . In this chapter, we consider the case when $M = 2$ as this is the same as the 2-D source monitoring problem.

4.2 Source Monitoring

As in chapter 2 and 3, suppose we use RSS measurements to get distance estimates. Without loss of generality, we can assume that $y = 0$ and that the sensors need to be placed at a safe distance $r_2 = 1$. Also assume that $x_i \in \mathbb{R}^2$ represent the sensor locations. Recall that distances from three non-collinear sources are necessary to localize, [22]. This scenario also applies to the case where only three sensors survive hostilities.

Suppose the set indices of sensors that are active is denoted by KS and $K = |KS|$. Then we are interested in the design of optimum sensor placement such that we achieve the best worst case performance i.e. the best performance when only 3 sensors are active. We would like to maximize the minimum eigenvalue of the underlying FIM in (4.2) overall possible active sensors. In view of the fact that the *minimum K needed for source monitoring is three*, in the rest of this chapter we consider $K = 3$.

$$F_{KS} = \sum_{i \in KS} x_i x_i^T, \quad (4.2)$$

With A_{KS} having columns x_i , $i \in KS$, we have $F_{KS} = A_{KS} A_{KS}^T$. Since $\|x_i\| = 1 \forall i \in \{1, 2, \dots, N\}$, the trace of the underlying FIM given by F_{KS} in (4.2) is a constant. Also as $F_{KS} \in \mathbb{R}^{2 \times 2}$, maximizing minimum eigenvalue of F_{KS} minimizes the maximum eigenvalue of F_{KS} thereby minimizing the condition number. However, since we are interested in the best worst case performance, we would like to minimize the maximum condition number over all possible KS . Thus the formal problem considered in this chapter is as follows.

Problem: Minimize the maximum condition number of F_{KS} among all KS with cardinality 3 i.e.

$$\min_{A \in \mathbb{R}^{M \times N} \text{ with unit-normed columns}} \left\{ \max_{KS \subseteq \{1, 2, \dots, N\}} \frac{\lambda_{\max}(\tilde{A}_{KS})}{\lambda_{\min}(\tilde{A}_{KS})} \right\}. \quad (4.3)$$

Suppose $x_i = (\cos \theta_i, \sin \theta_i)^T$ then following similar calculations presented in Section 3.2, leads us to the equivalent problem described below.

Problem:

$$\min_{\theta_1, \dots, \theta_N} \max_{KS = \{i_1, i_2, \dots, i_K\}} \sum_{j=1}^K \sum_{l=j+1}^K \cos 2(\theta_{i_l} - \theta_{i_j}).$$

We solve the problem by splitting it into two cases.

1. The number of sensors in the network N is even.
2. The number of sensors in the network N is odd.

4.3 $K = 3$, N is an even number

Theorem 4.3.1 *Let $K = 3$ and N be an even number. Then the set of angles $\theta_i = \frac{2\pi(i-1)}{N} \bmod \pi$, $1 \leq i \leq N$, minimizes the maximum condition number among all sub-matrices with K columns. Moreover, they are the unique set of angles that achieve the smallest maximum condition number for $N \geq 6$.*

Proof: We first derive a lower bound for the maximum condition number among all sub-matrices with $K = 3$ columns; and then show the given set of angles achieve

this lower bound.

Suppose that the set of angles $0 \leq \theta_i^* < \pi$, $1 \leq i \leq N$, achieve the smallest maximum condition number for all submatrices with $K = 3$ columns. Without loss of generality, let $\theta_1^* = 0$; and let θ_i^* , $1 \leq i \leq N$, appear sequentially in a counter-clockwise order. Let $\tilde{\theta}_i = 2\theta_i^*$, so we have $0 \leq \tilde{\theta}_i < 2\pi$.

Lower bound for maximum condition number

Consider $|(\tilde{\theta}_{(i+2) \bmod N} - \tilde{\theta}_i) \bmod (2\pi)|$ which is the counter-clockwise region going from $\tilde{\theta}_i$ to $\tilde{\theta}_{(i+2) \bmod N}$. So the summation $\sum_{i=1}^N |(\tilde{\theta}_{(i+2) \bmod N} - \tilde{\theta}_i) \bmod (2\pi)| = 2 \times (2\pi)$ because each counter-clockwise region between two adjacent angles is summed twice (see Figure. 4.1). Thus there must exist an index $1 \leq i \leq N$ such that for $\tilde{\theta}_i$, $\tilde{\theta}_{(i+1) \bmod N}$, and $\tilde{\theta}_{(i+2) \bmod N}$, $|(\tilde{\theta}_{(i+2) \bmod N} - \tilde{\theta}_i) \bmod (2\pi)| \leq \frac{4\pi}{N}$.

For simplicity of notations, we denote these three angles $\tilde{\theta}_i$, $\tilde{\theta}_{(i+1) \bmod N}$, and $\tilde{\theta}_{(i+2) \bmod N}$ as t_1 , t_2 and t_3 . Without loss of generality, we assume that $0 = t_1 \leq t_2 \leq t_3 \leq \frac{4\pi}{N}$. We now show that the smallest condition number that these three angles t_1 , t_2 , and t_3 can achieve is when $t_2 = t_1$ or $t_2 = t_3$.

We consider the scenario where $|\theta_3 - \theta_1| \leq \frac{4\pi}{N}$ remains as a fixed constant.

Define $f(\theta_2)$ as

$$f(t_2) = \cos(t_1 - t_2) + \cos(t_1 - t_3) + \cos(t_2 - t_3).$$

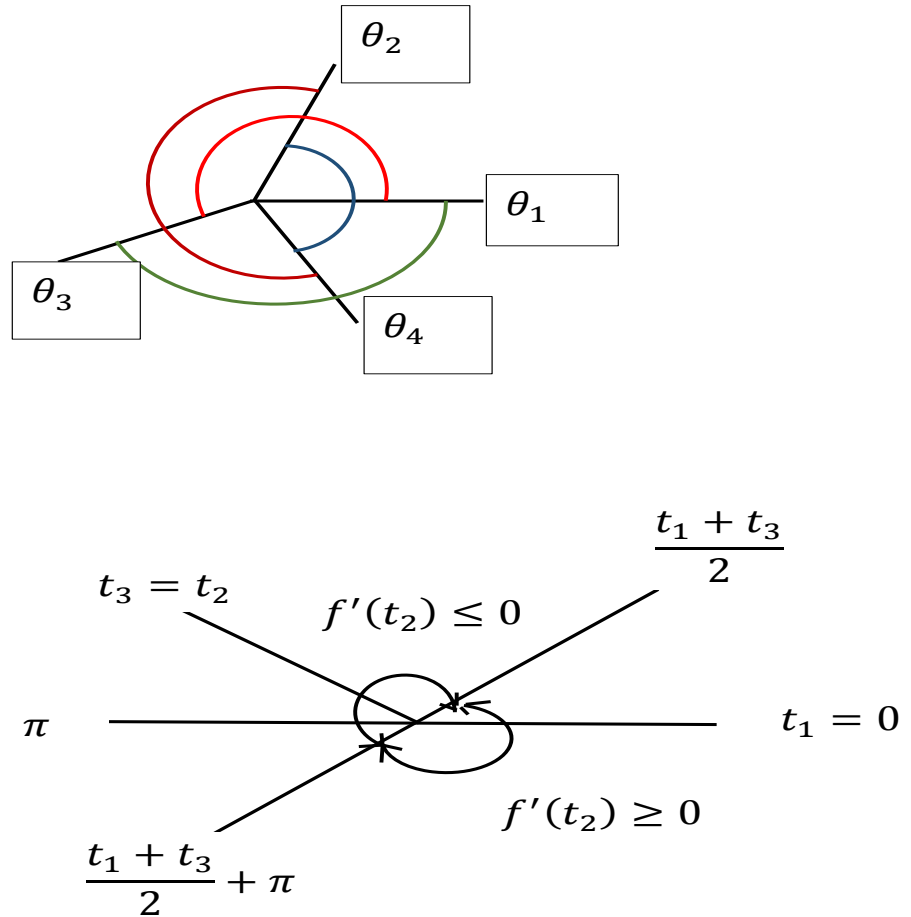


Figure 4.1: Top: Illustration of the $\sum_{i=1}^N |(\tilde{\theta}_{(i+2) \bmod N} - \tilde{\theta}_i) \bmod (2\pi)| = 2 \times (2\pi)$ for a 4 sensor network. Bottom: Illustration of the regions where $f'(t_2) \geq 0$ and $f'(t_2) \leq 0$.

Its derivative is

$$\begin{aligned} f'(t_2) &= -\sin(t_2 - t_1) + \sin(t_3 - t_2) \\ &= 2 \sin\left(\frac{t_3 + t_1}{2} - t_2\right) \cos\left(\frac{t_3 - t_1}{2}\right). \end{aligned}$$

So if $(t_3 - t_1) \leq \pi$, the derivative $f'(t_2)$ is non-positive for $\frac{t_3 + t_1}{2} \leq t_2 \leq \frac{t_3 + t_1}{2} + \pi$; and it is non-negative for $\frac{t_3 + t_1}{2} + \pi \leq t_2 \leq \frac{t_3 + t_1}{2} + 2\pi$. So if $0 = t_1 \leq t_2 \leq t_3 \leq \frac{4\pi}{N}$, $f(t_2)$ is minimized when $t_2 = t_1$ or $t_2 = t_3$ (see Figure. 4.1). The corresponding $f(t_2)$ is

$$f(t_2 = t_1) = f(t_2 = t_3) = 1 + 2 \cos(t_1 - t_3) \geq 1 + 2 \cos\left(\frac{4\pi}{N}\right).$$

Achievability

Finishing the proof requires us to that the given set of angles $\theta_i = \frac{2\pi(i-1)}{N} \bmod \pi$, $1 \leq i \leq N$, achieve the lower bound $1 + 2 \cos\left(\frac{4\pi}{N}\right)$. Let $\ddot{\theta}_i = 2\theta_i$, thus $0 \leq \ddot{\theta}_i < 2\pi$. In the Counter-clockwise, starting from the two angles $\ddot{\theta}_i = 0$ and $\ddot{\theta}_{\frac{N}{2}+1} = 0$ (which are in fact two angles in the same position), *re-label* these N angles sequentially as $\hat{\theta}_1, \hat{\theta}_2, \dots$, and $\hat{\theta}_N$.

Thus the following needs to be proved. For any 3 angles r_1, r_2 and r_3 from the given set of angles $\hat{\theta}_i$ satisfy

$$\cos(r_1 - r_2) + \cos(r_2 - r_3) + \cos(r_1 - r_3) \leq 1 + 2 \cos\left(\frac{4\pi}{N}\right).$$

Without loss of generality, one can assume that r_1, r_2 and r_3 are in a counter-

clockwise order; and that $|(r_2 - r_1) \bmod (2\pi)|$ is the smallest among $|(r_2 - r_1) \bmod (2\pi)|$, $|(r_3 - r_2) \bmod (2\pi)|$ and $|(r_1 - r_3) \bmod (2\pi)|$. Clearly, $|(r_2 - r_1) \bmod (2\pi)| \leq \frac{2\pi}{3}$, and $|(r_2 - r_1) \bmod (2\pi)|$ is an integer multiple of $\frac{4\pi}{N}$.

Suppose $|(r_2 - r_1) \bmod (2\pi)| = 0$. Then $r_2 = r_1$ and $|(r_1 - r_3) \bmod (2\pi)| = |(r_3 - r_2) \bmod (2\pi)| \geq \frac{4\pi}{N}$. Similar to the proof of “lower bound”, for such a setting, the function

$$f(r_3) = \cos(r_1 - r_2) + \cos(r_1 - r_3) + \cos(r_2 - r_3)$$

is a decreasing function of r_3 for $r_3 \in [r_1, (r_1 + \pi) \bmod (2\pi)]$; and an increasing function of r_3 for $r_3 \in [(r_1 + \pi) \bmod (2\pi), (r_1 + 2\pi) \bmod (2\pi)]$. So the maximum of $f(r_3)$ is achieved when $|(r_1 - r_3) \bmod (2\pi)| = \frac{4\pi}{N}$, where $f(r_3) = 1 + 2 \cos(\frac{4\pi}{N})$.

Suppose $|(r_2 - r_1) \bmod (2\pi)| = \frac{4\pi}{N}$. Then $|(r_1 - r_3) \bmod (2\pi)| \geq \frac{4\pi}{N}$ and $|(r_3 - r_2) \bmod (2\pi)| \geq \frac{4\pi}{N}$. Similar to the reasoning in the “lower bound” part, the maximum for $f(r_3) = \cos(r_1 - r_2) + \cos(r_1 - r_3) + \cos(r_2 - r_3)$ is achieved when $|(r_3 - r_2) \bmod (2\pi)| = \frac{4\pi}{N}$, $r_3 \neq r_1$; or $|(r_1 - r_3) \bmod (2\pi)| = \frac{4\pi}{N}$ and $r_3 \neq r_2$. In both cases, $f(r_3) = 2 \cos(\frac{4\pi}{N}) + \cos(\frac{8\pi}{N})$, which is smaller than the lower bound $1 + 2 \cos(\frac{4\pi}{N})$.

Now suppose $|(r_2 - r_1) \bmod (2\pi)| > \frac{4\pi}{N}$. Since $|(r_2 - r_1) \bmod (2\pi)| \leq \frac{2\pi}{3}$ and r_3 is certainly outside the counter-clockwise region going from r_1 to r_2 , using the same reasoning in proving the lower bound, the function

$$f(r_3) = \cos(r_1 - r_2) + \cos(r_1 - r_3) + \cos(r_2 - r_3)$$

achieves its maximum when $r_3 = r_2$ or $r_3 = r_1$. This maximum is

$$f(r_3 = r_1) = 1 + 2 \cos(r_1 - r_2),$$

which is certainly no bigger than $1 + 2 \cos(\frac{4\pi}{N})$.

So the given set of angles indeed achieves the lower bound $1 + 2 \cos(\frac{4\pi}{N})$, and we have proven the optimality of the given set of angles in minimizing the maximum condition number among all submatrices with 3 columns.

(Uniqueness)

Moreover, in the proof of the lower bound, when $N \geq 6$, $(t_3 - t_1) < \pi$, the derivative $f'(t_2)$ is negative for $\frac{t_3+t_1}{2} < t_2 < \frac{t_3+t_1}{2} + \pi$; and positive for $\frac{t_3+t_1}{2} + \pi < t_2 < \frac{t_3+t_1}{2} + 2\pi$. So $t_3 = t_1$ or $t_3 = t_2$ are the only two places where $f(t_3)$ achieves the lower bound $1 + 2 \cos(\frac{4\pi}{N})$. We further notice that the lower bound is achieved only when the counter-clockwise region between any 3 adjacent angles from $\tilde{\theta}_i$, $1 \leq i \leq N$, is equal to $\frac{4\pi}{N}$. Otherwise, if there exist one set of 3 adjacent angles from $\tilde{\theta}$ such that the region between them is larger than $\frac{4\pi}{N}$, there must exist another set of 3 adjacent angles from $\tilde{\theta}_i$, $1 \leq i \leq N$, such that the counter-clockwise region between them is smaller than $\frac{4\pi}{N}$. This is because $\sum_{i=1}^N |(\tilde{\theta}_{(i+2) \bmod N} - \tilde{\theta}_i) \bmod 2\pi| = 2 \times (2\pi)$. For these sets of 3 angles, their corresponding cost function $f(\cdot)$ is larger than the derived cost function lower bound $1 + 2 \cos(\frac{4\pi}{N})$, thus bringing a larger maximum condition number. This proves for $N \geq 6$, $\theta_i = \frac{2\pi(i-1)}{N} \bmod \pi$, $1 \leq i \leq N$ are the unique set of angles that minimize the maximum condition number.

It is worth mentioning that when $N = 4$, the design given in Theorem 4.3.1 is still optimal. However, we have more than one design that can minimize the maximum condition number. This is because, when counter-clockwise region covered by 3 angles is π , no matter where the middle angle is, the cost function is -1 .

Theorem 4.3.2 *For $N = 4$, $K = 3$ and $M = 2$, the set of $\hat{\Theta} = 2\Theta = \{\tilde{\theta}_1, \tilde{\theta}_2, \tilde{\theta}_1 + \pi, \tilde{\theta}_2 + \pi\}$, where $0 \leq \tilde{\theta}_1 < \pi$, $0 \leq \tilde{\theta}_2 < \pi$, minimizes the maximum condition number over all possible 3×3 submatrices.*

4.4 $K = 3$, $N = 3$ or 5

Interestingly, when $K = 3$, except for the trivial case $N = 3$, $N = 5$ is the only other case where a uniform distributed design indeed minimizes the maximum condition number.

Theorem 4.4.1 *Let $K = 3$ and $N = 3$ or 5. Then the set of angles $\theta_i = \frac{\pi(i-1)}{N}$, $1 \leq i \leq N$, minimizes the maximum condition number among all sub-matrices with $K = 3$ columns.*

Proof: The case for $N = 3$ is trivial, so now we only focus on proving the claim for $N = 5$.

For the set of angles $\hat{\theta}_i = 2\theta_i = \frac{2\pi(i-1)}{N}$, $1 \leq i \leq N$, it is not hard to check that 3 adjacent angles, denoted by r_1 , r_2 and r_3 , give the maximum cost function

$$\cos(r_1 - r_2) + \cos(r_1 - r_3) + \cos(r_2 - r_3) = 2 \cos\left(\frac{2\pi}{5}\right) + \cos\left(\frac{4\pi}{5}\right),$$

which corresponds to largest condition number.

Let $0 \leq \theta_i^* < \pi$, $1 \leq i \leq N$, be a set of N angles which minimizes the maximum condition number of all submatrices with 3 columns. For convenience, we consider the corresponding N angles $\tilde{\theta}_i = 2\theta_i^*$, $1 \leq i \leq N$. Without loss of generality, we assume $\tilde{\theta}_1 = 0$; and $0 \leq \tilde{\theta}_i < 2\pi$ are arranged sequentially in a counter-clockwise order as i ranges from 1 to N . We first prove the following two lemmas before proving that there must exist at least 4 adjacent-3-angle sets which give the maximum condition number.

Lemma 4.4.1 *The counter-clockwise region between any two adjacent angles (for example $\tilde{\theta}_i$ and $\tilde{\theta}_{(i+1) \bmod N}$ for some i) is smaller than π .*

Proof: Note that the 5 angles partition the circle into 5 regions. If instead the counter-clockwise region going from $\tilde{\theta}_i$ to $\tilde{\theta}_{(i+1) \bmod N}$ is at least π , because the other 4 regions occupy at most π , there must exist three adjacent angles for which the two counter-clockwise regions covered by them is no bigger than $\frac{\pi}{2}$. For those three angles, from the same calculation as in Theorem 4.3.1, the smallest cost function these 3 angles can achieve is

$$\cos\left(\frac{\pi}{2} - \frac{\pi}{2}\right) + \cos\left(0 - \frac{\pi}{2}\right) + \cos\left(0 - \frac{\pi}{2}\right) = 1,$$

which is already bigger than the cost $2\cos\left(\frac{2\pi}{5}\right) + \cos\left(\frac{4\pi}{5}\right)$ achieved by the 5 angles $\hat{\theta}_i = 2\theta_i = \frac{2\pi(i-1)}{N}$, $1 \leq i \leq N$.

Lemma 4.4.2 *Let $N = 5$. In the optimal design $\tilde{\theta}_i$, $1 \leq i \leq N$, consider 4 adjacent*

angles r_1, r_2, r_3 and r_4 , where they are arranged in a counter-clockwise order; and r_2 and r_3 are inside the counter-clockwise region going from r_1 to r_4 . (r_1, r_2, r_3) and (r_2, r_3, r_4) give the same condition number if and only if $(r_2 - r_1) \bmod (2\pi) = (r_4 - r_3) \bmod (2\pi)$.

Proof: Without loss of generality, we assume $r_1 = 0$ such that $r_i, 1 \leq i \leq 4$, are all within $[0, 2\pi)$. Now we only need to show (r_1, r_2, r_3) and (r_2, r_3, r_4) give the same condition number if and only if $r_2 - r_1 = r_4 - r_3$.

If (r_1, r_2, r_3) and (r_2, r_3, r_4) give the same condition number, we have

$$\begin{aligned} & \cos(r_1 - r_2) + \cos(r_1 - r_3) + \cos(r_2 - r_3) \\ = & \cos(r_3 - r_2) + \cos(r_4 - r_2) + \cos(r_4 - r_3). \end{aligned}$$

This means

$$\begin{aligned} & 2 \cos\left(\frac{r_3 - r_2}{2} + r_2 - r_1\right) \cos\left(\frac{r_3 - r_2}{2}\right) \\ = & 2 \cos\left(\frac{r_3 - r_2}{2} + r_4 - r_3\right) \cos\left(\frac{r_3 - r_2}{2}\right). \end{aligned}$$

Since we have just shown that $r_3 - r_2$ is smaller than π , we have

$$\cos\left(\frac{r_3 - r_2}{2} + r_2 - r_1\right) = \cos\left(\frac{r_3 - r_2}{2} + r_4 - r_3\right).$$

This means either $r_2 - r_1 = r_4 - r_3$ or $r_4 - r_1 = 2\pi$. The latter is not possible for a set of angles which achieve the smallest maximum condition number, because

$r_4 - r_1 = 2\pi$ forces the next angle r_5 to be aligned with both r_1 and r_4 . This gives a condition number of ∞ for the three angles r_1 , r_4 and r_5 . So we must have $r_2 - r_1 = r_4 - r_3$.

In the optimal design $\tilde{\theta}_i$, $1 \leq i \leq N$, we assume that $\{\tilde{\theta}_1, \tilde{\theta}_2, \tilde{\theta}_3\}$ is an adjacent-3-set which corresponds to the maximum condition number.

4.4.1 (At Least 2 adjacent-3-angle Sets Giving the Maximum Condition Number)

Lemma 4.4.3 $\tilde{\theta}_1$, $\tilde{\theta}_2$ and $\tilde{\theta}_3$ can not be the unique set of 3 angles that have the largest condition number.

Proof: We prove by contradiction. Suppose $\{\tilde{\theta}_1, \tilde{\theta}_2, \tilde{\theta}_3\}$ is the unique set of 3 adjacent angles that have the largest condition number. Then we must have $\tilde{\theta}_3 - \tilde{\theta}_1 < \pi$. Suppose instead that $\tilde{\theta}_3 - \tilde{\theta}_1 = \pi$ or $\tilde{\theta}_3 - \tilde{\theta}_1 > \pi$.

If $\tilde{\theta}_3 - \tilde{\theta}_1 = \pi$, the cost function for the set of 3 angles $\tilde{\theta}_1$, $\tilde{\theta}_2$ and $\tilde{\theta}_3$ is equal to the cost function for the set of 3 angles $\tilde{\theta}_3$, $\tilde{\theta}_5$ and $\tilde{\theta}_1$. This is a contradiction to our assumption.

If $\tilde{\theta}_3 - \tilde{\theta}_1 > \pi$, then $\tilde{\theta}_2 - \tilde{\theta}_1 = \tilde{\theta}_3 - \tilde{\theta}_2$. Otherwise, we can always shift $\tilde{\theta}_2$ towards $\frac{\tilde{\theta}_1 + \tilde{\theta}_3}{2}$ by a sufficiently small amount and strictly decrease the cost function for $\tilde{\theta}_1$, $\tilde{\theta}_2$ and $\tilde{\theta}_3$. Since the cost functions for any other 3 adjacent angles are strictly smaller than the original cost function of $\tilde{\theta}_1$, $\tilde{\theta}_2$ and $\tilde{\theta}_3$, their cost functions will remain smaller than the new revised cost function of $\tilde{\theta}_1$, $\tilde{\theta}_2$ and $\tilde{\theta}_3$. So we have just decreased the largest condition number, which is a contradiction. So we must have $\tilde{\theta}_2 - \tilde{\theta}_1 = \tilde{\theta}_3 - \tilde{\theta}_2$. However the cost function for $\tilde{\theta}_4$, $\tilde{\theta}_5$ and $\tilde{\theta}_1$ is lower bounded by

$2 \cos(\frac{\pi}{2}) + \cos(\pi) = -1$, which is larger than the cost function for $\tilde{\theta}_1$, $\tilde{\theta}_2$ and $\tilde{\theta}_3$. This is contradictory to the assumption that the set of $\tilde{\theta}_1$, $\tilde{\theta}_2$ and $\tilde{\theta}_3$ corresponds to the maximum condition number.

So we must have $\tilde{\theta}_3 - \tilde{\theta}_1 < \pi$. In this case, if we shift $\tilde{\theta}_3$ counter-clockwise by a sufficiently small amount δ , we will strictly decrease the cost function for $\tilde{\theta}_1$, $\tilde{\theta}_2$ and $\tilde{\theta}_3$. Since by our assumption, the cost function of any other 3 adjacent angles were *strictly* smaller than the original cost function of $\{\tilde{\theta}_1, \tilde{\theta}_2, \tilde{\theta}_3\}$, their cost functions will stay smaller than the new revised cost function for $\{\tilde{\theta}_1, \tilde{\theta}_2, \tilde{\theta}_3\}$. So we have just strictly decreased the maximum condition number of the optimal design, which is not possible.

4.4.2 (At Least 3 adjacent-3-angle Sets Giving the Maximum Condition Number)

Lemma 4.4.4 $\{\tilde{\theta}_1, \tilde{\theta}_2, \tilde{\theta}_3\}$ and $\{\tilde{\theta}_2, \tilde{\theta}_3, \tilde{\theta}_4\}$ can not be the only 2 sets of 3 adjacent angles which correspond to the maximum condition number.

Proof: We prove by contradiction. Suppose $\{\tilde{\theta}_1, \tilde{\theta}_2, \tilde{\theta}_3\}$ and $\{\tilde{\theta}_2, \tilde{\theta}_3, \tilde{\theta}_4\}$ are the only two sets of 3 adjacent angles that have the largest condition number. This means $\tilde{\theta}_4 - \tilde{\theta}_3 = \tilde{\theta}_2 - \tilde{\theta}_1 = \alpha$ for some $\alpha \geq 0$; and $\tilde{\theta}_2 - \tilde{\theta}_1 = \beta$ for some $\beta \geq 0$. Note that $2\alpha + \beta < 2\pi$ because, otherwise, $\tilde{\theta}_4$, $\tilde{\theta}_5$ and $\tilde{\theta}_1$ are forced to be in the same position, giving rise to a condition number of ∞ for these three angles.

From Lemma 4.4.1, we know $\beta < \pi$. For such a β , it is not hard to check that under the constraint $2\alpha + \beta \leq 2\pi$, the cost function $\cos(\alpha) + \cos(\beta) + \cos(\alpha + \beta)$ achieves its unique minimum when $2\alpha + \beta = 2\pi$. Moreover, the cost function is a

strictly decreasing function as α grows from 0 to $\pi - \frac{\beta}{2}$. So if we shift $\tilde{\theta}_4$ counterclockwise by a small amount $\delta > 0$ and shift $\tilde{\theta}_1$ clockwise by the same small amount $\delta > 0$, then as long as $2\alpha + \beta < 2\pi$, this will strictly decrease the condition numbers simultaneously for $\{\tilde{\theta}_1, \tilde{\theta}_2, \tilde{\theta}_3\}$ and $\{\tilde{\theta}_2, \tilde{\theta}_3, \tilde{\theta}_4\}$.

Since the cost functions for any other 3 adjacent angles were strictly smaller than the original cost function of $\{\tilde{\theta}_1, \tilde{\theta}_2, \tilde{\theta}_3\}$, their cost functions will stay smaller than the new revised cost function of $\{\tilde{\theta}_1, \tilde{\theta}_2, \tilde{\theta}_3\}$. So we have just strictly decreased the maximum condition number, which is a contradiction to our assumption of an optimal design.

By symmetry, in the same spirit, we have

Lemma 4.4.5 $\{\tilde{\theta}_1, \tilde{\theta}_2, \tilde{\theta}_3\}$ and $\{\tilde{\theta}_1, \tilde{\theta}_2, \tilde{\theta}_5\}$ can not be the only 2 sets of 3 adjacent angles which have the largest condition number.

We can also prove:

Lemma 4.4.6 $\{\tilde{\theta}_1, \tilde{\theta}_2, \tilde{\theta}_3\}$ and $\{\tilde{\theta}_3, \tilde{\theta}_4, \tilde{\theta}_5\}$ can not be the only 2 sets of 3 adjacent angles which correspond to the maximum condition number.

Proof: Again, we prove by contradiction. Suppose $\{\tilde{\theta}_1, \tilde{\theta}_2, \tilde{\theta}_3\}$ and $\{\tilde{\theta}_3, \tilde{\theta}_4, \tilde{\theta}_5\}$ are the only two sets of 3 adjacent angles that have the largest condition number.

We first assume that $\tilde{\theta}_5 - \tilde{\theta}_3 \neq \pi$.

We claim that if $\tilde{\theta}_5 - \tilde{\theta}_3 > \pi$, then $\tilde{\theta}_4 = \frac{\tilde{\theta}_3 + \tilde{\theta}_5}{2}$. This is because otherwise, we can shift $\tilde{\theta}_4$ toward the middle point $\frac{\tilde{\theta}_3 + \tilde{\theta}_5}{2}$ by a sufficiently small amount, thus strictly decreasing the condition number for $\{\tilde{\theta}_3, \tilde{\theta}_4, \tilde{\theta}_5\}$. This will leave $\{\tilde{\theta}_1, \tilde{\theta}_2, \tilde{\theta}_3\}$ as

the unique adjacent-3-set with the maximum condition number, which is not possible by Lemma 4.4.3.

But if $\tilde{\theta}_5 - \tilde{\theta}_3 > \pi$, we must have $\tilde{\theta}_3 - \tilde{\theta}_1 < \pi$. However, then $\{\tilde{\theta}_1, \tilde{\theta}_2, \tilde{\theta}_3\}$ and $\{\tilde{\theta}_3, \tilde{\theta}_4, \tilde{\theta}_5\}$ can not have the same condition number. In fact, from analyzing the cost function, when $\tilde{\theta}_3 - \tilde{\theta}_1 < \pi$, $\tilde{\theta}_5 - \tilde{\theta}_3 > \pi$ and $\tilde{\theta}_4 = \frac{\tilde{\theta}_3 + \tilde{\theta}_5}{2}$, $\{\tilde{\theta}_3, \tilde{\theta}_4, \tilde{\theta}_5\}$ has a strictly smaller condition number than $\{\tilde{\theta}_1, \tilde{\theta}_2, \tilde{\theta}_3\}$.

So when $\tilde{\theta}_5 - \tilde{\theta}_3 \neq \pi$, we must have $\tilde{\theta}_5 - \tilde{\theta}_3 < \pi$ and, symmetrically, $\tilde{\theta}_3 - \tilde{\theta}_1 < \pi$. Then $\tilde{\theta}_4 = \tilde{\theta}_3$ or $\tilde{\theta}_5$; $\tilde{\theta}_2 = \tilde{\theta}_1$ or $\tilde{\theta}_3$; and $\tilde{\theta}_3 - \tilde{\theta}_1 = \tilde{\theta}_5 - \tilde{\theta}_3$. This is because, if $\tilde{\theta}_4 \neq \tilde{\theta}_3$ and $\tilde{\theta}_4 \neq \tilde{\theta}_5$, we can always shift $\tilde{\theta}_4$ towards whatever is closer to $\tilde{\theta}_4$ among $\tilde{\theta}_3$ and $\tilde{\theta}_5$. This will strictly decrease the corresponding cost function, and leaving only one adjacent-3-angle set having the maximum condition number, which is not possible by Lemma 4.4.3.

But then by increasing $\tilde{\theta}_3 - \tilde{\theta}_1 = \tilde{\theta}_5 - \tilde{\theta}_3$ by a sufficiently small amount $\delta > 0$, we will strictly decrease the condition numbers for $\{\tilde{\theta}_1, \tilde{\theta}_2, \tilde{\theta}_3\}$ and $\{\tilde{\theta}_3, \tilde{\theta}_4, \tilde{\theta}_5\}$. Since the cost functions for the other sets of 3 adjacent angles were strictly smaller than the original cost function of $\{\tilde{\theta}_1, \tilde{\theta}_2, \tilde{\theta}_3\}$ and $\{\tilde{\theta}_3, \tilde{\theta}_4, \tilde{\theta}_5\}$, their cost functions will remain smaller than the new revised cost function of $\{\tilde{\theta}_3, \tilde{\theta}_4, \tilde{\theta}_5\}$. So we have just decreased the maximum condition number of the optimal design, which is not possible.

We now consider the possibility that $\tilde{\theta}_5 - \tilde{\theta}_3 = \pi$. Because $\{\tilde{\theta}_3, \tilde{\theta}_4, \tilde{\theta}_5\}$ and $\{\tilde{\theta}_1, \tilde{\theta}_2, \tilde{\theta}_3\}$ both have the maximum condition number; and $(\tilde{\theta}_3 - \tilde{\theta}_1) + (\tilde{\theta}_5 - \tilde{\theta}_3) \leq 2\pi$, with the cost function $\cos(\alpha) + \cos(\beta) + \cos(\alpha + \beta)$ achieving the minimum -1 when $\alpha + \beta \leq \pi$, we must have $\tilde{\theta}_3 - \tilde{\theta}_1 = \pi$ too. Then $\tilde{\theta}_5$ and $\tilde{\theta}_1$ must be in the same

position, and so $\{\tilde{\theta}_1, \tilde{\theta}_2, \tilde{\theta}_5\}$ must have a condition number no smaller than $\{\tilde{\theta}_1, \tilde{\theta}_2, \tilde{\theta}_3\}$ since $\cos(\tilde{\theta}_2 - \tilde{\theta}_1) + \cos(\tilde{\theta}_1 - \tilde{\theta}_5 + 2\pi) + \cos(\tilde{\theta}_2 - \tilde{\theta}_5 + 2\pi)$ achieves its minimum -1 with $\tilde{\theta}_2 = \pi$ when $\tilde{\theta}_2 \leq \pi$. This is contradictory to our assumption that $\{\tilde{\theta}_1, \tilde{\theta}_2, \tilde{\theta}_3\}$ and $\{\tilde{\theta}_3, \tilde{\theta}_4, \tilde{\theta}_5\}$ are the only 2 sets of 3 adjacent angles which have the maximum condition number.

By symmetry, we can also prove

Lemma 4.4.7 $\{\tilde{\theta}_1, \tilde{\theta}_2, \tilde{\theta}_3\}$ and $\{\tilde{\theta}_4, \tilde{\theta}_5, \tilde{\theta}_1\}$ can not be the only 2 sets of 3 adjacent angles which have the largest condition number.

4.4.3 (At Least 4 adjacent-3-angle Sets Giving the Maximum Condition Number)

Now we consider the cases where more angle sets have the maximum condition number.

Lemma 4.4.8 $\{\tilde{\theta}_1, \tilde{\theta}_2, \tilde{\theta}_3\}$, $\{\tilde{\theta}_2, \tilde{\theta}_3, \tilde{\theta}_4\}$ and $\{\tilde{\theta}_3, \tilde{\theta}_4, \tilde{\theta}_5\}$ can not be the only 3 sets of 3 adjacent angles which have the largest condition number.

Proof: We prove by contradiction. Let us assume $\{\tilde{\theta}_1, \tilde{\theta}_2, \tilde{\theta}_3\}$, $\{\tilde{\theta}_2, \tilde{\theta}_3, \tilde{\theta}_4\}$ and $\{\tilde{\theta}_3, \tilde{\theta}_4, \tilde{\theta}_5\}$ are the only 3 sets of 3 adjacent angles which have the largest condition number. Apparently, $\tilde{\theta}_2 - \tilde{\theta}_1 = \tilde{\theta}_4 - \tilde{\theta}_3 = \alpha$ and $\tilde{\theta}_3 - \tilde{\theta}_2 = \tilde{\theta}_5 - \tilde{\theta}_4 = \beta$ for some $\alpha \geq 0$ and $\beta \geq 0$.

We must have $\alpha + \beta < \pi$. Otherwise, angle $\tilde{\theta}_5$ will be in the same position as $\tilde{\theta}_1$. But, as argued in Lemma 4.4.6, this implies $\{\tilde{\theta}_5, \tilde{\theta}_1, \tilde{\theta}_2\}$ can not have a smaller condition number than $\{\tilde{\theta}_1, \tilde{\theta}_2, \tilde{\theta}_3\}$, which is a contradiction to the assumption that $\{\tilde{\theta}_1, \tilde{\theta}_2, \tilde{\theta}_3\}$, $\{\tilde{\theta}_2, \tilde{\theta}_3, \tilde{\theta}_4\}$ and $\{\tilde{\theta}_3, \tilde{\theta}_4, \tilde{\theta}_5\}$ are the only 3 sets of 3 adjacent angles which

have the largest condition number.

So we can always increase α and β by a sufficiently small amount δ to decrease the condition number for $\{\tilde{\theta}_1, \tilde{\theta}_2, \tilde{\theta}_3\}$, $\{\tilde{\theta}_2, \tilde{\theta}_3, \tilde{\theta}_4\}$ and $\{\tilde{\theta}_3, \tilde{\theta}_4, \tilde{\theta}_5\}$. Since the cost functions for any other 3 adjacent angles were strictly smaller than the original cost function of $\{\tilde{\theta}_1, \tilde{\theta}_2, \tilde{\theta}_3\}$, $\{\tilde{\theta}_2, \tilde{\theta}_3, \tilde{\theta}_4\}$ and $\{\tilde{\theta}_3, \tilde{\theta}_4, \tilde{\theta}_5\}$, their cost functions will remain smaller than the new revised cost function of $\tilde{\theta}_1$, $\tilde{\theta}_2$ and $\tilde{\theta}_3$. So we have just decreased the maximum condition number, which is a contradiction to our assumption.

We also have:

Lemma 4.4.9 $\{\tilde{\theta}_1, \tilde{\theta}_2, \tilde{\theta}_3\}$, $\{\tilde{\theta}_2, \tilde{\theta}_3, \tilde{\theta}_4\}$ and $\{\tilde{\theta}_4, \tilde{\theta}_5, \tilde{\theta}_1\}$ can not be the only 3 sets of 3 adjacent angles which have the largest condition number.

Proof: Again, we prove by contradiction. Suppose that $\{\tilde{\theta}_1, \tilde{\theta}_2, \tilde{\theta}_3\}$, $\{\tilde{\theta}_2, \tilde{\theta}_3, \tilde{\theta}_4\}$ and $\{\tilde{\theta}_4, \tilde{\theta}_5, \tilde{\theta}_1\}$ are the only 3 sets of 3 adjacent angles which have the largest condition number.

Firstly, we assume that the counter-clockwise region between angle $\tilde{\theta}_4$ and angle $\tilde{\theta}_1$ is smaller than π . Then we know angle $\tilde{\theta}_5$ must be in the same position as angle $\tilde{\theta}_4$ or angle $\tilde{\theta}_1$. Otherwise, as we discussed earlier, we can always shift $\tilde{\theta}_5$ such that the cost function for $\{\tilde{\theta}_4, \tilde{\theta}_5, \tilde{\theta}_1\}$ is decreased, which will reduce us to the scenario in Lemma 4.4.4.

Suppose $\tilde{\theta}_5$ is in the same position as angle $\tilde{\theta}_4$. From our assumption, the cost function for $\{\tilde{\theta}_3, \tilde{\theta}_4, \tilde{\theta}_5\}$ is smaller than the cost function for $\{\tilde{\theta}_2, \tilde{\theta}_3, \tilde{\theta}_4\}$. This is not possible, because $\tilde{\theta}_4 - \tilde{\theta}_3 < \pi$, and $\tilde{\theta}_5 - \tilde{\theta}_4 = 0$ and the cost function for $\{\tilde{\theta}_2, \tilde{\theta}_3, \tilde{\theta}_4\}$ is

maximized when $\tilde{\theta}_2 = \tilde{\theta}_3$ under the condition $\tilde{\theta}_2 \leq \tilde{\theta}_3$.

By symmetry of $\tilde{\theta}_5$ with respect to $\tilde{\theta}_4$ and $\tilde{\theta}_1$, when $\tilde{\theta}_5$ is in the same position as $\tilde{\theta}_1$, we also get a contradiction.

Secondly, we assume that the counter-clockwise region going from $\tilde{\theta}_4$ to $\tilde{\theta}_1$ is equal to π . In this case, the cost function for $\{\tilde{\theta}_5, \tilde{\theta}_1, \tilde{\theta}_4\}$ does not depend on the location of angle $\tilde{\theta}_5$. Since the cost function for $\{\tilde{\theta}_4, \tilde{\theta}_5, \tilde{\theta}_1\}$ is -1 and $\tilde{\theta}_4 - \tilde{\theta}_1$, in order for $\{\tilde{\theta}_1, \tilde{\theta}_2, \tilde{\theta}_3\}$, $\{\tilde{\theta}_2, \tilde{\theta}_3, \tilde{\theta}_4\}$ and $\{\tilde{\theta}_4, \tilde{\theta}_5, \tilde{\theta}_1\}$ to have the same cost function, we must have $\tilde{\theta}_2 = \tilde{\theta}_1 = 0$ and $\tilde{\theta}_3 = \tilde{\theta}_4 = \pi$. This is contradictory to the assumption that $\{\tilde{\theta}_2, \tilde{\theta}_3, \tilde{\theta}_4\}$ has a larger cost function than $\{\tilde{\theta}_3, \tilde{\theta}_4, \tilde{\theta}_5\}$.

Thirdly, we assume that the counter-clockwise region going from $\tilde{\theta}_4$ to $\tilde{\theta}_1$ is larger than π . Similar to earlier analysis, $\tilde{\theta}_5$ must at the middle point of the counter-clockwise region going from $\tilde{\theta}_4$ to $\tilde{\theta}_1$. However, we get a contradiction because the cost function for $\{\tilde{\theta}_4, \tilde{\theta}_5, \tilde{\theta}_1\}$ is no bigger than -1 ; while the cost function for $\{\tilde{\theta}_1, \tilde{\theta}_2, \tilde{\theta}_3\}$ is bigger than -1 since $\tilde{\theta}_3 - \tilde{\theta}_1 < \pi$.

So in summary, we have proven this lemma.

In the same spirit, we can prove

Lemma 4.4.10 $\{\tilde{\theta}_1, \tilde{\theta}_2, \tilde{\theta}_3\}$, $\{\tilde{\theta}_3, \tilde{\theta}_4, \tilde{\theta}_5\}$ and $\{\tilde{\theta}_5, \tilde{\theta}_1, \tilde{\theta}_2\}$ can not be the only 3 sets of 3 adjacent angles which have the largest condition number.

Lemma 4.4.11 $\{\tilde{\theta}_1, \tilde{\theta}_2, \tilde{\theta}_3\}$, $\{\tilde{\theta}_3, \tilde{\theta}_4, \tilde{\theta}_5\}$ and $\{\tilde{\theta}_4, \tilde{\theta}_5, \tilde{\theta}_1\}$ can not be the only 3 sets of 3 adjacent angles which have the largest condition number.

So the only left four possibilities are

- $\{\tilde{\theta}_1, \tilde{\theta}_2, \tilde{\theta}_3\}$, $\{\tilde{\theta}_2, \tilde{\theta}_3, \tilde{\theta}_4\}$, $\{\tilde{\theta}_3, \tilde{\theta}_4, \tilde{\theta}_5\}$, and $\{\tilde{\theta}_4, \tilde{\theta}_5, \tilde{\theta}_1\}$ are the sets of 3 adjacent angles which have the largest condition number.
- $\{\tilde{\theta}_1, \tilde{\theta}_2, \tilde{\theta}_3\}$, $\{\tilde{\theta}_2, \tilde{\theta}_1, \tilde{\theta}_5\}$, $\{\tilde{\theta}_1, \tilde{\theta}_5, \tilde{\theta}_4\}$, and $\{\tilde{\theta}_5, \tilde{\theta}_4, \tilde{\theta}_3\}$ are the sets of 3 adjacent angles which have the largest condition number.
- $\{\tilde{\theta}_1, \tilde{\theta}_2, \tilde{\theta}_3\}$, $\{\tilde{\theta}_2, \tilde{\theta}_3, \tilde{\theta}_4\}$, $\{\tilde{\theta}_3, \tilde{\theta}_4, \tilde{\theta}_5\}$, and $\{\tilde{\theta}_5, \tilde{\theta}_1, \tilde{\theta}_2\}$ are the sets of 3 adjacent angles which have the largest condition number.
- $\{\tilde{\theta}_1, \tilde{\theta}_2, \tilde{\theta}_3\}$, $\{\tilde{\theta}_2, \tilde{\theta}_3, \tilde{\theta}_4\}$, $\{\tilde{\theta}_4, \tilde{\theta}_5, \tilde{\theta}_1\}$, and $\{\tilde{\theta}_5, \tilde{\theta}_1, \tilde{\theta}_2\}$ are the sets of 3 adjacent angles which have the largest condition number.

These four cases are symmetric to each other, so we consider the first case and the conclusion carries over to the other three cases accordingly.

The first case implies that $\tilde{\theta}_2 - \tilde{\theta}_1 = \tilde{\theta}_4 - \tilde{\theta}_3 = \tilde{\theta}_1 - \tilde{\theta}_5 + 2\pi = \alpha$ for some constant $\alpha \geq 0$; and $\tilde{\theta}_3 - \tilde{\theta}_2 = \tilde{\theta}_5 - \tilde{\theta}_4 = \beta$ for some constant $\beta \geq 0$.

We note that $\{\tilde{\theta}_1, \tilde{\theta}_2, \tilde{\theta}_5\}$ are adjacent 3 angles with α between $\tilde{\theta}_1$ and $\tilde{\theta}_2$; and α between $\{\tilde{\theta}_1$ and $\tilde{\theta}_5\}$. We also notice that $\alpha \geq \beta \geq 0$ (because $\alpha + \beta \leq \pi$ and $2\alpha + \beta \leq 2\pi$. Under these constraints, it is not hard to check that the cost function $\cos(\alpha) + \cos(\alpha) + \cos(2\alpha)$ for $\{\tilde{\theta}_5, \tilde{\theta}_1, \tilde{\theta}_2\}$ is bigger than the cost function $\cos(\alpha) + \cos(\beta) + \cos(\alpha + \beta)$ for $\{\tilde{\theta}_1, \tilde{\theta}_2, \tilde{\theta}_3\}$ if and only if $\alpha \geq \beta$.) and $3\alpha + 2\beta = 2\pi$. In order to minimize the largest condition number, we should make the cost function $\cos(\alpha) + \cos(\beta) + \cos(\alpha + \beta)$ as small as possible.

Under the constraints that $\alpha \geq \beta \geq 0$ and $3\alpha + 2\beta = 2\pi$, we have $\frac{2\pi}{5} \leq \alpha \leq \frac{2\pi}{3}$. Within this range, the cost function $\cos(\alpha) + \cos(\beta) + \cos(\alpha + \beta)$ achieves its minimum when $\alpha = \beta = \frac{2\pi}{5}$. If $\alpha = \beta$, the cost function is equal to $2\cos(\frac{2\pi}{5}) + \cos(\frac{4\pi}{5}) \approx$

−0.1910.

So indeed the optimal solution is given by $\theta_i = \frac{\pi(i-1)}{N}$, $1 \leq i \leq N$.

4.5 $K = 3, N = 7$

One might think that the uniform distributed design is optimal for $N = 7$.

However, this is not true from the following lemma.

Theorem 4.5.1 *Let $K = 3$ and $N = 7$. Then $\theta_i = \frac{2\pi(i-1)}{N+1} \pmod{\pi}$, $1 \leq i \leq N$, minimizes the maximum condition number among all sub-matrices with $K = 3$ columns.*

Proof: Among $\hat{\theta}_i = 2\theta_i = \frac{4\pi(i-1)}{N+1} \pmod{2\pi}$, $1 \leq i \leq N$, it is not hard to check that 3 adjacent angles, denoted by r_1, r_2 and r_3 with $r_1 = r_2$, give the maximum cost function

$$\cos(r_1 - r_2) + \cos(r_1 - r_3) + \cos(r_2 - r_3) = 2 \cos\left(\frac{4\pi}{N+1}\right) + 1.$$

This means the submatrix corresponding to such 3 adjacent angles generate the maximum condition number among all possible 3-column submatrices.

So in order to prove that $\hat{\theta}_i = 2\theta_i = \frac{4\pi(i-1)}{N+1} \pmod{2\pi}$, $1 \leq i \leq N$, minimizes the maximum condition number among all 3-column submatrices, it is enough to show $\hat{\theta}_i = 2\theta_i = \frac{4\pi(i-1)}{N+1} \pmod{2\pi}$, $1 \leq i \leq N$, minimizes the maximum condition number among all the adjacent-3-angle sets. Let us assume that N angles $0 \leq \tilde{\theta} = 2\theta_i^* < 2\pi$, $1 \leq i \leq N$ achieves the smallest maximum condition number among all the adjacent-

3-angle sets. Without sacrificing generality, let $\tilde{\theta}_1 = 0$ and $\tilde{\theta}_i$ be arranged sequentially in a counter-clockwise order as i goes from 1 to N .

Lemma 4.5.1 *In the optimal design $\tilde{\theta}_i$, $1 \leq i \leq N$, the counter-clockwise region covered by any three adjacent angles is no bigger than π for $N = 7$; and smaller than π for $N \geq 9$. The only scenario where the counter-clockwise region covered by one adjacent-3-angle set is π is when $N = 7$ and the 7 angles are respectively $0, 0, \pi/2, \pi/2, \pi, \pi$ and $\frac{3\pi}{2}$ (up to rotations of these angles).*

Proof: Suppose instead in the optimal design, the counter-clockwise region covered by some three adjacent angles r_1, r_2 and r_3 is larger than π . Then there must exist 3 adjacent angles for which the counter-clockwise region covered by them is smaller than $\frac{3\pi}{N-1} \leq \frac{\pi}{2}$ because the sum of the counter-clockwise regions covered by all the 3 adjacent angles is 4π (Please see the proof in Theorem 4.3.1). This means that the cost function for r_1, r_2 and r_3 is larger than $2 \cos(\frac{3\pi}{N-1}) + 1$ (when r_2 is aligned with r_1 or r_3). Note that, $2 \cos(\frac{3\pi}{N-1}) + 1$ is equal to the maximum cost function $2 \cos(\frac{4\pi}{N+1}) + 1$ given by the to-be-proven optimal design $\hat{\theta}_i = 2\theta_i = \frac{4\pi(i-1)}{N+1} \bmod 2\pi$, $1 \leq i \leq N$, when $N = 7$; and is bigger than $2 \cos(\frac{4\pi}{N+1}) + 1$ when $N \geq 9$. This is contradictory to our optimal design. So in the optimal design $\hat{\theta}_i = 2\theta_i = \frac{4\pi(i-1)}{N+1} \bmod 2\pi$, the counter-clockwise region covered by any three adjacent angles is no bigger than π for $N \geq 7$.

When $N = 7$ and the counter-clockwise region covered by one adjacent-3-angle set is π , the counter-clockwise region covered by each one of the other adjacent-3-

angle sets is forced to be $\frac{\pi^i}{2}$, The only way for that to happen is that the 7 angles $\tilde{\theta}_i$, $1 \leq i \leq N$, are $0, 0, \pi/2, \pi/2, \pi, \pi$ and $\frac{3\pi}{2}$ (up to rotations of these angles).

Note that the same argument can show that the counter-clockwise region covered by any three adjacent angles is smaller than π for $N \geq 9$.

In the optimal design $\tilde{\theta}_i$, $1 \leq i \leq N$, there are N sets of 3 adjacent angles, and we denote each set by its counter-clockwise central angle. For example, we denote the set of three angles $\{\tilde{\theta}_{(j-1) \bmod N}, \tilde{\theta}_j, \tilde{\theta}_{(j+1) \bmod N}\}$ for some $1 \leq j \leq N$ as its central angle $\{\tilde{\theta}_j\}$. We assume that $\tilde{\theta}_1, \tilde{\theta}_2$ and $\tilde{\theta}_3$ are three angles which correspond to the largest condition number.

We now prove the following lemma:

Lemma 4.5.2 *In the optimal design $\tilde{\theta}_i$, $1 \leq i \leq N$, $N \geq 7$, there do not exist ≥ 2 consecutive adjacent-3-angle sets (for example $\{\tilde{\theta}_j\}$ and $\{\tilde{\theta}_{(j+1) \bmod N}\}$ for some $1 \leq j \leq N$) which have smaller condition numbers than the maximum condition number.*

Proof: We prove by contradiction. Suppose that for some j , $\{\tilde{\theta}_j\}$ and $\{\tilde{\theta}_{(j+1) \bmod N}\}$ both have smaller condition numbers than the maximum condition number. We also assume that one of $\{\tilde{\theta}_{(j-1) \bmod N}\}$ and $\{\tilde{\theta}_{(j+2) \bmod N}\}$ is an adjacent-3-angle set corresponding to the maximum condition number. Notice that we can always find such a j if there exist ≥ 2 consecutive adjacent-3-angle sets which have smaller condition numbers than the maximum condition number.

By Lemma 4.5.1, any adjacent angle widths γ_1 and γ_2 satisfy $\gamma_1 + \gamma_2 \leq \pi$. The cost function for $\cos(\gamma_1) + \cos(\gamma_2) + \cos(\gamma_1 + \gamma_2)$ strictly decreases if we increase γ_1 and γ_2 simultaneously by a sufficiently small amount.

Suppose that $\{\tilde{\theta}_j\}$ spans two regions with counter-clockwise angle width $\alpha \geq 0$ and $\beta \geq 0$; and that $\{\tilde{\theta}_{(j+1) \bmod N}\}$ spans two regions with counter-clockwise angle width β and γ .

If $\beta > 0$, we can always reduce β by a sufficiently small enough amount and increase every region involved in all the adjacent-3-angle sets corresponding to the maximum condition number by an appropriate small amount such that the angle widths of the N regions still sum up to 2π . In this way, we have just strictly decreased the maximum condition number among all the adjacent-3-angle sets. This is contradictory to the optimal design assumption.

If $\beta = 0$, since every two adjacent angles are no more than π apart, $\{\tilde{\theta}_{(j-1) \bmod N}\}$ has no bigger condition number than $\{\tilde{\theta}_j\}$ and $\{\tilde{\theta}_{(j+2) \bmod N}\}$ has no bigger condition number than $\{\tilde{\theta}_{(j+1) \bmod N}\}$. This is contradictory to the assumption that $\{\tilde{\theta}_j\}$ and $\{\tilde{\theta}_{(j+1) \bmod N}\}$ both have smaller condition numbers than the maximum condition number; and one of $\{\tilde{\theta}_{(j-1) \bmod N}\}$ and $\{\tilde{\theta}_{(j+2) \bmod N}\}$ is an adjacent-3-angle set corresponding to the maximum condition number.

Lemma 4.5.3 *Let $N = 7$. Suppose $\tilde{\theta}_i$, $1 \leq i \leq N$, is an optimal design which minimizes the maximum condition number among all adjacent-3-angle sets. Then there exists at most 1 adjacent-3-angle set which has smaller condition number than the maximum condition number among all adjacent-3-angle sets.*

Proof: We prove this lemma by contradiction.

Without loss of generality, suppose that $\{\tilde{\theta}_1\}$ has a condition number smaller than the maximum condition number and there exist ≥ 2 adjacent-3-angle sets which have smaller condition numbers than the maximum condition number among all adjacent-3-angle sets. Then there must exist a sequence of consecutive angles, say $\tilde{\theta}_i$, $1 \leq i \leq l$, for some $3 \leq l \leq N$, such that any adjacent-3-angle set $\{\tilde{\theta}_j\}$, $2 \leq j \leq l-1$ has the maximum condition number while the first counter-clockwise adjacent-3-angle set $\{\tilde{\theta}_l\}$ and the first clockwise adjacent-3-angle set $\{\tilde{\theta}_1\}$ have smaller condition numbers than the maximum condition number.

Since $\{\tilde{\theta}_j\}$, $2 \leq j \leq l-1$, have the *equal* maximum condition number, the counter-clockwise regions between $\{\tilde{\theta}_j\}$, $1 \leq j \leq l$ must alternate between $\alpha \geq 0$ and $\beta \geq 0$, where $\alpha + \beta \leq \pi$. Without loss of generality, we assume that $\alpha \geq \beta$. For now we also assume that $\alpha + \beta < \pi$. From Lemma 4.5.1, when $\alpha + \beta = \pi$, only 1 adjacent-3-angle set has a smaller than the maximum condition number.

We first consider the case where l is an odd number, namely we have an even number of regions between angle $\tilde{\theta}_1$ and angle $\tilde{\theta}_l$. Since $\alpha + \beta < \pi$, we claim that β must be equal to 0. Suppose instead $\beta \neq 0$. Then we can shift the even-number-indexed angles $\tilde{\theta}_j$, $1 \leq j \leq l$, counter-clockwise by a sufficiently small amount. This will strictly decrease the condition numbers for $\{\tilde{\theta}_j\}$, $2 \leq j \leq l-1$. Since $\{\tilde{\theta}_l\}$ and $\{\tilde{\theta}_1\}$ also have strictly smaller condition numbers than the maximum condition number, thus we have ≥ 2 consecutive adjacent-3-angle sets which have the smaller condition number than the maximum condition number. This forms a contradiction

by Lemma 4.5.2.

So we must have $\beta = 0$. However, this implies $\{\tilde{\theta}_{(l+1) \bmod N}\}$ has a condition number no bigger than that of $\{\tilde{\theta}_l\}$. Thus we have two consecutive adjacent-3-angle sets $\{\tilde{\theta}_l\}$ and $\{\tilde{\theta}_{(l+1) \bmod N}\}$ which have smaller condition numbers than the maximum condition number. This forms a contradiction by Lemma 4.5.2.

We then consider the case where l is an even number. Since $l \geq 3$, such a number can only be $l = 4$ or $l = 6$.

When $l = 4$, then $\{\tilde{\theta}_6\}$ must also have a smaller condition number than the maximum condition number. This is because, from Lemma 4.5.2, $\{\tilde{\theta}_5\}$ and $\{\tilde{\theta}_7\}$ can not have smaller condition numbers than the maximum condition number. Moreover, if $\{\tilde{\theta}_6\}$ also has the maximum condition number, $\{\tilde{\theta}_j \bmod N\}$, $4 \leq j \leq N + 1$, are then consecutive angles such that $\{\tilde{\theta}_5\}$, $\{\tilde{\theta}_6\}$ and $\{\tilde{\theta}_7\}$ all have the maximum condition numbers, which is not possible by our previous discussion of the cases when l is an odd number.

However, when $\{\tilde{\theta}_6\}$ has a smaller condition number than the maximum condition number, there are an even number (in fact, 2,) of regions between angle $\tilde{\theta}_4$ and angle $\tilde{\theta}_6$, which is not possible by our previous discussion.

So in summary, the original assumption of ≥ 2 adjacent-3-angle sets having larger than maximum condition number cannot hold. There exists at most 1 adjacent-3-angle set which has smaller condition number than the maximum condition number.

If every adjacent-3-angle set has the same condition number as the maximum condition number, then the region between every angle must be equal. So the cost

function for the maximum condition number should be $2 \cos(\frac{2\pi}{7}) + \cos(\frac{4\pi}{7})$.

If there is exactly 1 adjacent-3-angle set which has a smaller condition number than the maximum condition number, and $\{\tilde{\theta}_1\}$ is the unique adjacent-3-angle set that has the smallest condition number, then $\tilde{\theta}_i$, $1 \leq i \leq 7$, can be respectively denoted by 0 , α , $\alpha + \beta$, $2\alpha + \beta$, $2(\alpha + \beta)$, $3\alpha + 2\beta$, and $3\alpha + 3\beta$, where $\alpha \geq 0$, $\beta \geq 0$ and $\alpha > \beta$ and $4\alpha + 3\beta = 2\pi$. The cost function for the maximum condition number $\cos(\alpha) + \cos(\beta) + \cos(\alpha + \beta)$ is thus minimized when $\beta = 0$ and $\alpha = \frac{2\pi}{4}$ for $\alpha \geq 0$, $\beta \geq 0$ and $\alpha > \beta$ and $4\alpha + 3\beta = 2\pi$. This cost function is smaller than the cost function of $2 \cos(\frac{2\pi}{7}) + \cos(\frac{4\pi}{7})$, so $\theta_i = \frac{2\pi(i-1)}{N+1} \bmod 2\pi$, $1 \leq i \leq N$ is indeed the optimal design.

4.6 $K = 3$, $N \geq 9$ is an Odd Number

Theorem 4.6.1 *Let $K = 3$ and $N \geq 9$ be an odd number. Then the set of angles $\theta_i = \frac{2\pi(i-1)}{N+1} \bmod \pi$, $1 \leq i \leq N$, minimizes the maximum condition number among all sub-matrices with $K = 3$ columns.*

Proof: The proof of this theorem follows the proof of Theorem 4.5.1. The complication compared with Theorem 4.5.1 comes from the fact that we need to prove the following lemma instead of Lemma 4.5.3.

Lemma 4.6.1 *Let us take $N \geq 9$. Suppose that $\tilde{\theta}_i$, $1 \leq i \leq N$, is an optimal design which minimizes the maximum condition number among all adjacent-3-angle sets. Then there exists at most 1 adjacent-3-angle set which has a smaller condition number than the maximum condition number among all adjacent-3-angle sets.*

Proof: We prove this lemma by contradiction.

Suppose that there exists ≥ 2 adjacent-3-angle sets which have smaller condition numbers than the maximum condition number among all adjacent-3-angle sets. From Lemma 4.5.2, we can always partition the N angles into distinct blocks by using $\tilde{\theta}_j$'s with $\{\tilde{\theta}_j\}$ having a strictly smaller condition number than the maximum condition number as the boundary angles between different blocks. From Lemma 4.5.2, there must exist at least one angle between two boundary angles. Without loss of generality, suppose $\tilde{\theta}_1$ and $\tilde{\theta}_l$, $3 \leq l \leq N$, are two neighboring boundary angles. Since $\{\tilde{\theta}_j\}$, $2 \leq j \leq l-1$, have the *equal* maximum condition number, the counter-clockwise regions between $\{\tilde{\theta}_j\}$, $1 \leq j \leq l$ must alternate between $\alpha \geq 0$ and $\beta \geq 0$, where $\alpha + \beta < \pi$ according to Lemma 4.5.1.

We first consider the case when l is an odd number, namely we have an even number of regions between angle $\tilde{\theta}_1$ and angle $\tilde{\theta}_l$. Without loss of generality, we assume that $\alpha \geq \beta$ when l is an odd number. Since $\alpha + \beta < \pi$, from the same reasoning as in the proof of Lemma 4.5.3 we know this is not possible.

We then consider the case when l is an even number. If l is an even number, we divide into two scenarios: $\alpha \geq \beta$ or $\alpha \leq \beta$.

If $\alpha \leq \beta$, we can simultaneously shift the even-numbered angles $\tilde{\theta}_j$, $j = 2, 4, \dots, l-2$, clockwise by the same sufficiently small angle $\delta > 0$. Note that this shift will not increase the maximum condition number if δ is sufficiently small. However, this will create two consecutive adjacent-3-angle sets $\{\tilde{\theta}_2\}$ and $\{\tilde{\theta}_1\}$ which have smaller condition numbers than the maximum condition number. According to Lemma 4.5.2,

this is contradictory to our assumption of an optimal design.

We now assume $\alpha > \beta$ and the number of regions in each block is an odd number. Consider two neighboring blocks separated by a single angle j such that $\{\tilde{\theta}_j\}$ is an adjacent-3-angle set which has a smaller condition number than the maximum condition number. Suppose that the second block is in the clockwise direction of the first block. The counter-clockwise region in the first block alternates between α and β ; the counter-clockwise region in the second block alternates between α_1 and β_1 with $\alpha_1 \geq \beta_1$ (otherwise we are done by the discussion in last paragraph). Since the adjacent-3-angle sets inside each block have the maximum condition number, without loss of generality, we have $\alpha_1 \leq \alpha$, and $\beta_1 \geq \beta$. If we change the regions of the 2-nd block to be $\beta_1, \alpha_1, \beta_1, \alpha_1, \dots, \alpha_1$, and α_1 . Since $\alpha_1 \leq \alpha$ and $\beta_1 \geq \beta$, in this change, we do not increase the condition number of $\{\tilde{\theta}_j\}$. It is not hard to check that as long as $\alpha_1 + \beta_1 < \pi$, the cost function $\cos(\alpha_1) + \cos(\alpha_1) + \cos(2\alpha_1)$ is smaller than the cost function $\cos(\alpha_1) + \cos(\beta_1) + \cos(\alpha_1 + \beta_1)$. So in this change, we do not increase the maximum condition number among adjacent-3-angle sets, while creating two consecutive adjacent-3-angle sets at the clockwise end of the second block, which is a contradiction from Lemma 4.5.2.

So in summary, there exists at most 1 adjacent-3-angle set which has smaller condition number than the maximum condition number.

So in the optimal design, the angles must alternate like $\alpha, \beta, \dots, \alpha, \beta, \alpha$, where $\alpha \geq \beta$, and $\frac{N+1}{2}\alpha + \frac{N-1}{2}\beta = 2\pi$. For $N \geq 9$, the optimal angle allocation for α is $\frac{4\pi}{N+1}$ and $\beta = 0$.

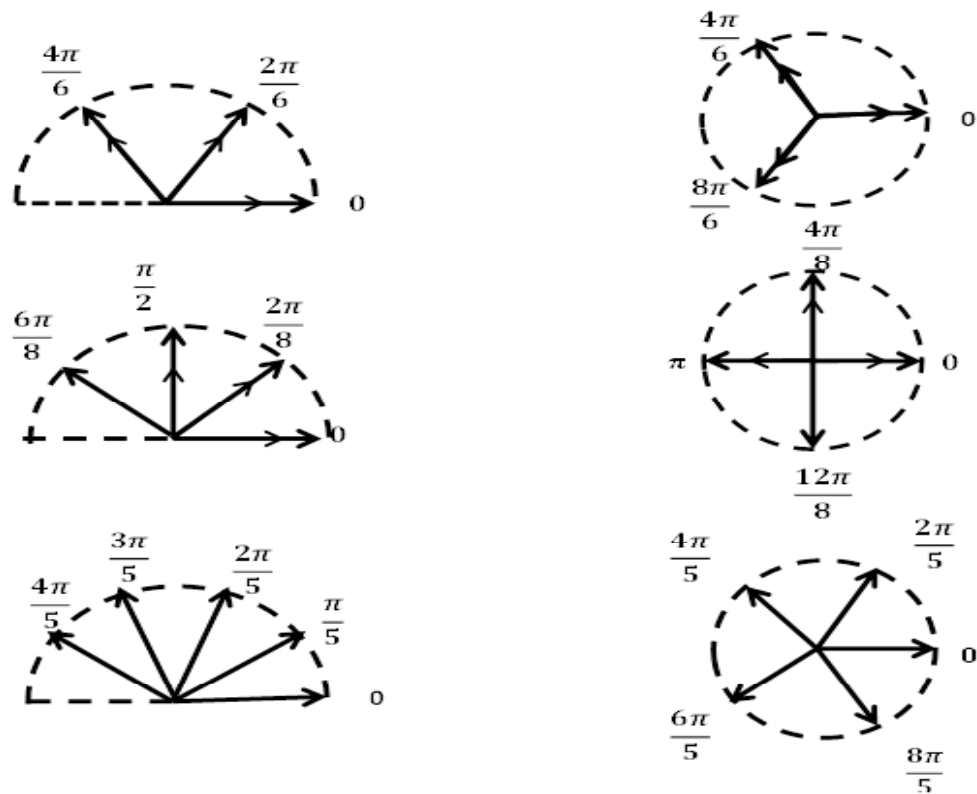


Figure 4.2: Illustration of angular separation between columns of the sensing matrix/sensors in the network. Top left and right figures represent the proposed angular separation for the columns of the sensing matrix (optimum sensor placement with 6 columns/sensors) and the doubled angles respectively. Middle figures represents design for the matrix with 7 columns while the bottom figures represent the optimum design for 5 columns/sensors.

Figure. 4.2 shows the proposed optimum angular separation between columns of the sensing matrix/sensors in the network that produce the best worst case condition number.

4.7 Simulation Results

We now present simulation results for 3 experiments.

1. We plot the worst case condition number versus the number of sensors in the network (N).
2. We plot the worst mean square signal estimation error versus the number of sensors in the network (N).
3. We also plot the mean square error in source location estimation versus the Signal to Noise Ratio.

4.7.1 Worst Case Condition Number vs N

We compare the maximum condition number among all the possible 2×3 submatrices in three different cases shown in Figure.4.4. The cases are, (i) when successive sensors are placed in a semicircle π/N apart, (ii) they are placed $2\pi/N$ apart, and (iii) they are placed in a manner specified by our theorems. That the performance of (ii) matches (iii) for even N conforms with earlier observations.

4.7.2 Worst mean square signal estimation error vs N

Consider the setting of Section 4.1 We compare in Figure. 4.5 the worst case mean square error (MSE) yielded by (i) above with that yielded by the postulated op-

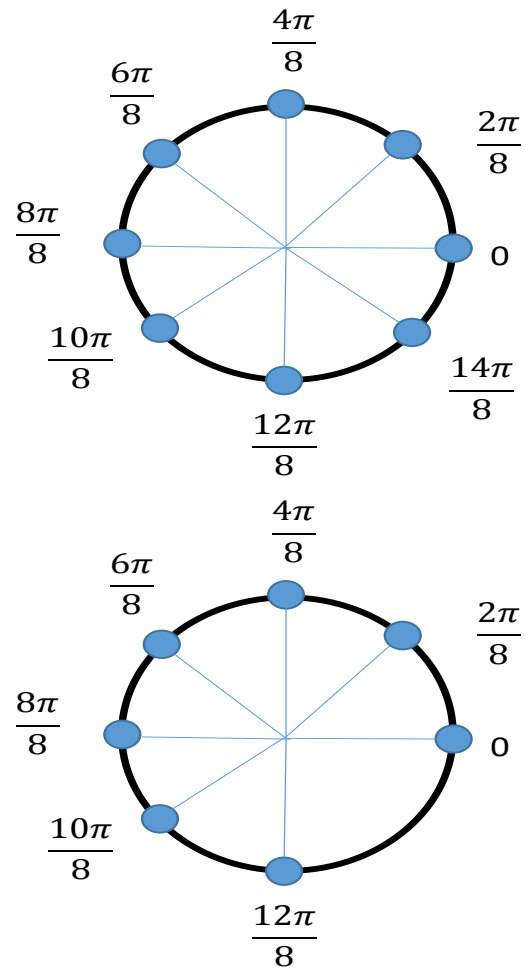


Figure 4.3: Illustration of the proposed solution for a 8 node network and a 7 node network angles in the range $[0, 2\pi)$

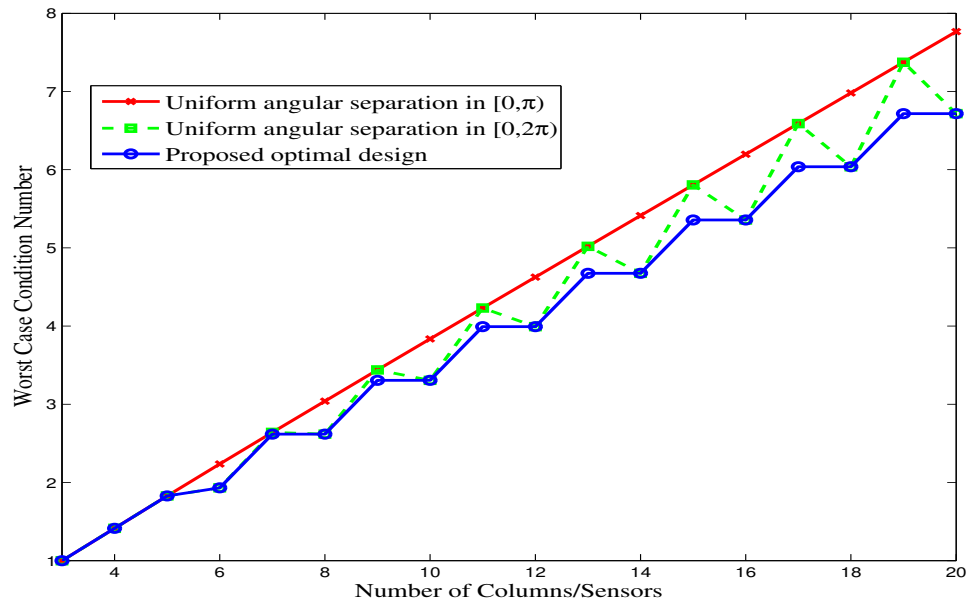


Figure 4.4: Worst case Condition Number Versus N

timum for sensors ranging in number from 3 to 15. The signal x in (4.1) is $[9, 9]^T$. The noise in each measurement is $\mathcal{N} \sim (0, 1)$. For each value N , the worst case estimation error $\|\hat{x} - x\|_2$ was averaged over 2000 iterations. Again the predicted optimal placement is superior.

4.7.3 Monitoring Error vs SNR

Fig. 4.6 compares the Maximum Likelihood estimation of a source at the origin with 10 sensor network, from RSS under log-normal shadowing in the case where the sensors are placed as in (i) against optimal placement. The latter's superiority is evident. The simulations are performed using gradient descent method on the ML cost function. The Signal to Noise Ratio (SNR) is defined as ratio of the average

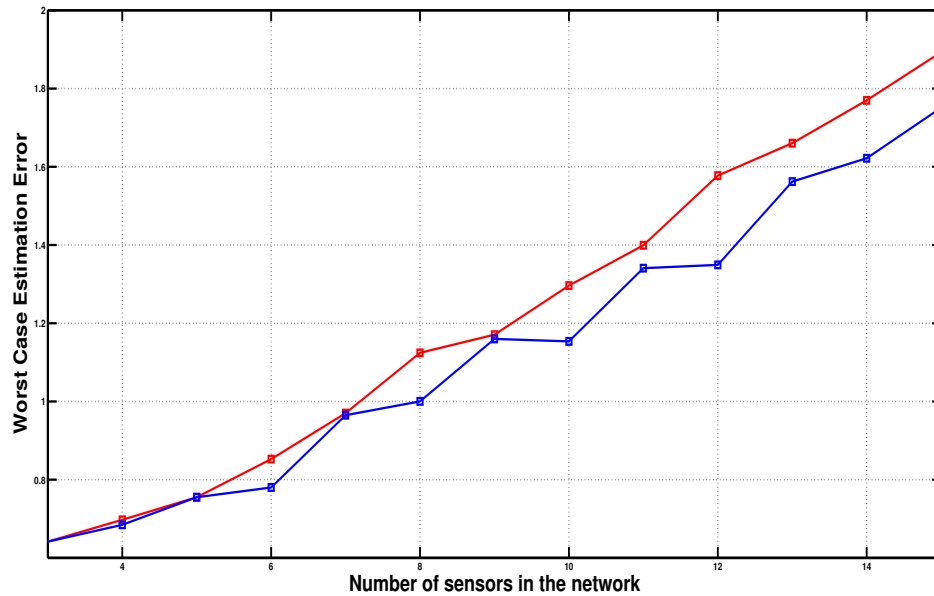


Figure 4.5: Worst case estimation error versus the number of columns in the sensing matrix.

signal strength over all the nodes in the network to the standard deviation of the gaussian term in log-normal shadowing model.

4.8 Conclusions

In this chapter we proposed the problem of designing optimal $2 \times N$ ($M \leq N$) sensing matrices which minimize the maximum condition number of all the submatrices of $K = 3$ columns. Such matrices minimize the worst-case estimation errors when only K sensors out of N sensors are available for sensing at a given time. An interesting observation to make is that minimizing the maximum coherence between columns does not always guarantee minimizing the maximum condition number which would have been the case if all the sensors were active.

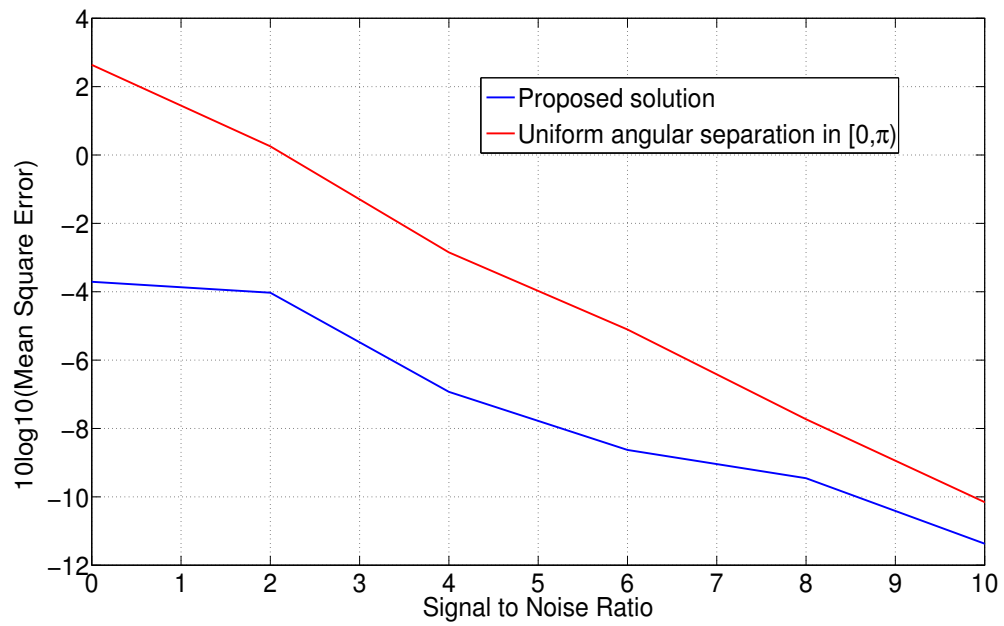


Figure 4.6: Mean square error(dB) in the source location estimate when the worst performing subset of sensors are active versus the Signal to Noise Ratio(dB).

CHAPTER 5 COPRIME CONDITIONS FOR FOURIER SAMPLING FOR SPARSE RECOVERY

As discussed in Chapter 1, the spark of a matrix is the smallest number of linearly dependent columns of a matrix. An alternate interpretation of the definition of the spark is *if the spark of a matrix is m , then any subset of $m - 1$ columns of the matrix are linearly independent*. This chapter considers the spark of $L \times N$ submatrices of the $N \times N$ Discrete Fourier Transform (DFT) matrix. The motivation comes from applications of compressed sensing such as MRI and synthetic aperture radar, where device physics dictates the measurements to be Fourier samples of the signal. Consequently the observation matrix comprises certain rows of the DFT matrix. To recover an arbitrary k -sparse signal, the spark of the observation matrix must exceed $2k + 1$. The technical question addressed in this work is how to choose the rows of the DFT matrix so that its spark equals the maximum possible value $L + 1$. This exposes certain coprimeness conditions that guarantee such a property.

5.1 Introduction

Depending on the method used to acquire the MR image, one can choose an appropriate transform domain that transforms the MR image into a sparse image that is compressible. Some such transform domains include Wavelet Transform and Fourier Transform. The inherent sparsity of the MR images in an appropriately chosen transform domain, motivates this chapter which is to provide a method for

designing a compressive sensing measurement matrix by choosing a subset of rows from the Discrete Fourier Transform (DFT) matrix.

Compressive sensing is a non-adaptive linear projection mechanism that samples signals at a lower rate than the Nyquist sampling rate. Recently, the compressive sensing problem has seen a wide variety of applications that include pattern recognition, machine learning, locality selective hashing, processing radar data, sensor networks, (Magnetic Resonance Imaging) MRI, spectrum sensing in cognitive radio applications, channel estimation and error correcting codes [31], [32].

A signal $N \times 1$ is said to be " k -sparse" if it can be written as a linear combination of $k \ll n$ basis vectors. In other words, a signal is k -sparse if $N - k$ elements of the signal are zero [32].

For the problem set up, consider a k -sparse $N \times 1$ vector x . Let A be a $M \times N$ ($M < N$) measurement or sensing matrix. Then the output of the measurement process defined by A is a $M \times 1$ vector y given by

$$y = Ax. \quad (5.1)$$

The measurement matrix A such be such that every k sparse $N \times 1$ vector x can be recovered from the observed $M \times 1$ vector. As discussed in chapter 1, the objective here is to design a measurement matrix A such that $\text{spark}(A) = M + 1$. Recollecting the definition of spark of a matrix, the spark of a matrix is the smallest number of linearly dependent columns of the matrix. More formally, the spark of a matrix A is given

$$\text{spark}(A) = \min_{s \neq 0} \|s\|_0 \quad (5.2)$$

such that $As = 0$.

Thus if the spark of a matrix is M , then any subset of $M - 1$ columns of the matrix are linearly independent.

5.2 Related Work

The observation matrices are submatrices of the $N \times N$ DFT matrix denoted by W_N . Specifically, with rows and column indices taking values from the set $\mathbb{Z}_N = \{0, 1, \dots, N - 1\}$, the il -th element of W_N is $e^{\frac{j2\pi il}{N}}$. Observe that these are the N -th roots of unity. We will assume that the observation matrix $A(\mathcal{M}, N)$ is obtained by retaining the rows of W_N that are indexed by $\mathcal{M} \subset \mathbb{Z}_N$. The key technical issue addressed in this paper is: *What conditions on \mathcal{M} and N ensure that $A(\mathcal{M}, N)$ has full spark?* In this section we summarize some key known results related to this question.

Suppose for some i and l , $\mathcal{M} = \{i, i+1, \dots, i+l-1\}$ i.e. contains consecutive elements of \mathbb{Z}_N . Define

$$z_n = e^{j\frac{2\pi n}{N}} \quad (5.3)$$

Then the matrix comprising any l columns of $A(\mathcal{M}, N)$, indexed by the integers

i_1, \dots, i_l can be expressed as

$$\begin{bmatrix} 1 & 1 & \cdots & 1 \\ z_{i_1} & z_{i_2} & \cdots & z_{i_l} \\ \vdots & \vdots & \vdots & \vdots \\ z_{i_1}^{l-1} & z_{i_2}^{l-1} & \cdots & z_{i_l}^{l-1} \end{bmatrix} \mathbf{diag} \{z_{i_1}^i, z_{i_2}^i, \dots, z_{i_l}^i\}. \quad (5.4)$$

and being a product of a Vandermonde and a nonsingular diagonal matrix, is thus non-singular for distinct z_{i_n} . Consequently, such an $A(\mathcal{M}, N)$ has full spark.

A less obvious result can be traced back to Chebotarëv in the early 20th century, (see [57]).

Theorem 5.2.1 *Suppose N is prime. Then for all $\mathcal{M} \subset \mathbb{Z}_N$, $A(\mathcal{M}, N)$ has full spark.*

The most sophisticated results are in [58]. As with Theorem 5.2.1 these results expose the role of prime factors of N and their relation to the set \mathcal{M} . The first is a set of necessary conditions.

Theorem 5.2.2 *Suppose for some $\mathcal{M} \subset \mathbb{Z}_N$, $A(\mathcal{M}, N)$ has full spark. Then so does:*

- (i) $A((\mathcal{M} + i) \bmod N, N)$ for all $i \in \mathbb{Z}_N$, i.e. the full spark condition is preserved under all translations.
- (ii) $A(M\mathcal{M}, N)$ for all M that is coprime with N .
- (iii) $A(\mathbb{Z}_N \setminus \mathcal{M}, N)$.

This theorem permits one to build entire classes of \mathcal{M}_i for which $A(\mathcal{M}_i, N)$ is full spark, from any \mathcal{M} for which $A(\mathcal{M}, N)$ is full spark.

The next result of note from [58] requires a definition. Observe a divisor d of N , partitions \mathbb{Z}_N into d cosets, the i -th coset being defined as

$$\mathcal{C}_i(d, N) = \{l \in \mathbb{Z}_N \mid l \bmod d = i\}, \quad i \in \{0, 1, \dots, d-1\}. \quad (5.5)$$

We say that \mathcal{M} is *uniformly distributed over the divisor d* if for each i the cardinality of $\mathcal{C}_i(d, N) \cap \mathcal{M}$ is either

$$\left\lceil \frac{|\mathcal{M}|}{d} \right\rceil \quad \text{or} \quad \left\lfloor \frac{|\mathcal{M}|}{d} \right\rfloor.$$

Then [58] proves the following remarkable theorem.

Theorem 5.2.3 *The matrix $A(\mathcal{M}, N)$ has full spark only if \mathcal{M} is uniformly distributed over all divisors of N . If N is a prime power then $A(\mathcal{M}, N)$ has full spark iff \mathcal{M} is uniformly distributed over all divisors of N .*

Furthermore, [58] disproves the conjecture that \mathcal{M} being uniformly distributed over all divisors of N suffices for $A(\mathcal{M}, N)$ to have full spark, regardless of whether N is a prime power, through the following counterexample.

Example 5.2.1 *Consider $N = 10$, $\mathcal{M} = \{0, 1, 3, 4\}$. This \mathcal{M} is uniformly distributed over 2 and 5. Yet the columns of $A(\mathcal{M}, 10)$ indexed by the set $\{0, 1, 2, 6\}$ are linearly dependent.*

5.3 Some General Results

This section provides two types of results. The first extends a consequence of (ii) of Theorem 5.2.2 using the following Lemma which can be found in [59].

Lemma 5.3.1 Consider integers $1 \leq M < N$. Then there exists $1 \leq n < N$ such that N divides Mn iff M and N are not coprime.

Using this lemma we now prove the following theorem.

Theorem 5.3.1 Suppose for positive integers M, K , $\mathcal{M} = \{i, i + M, i + 2M, \dots, i + (K - 1)M\}$, with $i + (K - 1)M < N$. Then $A(\mathcal{M}, N)$ has full spark iff M and N are coprime. Further if $A(\mathcal{M}, N)$ does not have full spark, then $\mathbf{spark}(A) = 2$.

Proof: Sufficiency follows from the facts that consecutive rows of W_N have full spark, and (i) and (ii) of Theorem 5.2.2.

With $n \in \{0, \dots, N - 1\}$, under (5.3), the l -th column of $A(\mathcal{M}, N)$ is: $a_l = z_l^i \begin{bmatrix} 1 & z_l^M & \dots & z_l^{(k-1)M} \end{bmatrix}^\top$ Thus with

$$b_l = \begin{bmatrix} 1 & z_l^M & \dots & z_l^{(k-1)M} \end{bmatrix}^\top \text{ and } B = [b_0 \ b_1 \ \dots \ b_{N-1}]$$

there holds: $A(\mathcal{M}, N) = B \mathbf{diag} \{z_l^i\}_{l=0}^{N-1}$. Thus $\mathbf{spark}(A(\mathcal{M}, N)) = \mathbf{spark}(B)$.

Now the Vandermonde structure of B ensures that B has full spark only if for all

$$0 \leq p < q < N$$

$$z_p^M \neq z_q^M. \quad (5.6)$$

From (5.3) this is equivalent to the nonexistence of an integer l such that

$$Mq = Mp + Nl$$

$$\Leftrightarrow M(q - p) = Nl.$$

As $0 < n = q - p < N$, the result follows from Lemma 5.3.1 and the fact that the violation of (5.6) implies $\mathbf{spark}(A(\mathcal{M}, N)) = 2$.

It is evident from Theorem 5.2.2 that using the fact that with $\mathcal{M} = \{0, 1, \dots, K\}$, the full spark nature of $A(\mathcal{M}, N)$ permits the construction of a plethora of subsets of \mathbb{Z}_N that yield the full spark property. The hallmark of $\mathcal{M} = \{0, 1, \dots, K\}$ is that consecutive rows of W_N comprise the observation matrix. The rest of the chapter focuses on the following question: What if a *single frame* from $\{0, 1, \dots, K\}$ is missing? What conditions guarantee full spark observation matrices? These sufficient conditions, together with Theorem 5.2.2 then generate a rich class of further row indices that guarantee full spark observations. On a related note, observe that Example 5.2.1 also has a missing frame. Our results directly explain why it lacks full spark.

We directly relate the lack of full spark to the notion of *vanishing sums of roots of unity*, [60]. The N -th roots of unity, $\{s_i\}_{i=1}^L$, s_i not necessarily distinct, form a *vanishing sum* if

$$\sum_{i=1}^L s_i = 0, \quad (5.7)$$

We emphasize that in $\{s_i\}_{i=1}^L$, s_k may equal s_l , even if $k \neq l$. The Lemma below, from [60], provides a necessary condition on L for $\{s_i\}_{i=1}^L$ to form a vanishing sum. The lemma refers to *nonnegative integer combination* of integers p_i : r is a nonnegative integer combination of integers p_i if there exist nonnegative integers n_i such that

$$r = \sum_i n_i p_i.$$

Lemma 5.3.2 *The possibly nondistinct N -th roots of unity $\{s_i\}_{i=1}^L$ form a vanishing sum only if L is a nonnegative integer combination of the prime factors of N . Further, should L be a nonnegative integer combination of the prime factors of N , then there is always a possibly nondistinct collection of N -th roots of unity $\{s_i\}_{i=1}^L$, that form a vanishing sum.*

As will be evident in the sequel, there emerges a new condition for full spark Fourier submatrices, that involves the integer combination of the prime factors of N . Towards such a result we first provide a fairly general theorem concerning the setting where a solitary row is missing from the index set $\{0, 1, \dots, K\}$. The theorem refers to the sum of m -products of a set of complex numbers. This is the sum of the products of the elements belonging to all subsets of the set with cardinality m . For example, the sum of 2-products of $\{a_1, a_2, a_3\}$ is $a_1a_2 + a_1a_3 + a_2a_3$.

Theorem 5.3.2 *For integers $1 \leq n < K < N$ and $\mathcal{M} = \{0, 1, \dots, K\} \setminus \{n\}$, $A(\mathcal{M}, N)$ does not have full spark iff there exist K distinct N -th roots of unity whose n -products form a vanishing sum.*

Proof: Since it has K rows, $A(\mathcal{M}, N)$ does not have full spark iff it has K distinct columns that are linearly dependent. Suppose these columns are indexed from the set $\{n_1, \dots, n_k\} \subset \mathbb{Z}_N$. Under (5.3), l -th of these columns comprises the powers $z_{n_l}^i$, $i \in \{0, 1, \dots, K\} \setminus \{n\}$. Thus, their linear dependence is equivalent to the existence of a nonzero polynomial, $\theta(z)$ of degree K with the coefficient of z^n zero, whose roots are z_{n_l} for each $l \in \{1, \dots, K\}$. The result follows from the easily verified fact that

the n -th coefficient of such a nonzero polynomial is, to within a sign, the sum of the n -products of its roots.

Consider Example 5.2.1 in which $N = 10$, $K = 4$, and $n = 2$. With $l \in \{0, 1, 2, 6\}$, it is readily checked that the sum of the six 2-products of the z_l is indeed zero.

In view of Lemma 5.3.2, and the pair of facts that the n -products of K distinct N -th roots of unity are $\binom{K}{n}$ in number, and are themselves N -th roots of unity, the following sufficient condition is then immediate.

Theorem 5.3.3 *For integers $1 \leq n < K < N$ and $\mathcal{M} = \{0, 1, \dots, K\} \setminus \{n\}$, $A(\mathcal{M}, N)$ has full spark if $\binom{K}{n}$ is not a nonnegative integer combination of the prime factors of N .*

Again with $N = 10$, $K = 4$, and $n = 2$, Example 5.2.1 violates the sufficient condition in Theorem 5.3.3 as $6 = \binom{4}{2}$ is a positive integer multiple of 2, a prime factor of 10. This Theorem again brings into sharp relief the role played by the prime factors of N .

Finally, we show that should for $1 \leq n < K < N$, and $\mathcal{M} = \{0, 1, \dots, K\} \setminus \{n\}$, $A(\mathcal{M}, N)$ not have full spark, then in fact it has spark even lower than K . To this end we need a lemma.

Lemma 5.3.3 *Suppose a nonzero polynomial with degree K has all its roots on the unit circle. Suppose also the coefficient of power of z^n , $0 < n < K$, in this polynomial is zero. Then so is the coefficient of power of z^{K-n} .*

Proof: Suppose s_1, \dots, s_K are the roots of this polynomial. The coefficient of z^n is the sum of all n -products of the s_i . Thus this coefficient is zero iff the sum of all n -products of the s_i is zero. Thus this sum divided by $\prod_{i=1}^K s_i$ is also zero. As s_i are on the unit circle $1/s_i = s_i^*$. Thus this ratio is the conjugate of the sum of all the $K - n$ products of the s_i . The result follows.

Using this theorem and the proof technique of Theorem 5.3.2 the following theorem obtains.

Theorem 5.3.4 *For integers $1 \leq n < K < N$ and $\mathcal{M} = \{0, 1, \dots, K\} \setminus \{n\}$, suppose $A(\mathcal{M}, N)$ does not have full spark. Then with $\mathcal{M}_1 = \{0, 1, \dots, K\} \setminus \{n, K - n\}$, $A(\mathcal{M}_1, N)$ does not have full spark either.*

5.4 Specialization to the case where N is a product of two primes

Theorem 5.3.2 characterizes conditions under which the full spark condition is satisfied when a single row is excluded from K consecutive rows of the DFT matrix, and links it to vanishing sums. Theorem 5.3.3 provides a sufficient condition on N , K and n for the full spark condition to hold. Between them, these two theorems do not however provide a necessary and sufficient condition on the integers N , K and n .

To partially address this gap we consider the special case where N is the product of two distinct prime factors, i.e. with p and q distinct primes

$$N = pq. \tag{5.8}$$

In this case [60] provides an easy characterization of the N -th roots of unity that

form a vanishing sum. Specifically, consider the two sets:

$$Z_q = \{lq \mid l \in \{0, \dots, p-1\}\} \quad (5.9)$$

and

$$Z_p = \{lp \mid l \in \{0, \dots, q-1\}\}. \quad (5.10)$$

Observe, for any a, b , (see (5.3)),

$$a \sum_{i \in Z_q} z_i = 0 \text{ and } b \sum_{i \in Z_p} z_i = 0$$

Then the sets of possibly nondistinct $\{z_i\}_{i=1}^L$ that form a vanishing sum obey two conditions:

- (A) For some nonnegative integers α and β the total number L of these z_i is $\alpha p + \beta q$.
- (B) The set $\{1, 2, \dots, L\}$ can be partitioned into α sets $\{S_{pi}\}_{i=1}^\alpha$ and β sets $\{S_{qi}\}_{i=1}^\beta$ such that for some integer r_i , $S_{pi} = r_i + Z_p$ and for some integer t_i , $S_{qi} = t_i + Z_q$.

In view of Theorems 5.3.2 and 5.3.3, this almost immediately yields the following result:

Theorem 5.4.1 *For distinct primes p and q , integers $1 < K < N = pq$, and $\mathcal{M} = \{0, 1, \dots, K\} \setminus \{1\}$ or $\mathcal{M} = \{0, 1, \dots, K\} \setminus \{K-1\}$, $A(\mathcal{M}, N)$ does not have full spark iff K is not a nonnegative integer combination of p and q .*

Observe this theorem exploits the fact that if K numbers on the unit circle sum to zero, then so do their $K-1$ products. Note also that a somewhat surprising

coprimeness condition has emerged involving the nonnegative integer combinations of the prime factors of N . Further, for N a product of two primes, the condition in Theorem 5.3.3 is both necessary and sufficient for $n = 1$ and $n = K - 1$.

For $n > 1$, while $K < N$ distinct roots of unity can be chosen arbitrarily, the n sums in general cannot be. Thus even if $\binom{K}{n}$ is a nonnegative integer combination of p and q , the n -products of K , N -th roots of unity need not partition in a manner mandated by (A) and (B) above. Thus for the case when $n \in \{2, 3\}$ we provide a less conservative than Theorem 5.3.3.

Towards this end, consider the following lemmas whose proofs are in Appendix A.

Lemma 5.4.1 *Consider two primes p and q , integers $1 < K < N = pq$, a set of k distinct integers $S = \{i_0, \dots, i_{K-1}\} \subset \{0, \dots, N - 1\}$, with $i_0 = 0$ and the integers*

$$m_{rl} = (i_l + i_r) \pmod{N}, \quad \{i_l, i_r\} \subset S, \quad i_l \neq i_r.$$

Consider the set of 2-tuples

$$\mathcal{I} = \{\{i, l\} \mid 0 \leq i < l \leq k - 1\}. \quad (5.11)$$

Suppose one can partition \mathcal{I} into sets \mathcal{I}_i each having the following properties.

(A) *Either $|\mathcal{I}_i| = q$ or $|\mathcal{I}_i| = p$.*

(B) The set

$$\mathcal{M}_i = \{m_{lr} \mid \{l, r\} \in \mathcal{I}_i\} \quad (5.12)$$

either equals

$$Z_p = \left\{ \frac{lN}{p} = lq \mid l \in \{0, \dots, p-1\} \right\} \quad (5.13)$$

or equals

$$Z_q = \left\{ \frac{lN}{q} = lp \mid l \in \{0, \dots, q-1\} \right\}. \quad (5.14)$$

Then there exist nonnegative integers α, β such that:

$$\alpha p + \beta q = k. \quad (5.15)$$

Lemma 5.4.2 Consider two primes p and q , integers $1 < n \leq K < N = pq$, a set of K distinct integers $S = \{i_0, \dots, i_{K-1}\} \subset \{0, \dots, N-1\}$, with $i_0 = 0$ and the integers

$$m_{(l_1, l_2, l_3)} = (i_{l_1} + i_{l_2} + i_{l_3}) \pmod{N}, \quad \{i_{l_1}, i_{l_2}, i_{l_3}\} \subset S, \quad i_u \neq i_v \forall u \neq v.$$

Consider the set of 3-tuples

$$\mathcal{I} = \{\{l_1, l_2, l_3\} \mid 0 \leq l_1 < l_2 < l_3 \leq k-1\}. \quad (5.16)$$

Suppose one can partition \mathcal{I} into sets \mathcal{I}_i each having the following properties.

(A) Either $|\mathcal{I}_i| = q$ or $|\mathcal{I}_i| = p$.

(B) The set

$$\mathcal{M}_i = \{m_{(l_1, l_2, l_3)} \mid \{l_1, l_2, l_3\} \in \mathcal{I}_i\} \quad (5.17)$$

either equals

$$Z_p = \left\{ \frac{lN}{p} = lq \mid l \in \{0, \dots, p-1\} \right\} \quad (5.18)$$

or equals

$$Z_q = \left\{ \frac{lN}{q} = lp \mid l \in \{0, \dots, q-1\} \right\}. \quad (5.19)$$

Then there exist nonnegative integers α, β such that:

$$\alpha p + \beta q = k. \quad (5.20)$$

Theorem 5.4.2 Suppose p and q are distinct primes, $N = pq$, $n \in \{2, 3\}$, $1 \leq n < K < N$ and $\mathcal{M} = \{0, 1, \dots, K\} \setminus \{n\}$. Then $A(\mathcal{M}, N)$ has full spark if K is not a nonnegative integer combination of the prime factors of p and q .

Proof: Suppose for the purpose of contradiction that $A(\mathcal{M}, N)$ does not have full spark though K is not a nonnegative integer combination of the prime factors of p and q . Consider Theorem 5.3.2 which is $A(\mathcal{M}, N)$ does not have full spark iff there exist K distinct $N - th$ roots of unity whose $n-$ products form a vanishing sum. Under (5.3), we know that the $n-$ products translates to $n-$ sums. Thus the indices form the partitions in Lemma. 5.4.1 and 5.4.2. Thus K is a non-negative integer combination of p and q leads us to a contradiction.

This is theorem is less conservative than Theorem 5.3.3 as Theorem 5.3.3

allows $\binom{K}{n}$ to be a nonnegative integer combination of p and q , even if K is not.

5.5 Conclusion

We have derived certain coprimeness conditions that guarantee that full spark matrices result from appropriate Fourier sampling. In the first result we show that the rows of W_N chosen from the index set $\{i+nM, i+(n+1)M, \dots, i+(n+L-1)M\}$, yields a full spark matrix iff M and N are coprime. We then turn to the case where the index set comprises $\{0, \dots, K\} \setminus \{i\}$ where $1 < i < K$. Because of Theorem 5.2.2, the full spark nature of such a set yields several others with the same property. We show that full spark is equivalent to the existence of K , N -th roots of unity sum of whose i -products is zero. A sufficient condition is that $\binom{K}{i}$ not be a nonnegative integer combination of the prime factors of N . We strengthen this result for the special case when N is the product of two primes and $i \in \{1, 2, 3\}$ by showing that full spark results if K is not a nonnegative integer combination of p and q .

CHAPTER 6 SUMMARY AND FUTURE WORK

6.1 Summary

This thesis address the design of optimal sensing matrices in the context of two cases. The first is the source localization problem where the objective is to find an optimum sensor geometry in order to locate a source such the underlying Fisher Information Matrix (FIM) is optimized. The second is the design of a measurement matrix for compressed sensing in Magnetic Resonance Imaging (MRI).

The specific problems addressed are:

- Optimum sensor placement for source localization in $N \geq 2$ dimensions under log-normal shadowing.
- Energy aware optimum sensor placement for source monitoring in two dimensions under log-normal shadowing.
- Distributed control law for optimum sensor placement for source localization.
- Coprime Conditions for Fourier Analysis for Sparse Recovery for MRI.

Of these, the first problem presented in Chapter 2 is based on the assumption that the source could be hazardous and thus the sensors need to be sufficiently far away from the harmful effects of the source. We have assumed that the source location has a radially symmetric probability density function in a sphere of a given radius. We have characterized the expectation of the Fisher Information Matrix (FIM) for optimum sensor placement for source localization in $N > 2$ dimensions that simul-

taneously achieves optimality criteria on the minimum eigenvalue, determinant and trace of the inverse. Our analysis shows that the expectation of FIM needs to be a scaled identity. We have also proposed a canonical sensor placement solution using an iterative the placement strategy

$$x_i = Q^{i-1}x_1 \quad (6.1)$$

where Q is an orthogonal matrix and we call it the sensor placement matrix. x_1 is the position of the first sensor on the concentric sphere. While the canonical solution that we designed for the 2D problem represents optimum spherical codes, the study of 3 or higher dimensional design provides great insights into the design of measurement matrices with equal norm columns that have the smallest possible condition number.

In Chapter 3, we present a distributed control law that guides the motion of the sensors on the circumference of circle so that the sensors achieve the optimum sensor placement for 2-D source localization proposed in Chapter 2. The proposed algorithm has the least communication overhead. Each sensor communicates with one closest neighbor node in the clockwise direction and one closest neighbor in the counter clockwise direction. The proposed algorithm is a modification of the gradient descent algorithm. The gradient of the cost function is modified to include a repulsion function between the sensor nodes. This prevents collisions among sensors. We proved the stability of the proposed distributed control law using Lasalle's invariance theorem.

In chapter 4, we presented the solution for an energy aware optimum sensor

placement for source monitoring in two dimensions. The problem was to find an optimum geometry for the sensors in order to best monitor a source in the worst case. The worst case in this context being the case when only 3 sensors are active and the rest are either switched off for energy conservation or have been destroyed due to extreme environmental conditions. The solutions presented were based on the assumption that the source is at the origin/ center of a circle and the sensors need to be placed on the circumference of this circle. The placement was thus an angular geometry. The FIM is the same as in the case of the source localization problem. The geometry depended on the number of sensors that were to be deployed. Specifically, the angular geometry for the even case was different from that of the odd case. This work dealt with the estimation of a 2 dimensional signal.

In Chapter 5, we derived certain coprimeness conditions which guarantee that full spark matrices result from appropriate Fourier sampling. In the first result we show that the rows of Discrete Fourier Transform matrix denoted by W_N chosen from the index set $\{i + nM, i + (n + 1)M, \dots, i + (n + L - 1)M\}$, yields a full spark matrix iff M and N are coprime. We then turn to the case where the index set comprises $\{0, \dots, K\} \setminus \{i\}$ where $1 < i < K$. Because of Theorem 5.2.2, the full spark nature of such a set yields several others with the same property. We showed that full spark is equivalent to the existence of K , N -th roots of unity sum of whose i -products is zero. A sufficient condition is that $\binom{K}{i}$ not be a nonnegative integer combination of the prime factors of N . We strengthen this result for the special case when N is the product of two primes by showing that full spark results if K is not a nonnegative

integer combination of p and q .

6.2 Future Work

An interesting extension of the work in Chapter 2 includes study of optimum sensor placement for indoor localization where the source location follows probability density functions that are different from the radial symmetric distribution. Other interesting fields of extension are the design of optimum deployment strategies for base station and/or relays for next generation communication networks for improved energy efficiency, reduced latency and interference. Another interesting problem to pursue is the placement of high altitude satellites and drones around the earth for seamless connectivity around the world.

The work in Chapter 3 can be used to develop a discrete time distributed control algorithm for optimum sensor placement for source localization. The work in Chapter 2 focused on the estimation of a $2D$ signal using 3 or more sensors. This work can be extended to estimation of higher dimensional signals which have several sensing applications such as seismic tomography, ionospheric tomography to name a few. Another interesting extension of the work in Chapter 2 would be to consider the case where the number of sensors that are active denoted by K is more than 3 and less than $\frac{N}{2}$. This work provides insights into the functioning of the network when half or fewer sensors in the network are active.

Chapter 5 considered the selection procedure for the rows from the DFT matrix when the size of the matrix is a product of two primes. Interesting future direction

is to study the case where N , the size of the DFT matrix is a product of more than 2 primes.

APPENDIX

The derivative of $H(Re_i)$ with respect to R is positive for $1 < R < \sqrt{3}$

Proof:

Consider a density function

$$f_Z(z) = g(\|z\|), \quad \forall z \in \mathbb{R}^3.$$

In terms of spherical coordinates $v = [r, \alpha, \beta]$, there holds:

$$z = \begin{bmatrix} r \cos \alpha \cos \beta \\ r \sin \alpha \cos \beta \\ r \sin \beta \end{bmatrix} = \begin{bmatrix} z_1 \\ z_2 \\ z_3 \end{bmatrix}.$$

The Jacobian is the determinant of

$$J(v) = \begin{bmatrix} \cos \alpha \cos \beta & \sin \alpha \cos \beta & \sin \beta \\ -r \sin \alpha \cos \beta & r \cos \alpha \cos \beta & 0 \\ -r \cos \alpha \sin \beta & -r \sin \alpha \sin \beta & r \cos \beta \end{bmatrix}$$

Observe:

$$\det \left(\begin{bmatrix} \cos \alpha \cos \beta & \sin \alpha \cos \beta \\ -r \sin \alpha \cos \beta & r \cos \alpha \cos \beta \end{bmatrix} \right) = r \cos^2 \beta.$$

Then unless $\cos \beta = 0$,

$$\begin{aligned} |\det(J(v))| &= r \left| \cos \beta \left(r \cos^2 \beta + r \sin^2 \beta [\cos \alpha \quad \sin \alpha] \begin{bmatrix} \cos \alpha & \sin \alpha \\ -\sin \alpha & \cos \alpha \end{bmatrix}^{-1} \begin{bmatrix} 1 \\ 0 \end{bmatrix} \right) \right| \\ &= r^2 |\cos \beta| \end{aligned}$$

Thus:

$$f_V(v) = r^2 |\cos \beta| g(r), \quad \forall z \in \mathbb{R}^3.$$

We will now examine the integral below with $R > 1$, focussing on whether it decreases with R . In the development below we use the substitution, $a = \sin \beta$.

$$\begin{aligned} H(Re_3) &= \int_{-\pi/2}^{\pi/2} \frac{(R - \sin \beta)^2}{((R - \sin \beta)^2 + \cos^2 \beta)^2} |\cos \beta| d\beta \\ &= \int_{-\pi/2}^{\pi/2} \frac{(R - \sin \beta)^2}{((R - \sin \beta)^2 + \cos^2 \beta)^2} \cos \beta d\beta \end{aligned} \quad (2)$$

$$= \int_{-1}^1 \frac{(R - a)^2}{((R - a)^2 + 1 - a^2)^2} da \quad (3)$$

Now observe that:

$$\begin{aligned} \frac{(R - a)^2}{(R^2 - 2Ra + 1)^2} &= \left(\frac{a - R}{2Ra - R^2 - 1} \right)^2 \\ &= \frac{1}{4R^2} \left(\frac{a - R}{a - \frac{R^2+1}{2R}} \right)^2 \\ &= \frac{1}{4R^2} \left(1 + \frac{\frac{R^2+1}{2R} - R}{a - \frac{R^2+1}{2R}} \right)^2 \\ &= \frac{1}{4R^2} \left(1 + \frac{\frac{1-R^2}{2R}}{a - \frac{R^2+1}{2R}} \right)^2 \\ &= \frac{1}{4R^2} \left(1 + \frac{\frac{1-R^2}{R}}{a - \frac{R^2+1}{2R}} + \left(\frac{\frac{1-R^2}{2R}}{a - \frac{R^2+1}{2R}} \right)^2 \right) \end{aligned}$$

Thus with

$$b = \frac{R^2 + 1}{2R}, \quad (4)$$

and $c = b - a$ there holds

$$\begin{aligned}
H(Re_3) &= \frac{1}{4R^2} \left(1 + \frac{R^2 - 1}{R} \int_{-1}^1 \frac{da}{b-a} + \left(\frac{1-R^2}{2R} \right)^2 \int_{-1}^1 \frac{da}{(b-a)^2} \right) \\
&= \frac{1}{4R^2} \left(1 + \frac{R^2 - 1}{R} \int_{b-1}^{b+1} \frac{dc}{c} + \left(\frac{1-R^2}{2R} \right)^2 \int_{b-1}^{b+1} \frac{dc}{c^2} \right) \\
&= \frac{1}{4R^2} \left(1 + \frac{R^2 - 1}{R} \ln \left(\frac{b+1}{b-1} \right) + \left(\frac{1-R^2}{2R} \right)^2 \left(\frac{1}{b-1} - \frac{1}{b+1} \right) \right) \\
&= \frac{1}{4R^2} \left(1 + \frac{R^2 - 1}{R} \ln \left(\frac{b+1}{b-1} \right) + 2 \left(\frac{1-R^2}{2R} \right)^2 \frac{1}{b^2 - 1} \right) \\
&= \frac{1}{4R^2} \left(1 + 2 \frac{R^2 - 1}{R} \ln \left(\frac{R+1}{R-1} \right) + 2 \left(\frac{1-R^2}{2R} \right)^2 \frac{1}{\left(\frac{R^2+1}{2R} \right)^2 - 1} \right) \\
&= \frac{1}{4R^2} \left(1 + 2 \frac{R^2 - 1}{R} \ln \left(\frac{R+1}{R-1} \right) + 2 \frac{(1-R^2)^2}{(R^2+1)^2 - 4R^2} \right) \\
&= \frac{1}{4R^2} \left(1 + 2 \frac{R^2 - 1}{R} \ln \left(\frac{R+1}{R-1} \right) + 2 \frac{(1-R^2)^2}{(R^2-1)^2} \right) \\
&= \frac{3}{4R^2} + \frac{R^2 - 1}{2R^3} \ln \left(\frac{R+1}{R-1} \right)
\end{aligned}$$

Now consider

$$\begin{aligned}
\frac{dH(Re_3)}{dR} &= -\frac{9}{4R^3} \\
&+ \frac{(R^2 - 1)(R - 1)}{2R^3(R + 1)} \frac{R - 1 - R - 1}{(R - 1)^2} + \ln \left(\frac{R + 1}{R - 1} \right) \frac{2R^4 - 3R^2(R^2 - 1)}{2R^6} \\
&= -\frac{9}{4R^3} - \frac{1}{R^3} + \ln \left(\frac{R + 1}{R - 1} \right) \frac{3R^2 - R^4}{R^4} \\
&= -\frac{13}{4R^3} + \ln \left(\frac{R + 1}{R - 1} \right) \frac{3 - R^2}{R^2}
\end{aligned}$$

Clearly for $1 < R < \sqrt{3}$,

$$\frac{dH(Re_3)}{dR} > 0. \quad (5)$$

Proofs of Lemma. 5.4.1

Theorem .0.1 Consider two primes p and q , integers $1 < n \leq k < N = pq$, a set of k distinct integers $S = \{i_0, \dots, i_{k-1}\} \subset \{0, \dots, N-1\}$, with $i_0 = 0$ and the integers

$$m_{(l_1, l_2, \dots, l_n)} = (i_{l_1} + i_{l_2} + \dots + i_{l_n}) \pmod{N}, \quad \{i_{l_1}, i_{l_2}, \dots, i_{l_n}\} \subset S, \quad i_{l_u} \neq i_{l_v} \forall u \neq v.$$

Consider the set of n -tuples

$$\mathcal{I} = \{\{l_1, \dots, l_n\} \mid 0 \leq l_1 < \dots < l_n \leq k-1\}. \quad (6)$$

Suppose one can partition \mathcal{I} into sets \mathcal{I}_i each having the following properties.

(A) Either $|\mathcal{I}_i| = q$ or $|\mathcal{I}_i| = p$.

(B) The set

$$\mathcal{M}_i = \{m_{(l_1, l_2, \dots, l_n)} \mid \{l_1, \dots, l_n\} \in \mathcal{I}_i\} \quad (7)$$

either equals

$$Z_p = \left\{ \frac{lN}{p} = lq \mid l \in \{0, \dots, p-1\} \right\} \quad (8)$$

or equals

$$Z_q = \left\{ \frac{lN}{q} = lp \mid l \in \{0, \dots, q-1\} \right\}. \quad (9)$$

Then there exist nonnegative integers α, β such that:

$$\alpha p + \beta q = k. \quad (10)$$

Proof: To establish a contradiction suppose there do not exist nonnegative integers α, β such that (16) holds. We will first prove this for 2-tuples and then extend it to $2 < n < k - 1$. As $0 \in S$ and every element of S is less than N , S can be partitioned into the nonempty sets $\{0\}$, S_p , S_q and S_o , such that $S_p \subset Z_p$ and $S_q \subset Z_q$. Further, every member of S_p is of the form iq for $i \in \{1, \dots, p-1\}$ and every member of S_q is of the form ip for $i \in \{1, \dots, q-1\}$. Finally, S_o comprises integers that are neither multiples of p nor multiples of q . By hypothesis its elements are all nonzero and less than N .

Consider now any element l of S_o . As $0 \in S$, and $l < N$, either $l \in Z_p$ or $l \in Z_q$. In the former case it is a multiple of q and in the latter case it is a multiple of p . Thus S_o is empty.

Next consider $np \in S_q$, for some $n \in \{1, \dots, q-1\}$ and $lq \in S_p$ for some $l \in \{1, \dots, p-1\}$. Now observe that as $N = pq$ and p and q are distinct primes,

$$(np + lq) \pmod{N} \notin Z_q,$$

as $l < p$ cannot be a multiple of p . Similarly,

$$(np + lq) \pmod{N} \notin Z_p$$

as $n < q$ cannot be a multiple of q . Thus one among S_p and S_q is empty.

Without loss of generality, assume S_p is empty. Thus $S \subset Z_q$. If $S = Z_q$, then indeed $k = q$ and (16) holds. Thus suppose $S \neq Z_q$. This implies $k < q$. As $0 \in S$, and $S \subset Z_q$, there is at least one $\mathcal{M}_i = Z_q$.

Now consider two cases.

Case I: Every $\mathcal{M}_i = Z_q$. Then for some positive integer m

$$\prod_{i=0}^{n-1} (k - i) = mq(n!).$$

Since q is prime and does not divide k it must divide $k - j$ for some $0 < j \leq n - 1$.

Thus for some positive integer L ,

$$k = Lq + j.$$

As $k < q$, $L = 0$ and $k = j \leq n - 1$, contradicting the assumption that $k > n$.

Case II: \exists an i for which $\mathcal{M}_i = Z_p$. Thus by this assumption \exists a set of distinct indices $\{u_i \in \{1, \dots, q - 1\} | i \in \{1, \dots, n\}\} \subset S_q$ such that

$$\left(\sum_{i=1}^n u_i p \right) \text{mod}(pq) = q \quad (11)$$

Consequently for some integer M

$$p \left(\sum_{i=1}^n u_i - Mq \right) = q.$$

This leads to a contradiction since q is a prime number.

This completes the proof for $n = 2$.

Proofs of Lemma. 5.4.2

Lemma .0.1 Consider two primes p and q , integers $1 < n \leq k < N = pq$, a set of k distinct integers $S = \{i_0, \dots, i_{k-1}\} \subset \{0, \dots, N-1\}$, with $i_0 = 0$ and the integers

$$m_{(l_1, l_2, l_3)} = (i_{l_1} + i_{l_2} + i_{l_3}) \pmod{N}, \quad \{i_{l_1}, i_{l_2}, i_{l_3}\} \subset S, \quad i_{l_u} \neq i_{l_v} \forall u \neq v.$$

Consider the set of 3-tuples

$$\mathcal{I} = \{\{l_1, l_2, l_3\} \mid 0 \leq l_1 < l_2 < l_3 \leq k-1\}. \quad (12)$$

Suppose one can partition \mathcal{I} into sets \mathcal{I}_i each having the following properties.

(A) Either $|\mathcal{I}_i| = q$ or $|\mathcal{I}_i| = p$.

(B) The set

$$\mathcal{M}_i = \{m_{(l_1, l_2, l_3)} \mid \{l_1, l_2, l_3\} \in \mathcal{I}_i\} \quad (13)$$

either equals

$$Z_p = \left\{ \frac{lN}{p} = lq \mid l \in \{0, \dots, p-1\} \right\} \quad (14)$$

or equals

$$Z_q = \left\{ \frac{lN}{q} = lp \mid l \in \{0, \dots, q-1\} \right\}. \quad (15)$$

Then there exist nonnegative integers α, β such that:

$$\alpha p + \beta q = k. \quad (16)$$

Proof: Let us now prove the result for 3 tuples. Consider the index set S . As we have done earlier, we can partition this set into 4 sets $\{0\}$, S_p , S_q and S_o . Clearly, from the result for 2-tuples, we know that adding indices from S_p to indices in S_q does not produce a sum that belongs to either Z_p or Z_q . Thus one of S_p or S_q is empty. Without loss of generality, let S_p be empty. We will now prove that S_o is empty.

Observe that if $|S_o| \leq n - 1$, one of S_p or S_q must be non-empty. To prove this assume to the contrary, then $|S| = k = n$. This contradicts the assumption that $k > n$. **Case** $|S_o| = 1$

Suppose for the purpose of contradiction that \exists a non-zero element $l \in S_o$. Now consider the 3-tuple, $(0, np, l)$ for some $n \in \{1, \dots, q-1\}$. Clearly in this case, the sum of these indices is not a multiple of p . Thus this 3 sum doesnot belong to Z_q . Suppose this 3 sum is a multiple of q . Then \exists an $m_1 \neq 0$ such that $(np + l) \bmod N = m_1 q$. Now by hypothesis (B), if there eixsts a 3-tuple that produced a sum which is a multiple of q there exist other 3 tuples that generate the other elements of Z_p . Since the indices in S_q cannot add upto a multiple of q , there must exist another integer $\tilde{n} \in \{1, \dots, q-1\}$ such that $n \neq \tilde{n}$ and $(\tilde{n}p + l) \bmod N = m_2 q$. Without loss of generality, $m_1 > m_2$. Now consider

$$(m_1 - m_2)q = (np + l) \bmod N - (\tilde{n}p + l) \bmod N = ((n - \tilde{n})p) \bmod N \quad (17)$$

i.e. for some integer \tilde{M} , we have

$$\tilde{L} = (m_1 - m_2)q = p((n - \tilde{n}) - \tilde{M}q) \quad (18)$$

Observe that $(m_1 - m_2) < p - 2$ and hence is not divisible by p . But from (18) p a prime factor of \tilde{L} . We have arrived at a contradiction since \tilde{L} must have a unique prime factorization. Thus S_o is empty.

Case $|S_o| = 2$

Let $S_o = \{l_1, l_2\}$. Observe that one of S_p or S_q is non-empty. Without loss of generality, we assume that S_q is non-empty. Consider the 3 tuple $(0, l_1, l_2)$. If the sum belongs neither to Z_p or Z_q , we are done. However, if the sum belongs to Z_p or Z_q , then consider the 3 tuple e 3-tuple, $(0, np, l)$ for some $n \in \{1, \dots, q - 1\}$. In this case the analysis is the same as the case, when $|S_o| = 1$. Thus S_o must be empty in this case too.

Case $|S_o| = 3$ and one of S_q or S_p is non-empty.

As earlier, let us assume that S_q is non-empty. Then S_p is empty. Let $S_o = \{l_1, l_2, l_3\}$. If the sum of these integers is neither in Z_p or Z_q , we are done. However, if it belongs to Z_p or Z_q , then the analysis is similar to the case with $|S_o| = 2$. Thus S_o is empty.

Case $|S_o| > 3$ and both S_p and S_q are empty.

All 3 sums belong to Z_p Observe that since $n < k$, then consider the 3 tuples of the form $(0, l_i, l_j)$. Specifically consider $(0, l_1, l_2)$. Let $(l_1 + l_2) \bmod N = mq$ for some integer $m \in \{1, \dots, p - 1\}$. Then since $l_1 + l_3 \in Z_p$, $\exists n$ such that $(l_1 + l_3) \bmod N = nq$

for some $n \neq m$ and $n \in \{1, \dots, p-1\}$. Now consider $(m-n)q = (l_3 - l_2) \bmod N$. Thus $(l_3 - l_2) \bmod N$ is a multiple of q . But $(l_2 + l_3) \bmod N$ is also a multiple of q . Thus l_3 is a multiple of q . We have arrived at a contradiction.

All 3 sums belong to Z_q The proof is the same as above.

Some 3 sums are in Z_p and some are in Z_q

Consider all 3 tuples that have the indices 0 and l_1 . Then either all of the 3-sums of this type of 3-tuples add up to multiples of q (say) or some of them add up to multiples of p and some add up to multiples of q . Since $|S_o| > 3$ and there are only two distinct prime factors of N , \exists 2 3 tuples $(0, l_1, l_i)$ and $(0, l_1, l_j)$ such that l_1, l_i and l_j are distinct and $(0 + l_1 + l_i) \bmod N \in Z_p$, $(0 + l_1 + l_j) \bmod N \in Z_p$. Thus $(l_i - l_j) \bmod N \in Z_p$. Thus we repeat the analysis as above to prove that S_o is empty.

Thus S_o must be empty. Thus we have $S \subset Z_q$. Thus \exists at least one \mathcal{M}_i such that $\mathcal{M}_i = Z_q$. As in the earlier case, we have two cases.

Now consider two cases. For $n \geq 2$

Case I: Every $\mathcal{M}_i = Z_q$. Then for some positive integer m

$$\prod_{i=0}^{n-1} (k - i) = mq(n!).$$

Since q is prime and does not divide k it must divide $k - j$ for some $0 < j \leq n - 1$.

Thus for some positive integer L ,

$$k = Lq + j.$$

As $k < q$, $L = 0$ and $k = j \leq n - 1$, contradicting the assumption that $k > n$.

Case II: \exists an i for which $\mathcal{M}_i = Z_p$. Thus by this assumption \exists a set of distinct indices $\{u_i \in \{1, \dots, q - 1\} | i \in \{1, \dots, n\}\} \subset S_q$ such that

$$\left(\sum_{i=1}^n u_i p \right) \text{mod}(pq) = q \quad (19)$$

Consequently for some integer M

$$p \left(\sum_{i=1}^n u_i - Mq \right) = q.$$

This leads to a contradiction since q is a prime number. This completes the proof for $n = 3$.

REFERENCES

- [1] Di Taranto, R. and Muppirisetty, S. and Raulefs, R. and Slock, D. and Svensson, T. and Wymeersch, H., “Location-Aware Communications for 5G Networks: How location information can improve scalability, latency, and robustness of 5G”, *IEEE Signal Processing Magazine*, vol. 31, no. 6, pp. 102-112, November 2014.
- [2] G. H. Forman and J. Zahorjan., “The challenges of mobile computing”, *IEEE Computer*, 27:38–47, 1994.
- [3] B. Karp and H T Kung., “GPSR: greedy perimeter stateless routing for wireless networks”, volume pages, pages 243–254. ACM, 2000.
- [4] M. Weiser., “Some computer science issues in ubiquitous computing”, *Commun. ACM*, 36(7):75–84, July 1993.
- [5] A.H. Sayed, A. Tarighat, and N. Khajehnouri., “Network-based wireless location: challenges faced in developing techniques for accurate wireless location information”, *Signal Processing Magazine, IEEE*, 22(4):24 – 40, july 2005.
- [6] C. D. Cordeiro and D.P. Agrawal., “Ad Hoc and Sensor Networks: Theory and Applications”, World Scientific, 2011.
- [7] Caicedo, D. and Pandharipande, A., “Distributed Ultrasonic Zoned Presence Sensing System”, In *Sensors Journal, IEEE*, vol.14, no.1, pp.234,243, Jan. 2014.
- [8] T. O’Donovan, J. O’Donoghue, C. Sreenan, D. Sammon, P. O’Reilly, and K.A., O’Connor. “A context aware wireless body area network (ban)”, In *Pervasive Computing Technologies for Healthcare, 2009. PervasiveHealth 2009. 3rd International Conference on*, pages 1 –8, april 2009.
- [9] J.T. Isaacs, D.J. Klein, and J.P. Hespanha., “Optimal sensor placement for time difference of arrival localization”, In *Decision and Control, 2009 held jointly with the 2009 28th Chinese Control Conference. CDC/CCC 2009. Proceedings of the 48th IEEE Conference on*, pages 7878 –7884, dec. 2009.
- [10] D. B. Jourdan and N. Roy., “Optimal sensor placement for agent localization”, *ACM Trans. Sen. Netw.*, 4(3):13:1–13:40, June 2008.

- [11] Lisa Ran, Sumi Helal, and Steve Moore., “Drishti: An integrated indoor/outdoor blind navigation system and service”, In *Proceedings of the Second IEEE International Conference on Pervasive Computing and Communications (PerCom'04)*, PERCOM '04, pages 23–, Washington, DC, USA, 2004, IEEE Computer Society.
- [12] S.H. Dandach, B. Fidan, S. Dasgupta, and B.D.O. Anderson., “Adaptive source localization by mobile agents”. In *45th IEEE Conference on Decision and Control*, pp. 2045 –2050, Dec. 2006.
- [13] N. Patwari, J.N. Ash, S. Kyperountas, III Hero, A.O., R.L. Moses, and N.S., Correal. “Locating the nodes: cooperative localization in wireless sensor networks”, *Signal Processing Magazine, IEEE*, 22(4):54 – 69, july 2005.
- [14] M.G. Rabbat and R.D. Nowak., “Decentralized source localization and tracking [wireless sensor networks]”, In *Acoustics, Speech, and Signal Processing, 2004. Proceedings. (ICASSP '04). IEEE International Conference on*, volume 3, pages iii – 921–4 vol.3, may 2004.
- [15] M. Rabbat and R. Nowak., “Distributed optimization in sensor networks”, In *Information Processing in Sensor Networks, 2004. IPSN 2004. Third International Symposium on*, pages 20 – 27, april 2004.
- [16] I.F. Akyildiz and M.C. Vuran., “Wireless Sensor Networks”, *Advanced Texts in Communications and Networking*. John Wiley & Sons, 2010.
- [17] E. Xu, Z. Ding and S. Dasgupta., “Source localization in wireless sensor networks from signal time-of-arrival measurements”, In *IEEE Transactions on Signal Processing*, pp. 2887-2897, 2009.
- [18] T.S. Rappaport., “Wireless communications: principles and practice”, Prentice Hall communications engineering and emerging technologies series. Prentice Hall PTR, 2002.
- [19] Bishop, A.N. and Jensfelt, P., “An optimality analysis of sensor-target geometries for signal strength based localization”, *Intelligent Sensors, Sensor Networks and Information Processing (ISSNIP), 2009 5th International Conference on*, pages 127-132.
- [20] Sichun Wang and Jackson, B.R. and Inkol, R.J., “Impact of Emitter-Sensor Geometry on Accuracy of Received Signal Strength Based Geolocation”, *Vehicular Technology Conference (VTC Fall), 2011 IEEE*, pages 1-5, San Francisco, CA, USA, 2011, IEEE Vehicular Technology Society.

- [21] Bishop, Adrian N. and Fidan, Baris and Anderson, Brian D. O. and Dogancay, Kutluyil and Pathirana, Pubudu N., “Optimality analysis of sensor-target localization geometries”, *Automatica*, vol 46 no 3 pp.479-492, March 2010.
- [22] B. Fidan, S. Dasgupta and B. D. O. Anderson., “Guaranteeing practical convergence in algorithms for sensor and source localization”, In *IEEE Transactions on Signal Processing*, pp. 4458-4469, 2008.
- [23] J.S. Abel., “Optimal sensor placement for passive source localization”, In *Acoustics, Speech, and Signal Processing, 1990. ICASSP-90., 1990 International Conference on*, pages 2927 –2930 vol.5, apr 1990.
- [24] R. Bodor, A. Drenner, P. Schrater, and N. Papanikolopoulos., “Optimal camera placement for automated surveillance tasks”. *J. Intell. Robotics Syst.*, 50(3):257–295, November 2007.
- [25] H.L. Van Trees., “Detection, Estimation, and Modulation Theory: Detection, estimation, and linear modulation theory”, Wiley, 2001.
- [26] Sonia Martnez and Francesco Bullo., “Optimal sensor placement and motion coordination for target tracking”, *Automatica*, 42(4):661 – 668, 2006.
- [27] Pukelsheim, F., “Optimal design of experiments”, Wiley, 1993.
- [28] S. Dasgupta, S. R. C. Ibeawuchi, and Z. Ding., “Optimum sensor placement for source monitoring under log-normal shadowing in three dimensions”, In *Proceedings of the 9th international conference on Communications and information technologies*, pages 376–381, Piscataway, NJ, USA, 2009. IEEE Press.
- [29] S. Dasgupta, S.C. Ibeawuchi, and Z. Ding., “Optimum sensor placement for localization under log-normal shadowing”, In *Proceedings of the International Symposium on Communications and Information Technologies (ISCIT)*, pages 204 –208, oct. 2010.
- [30] Ibeawuchi, Stella-Rita Chioma, ”Optimum sensor placement for source localization and monitoring from received signal strength *PhD diss., University of Iowa*, Available: <http://ir.uiowa.edu/etd/822>, 2010.
- [31] Donoho.D.L, ”Compressed Sensing” *IEEE Transactions on Information Theory*, vol. 52, No.4, pages 1289 - 1306.
- [32] Baraniuk, R.G., “Compressive Sensing [Lecture Notes]”, *Signal Processing Magazine, IEEE* , vol.24, no.4, pp.118-121, July 2007.

- [33] D. L. Donoho and M. Elad., “Optimally Sparse Recovery in general (nonorthogonal) dictionaries via l_1 minimization”, *Proceedings of National Academy of Sciences*, vol.100, no. 5, pp.2197-2203, 2003.
- [34] P. Feng and Y. Bresler., “Spectrum-blind minimum-rate sampling and reconstruction of multiband signals”, *IEEE International Conference on Acoustics, Speech, and Signal Processing*, vol. 3, pp. 1688-1691, 1996.
- [35] Calafiore, Giuseppe and Dabbene, Fabrizio and Tempo, Roberto., “Radial and Uniform Distributions in Vector and Matrix Spaces for Probabilistic Robustness” *Topics in Control and its Applications, Springer London*, pp. 17-31, 1999.
- [36] H. K. Achanta, S. Dasgupta and Z. Ding., “Optimum sensor placement for localization in three dimensional under log normal shadowing”, In *Proceedings of the 5th International Congress on Image and Signal Processing (CISP)*, pp. 1898-1901, October 2012.
- [37] Achanta, H.K. and Weiyu Xu and Dasgupta, S., “Matrix design for optimal sensing In *Acoustics, Speech and Signal Processing (ICASSP), IEEE International Conference on*, pages 4221– 4225, May, 2013.
- [38] Achanta, H.K. and Biswas, S. and Dasgupta, S. and Jacob, M. and Dasgupta, B.N. and Mudumbai, R., “Coprime conditions for Fourier sampling for sparse recovery”, *8th IEEE Workshop on Sensor Array and Multichannel Signal Processing*, pages 533-536, June 2014.
- [39] Achanta, H.K and Dassgupta, S. and Xu, W. and Mudumbai, R. and Bai, E., “A Distributed Control Law for Optimum Sensor Placement for Source Localization”, *International Conference on Computing, Communications and Informatics*, 2014 (accepted).
- [40] P. Lancaster and M. Tismenetsky., “The Theory of Matrices”, *ser. Computer Science and Applied Mathematics*, Academic Press, 1985.
- [41] C.T. Chen, “Linear System Theory and Design”, 4th Ed. 2013.
- [42] Louis L. Scharf and L.T. McWhorter., “Geometry of the cramer-rao bound”, *Signal Processing*, 31(3):301 – 311, 1993.
- [43] Wang, Yue and Xiong, Weiming., “Anchor-Based Three-Dimensional Localization Using Range Measurements”, *8th International Conference on Wireless Communications, Networking and Mobile Computing (WiCOM)*, 1-5, 2012.

- [44] Chaffee, J. and Abel, J., “GDOP and the Cramer-Rao bound”, *Position Location and Navigation Symposium, 1994.*, *IEEE*, 663-668, 1994.
- [45] Hing Cheung So and Lanxin Lin., “Linear Least Squares Approach for Accurate Received Signal Strength Based Source Localization”, *IEEE Transactions on Signal Processing*, vol. 59, no.8, pages 4035-4040.
- [46] Robertazzi, T.G. and Sarachik, P., “Self-organizing communication networks” *Communications Magazine, IEEE*, 24(1):28 – 33, January, 1986.
- [47] Mills, Kevin L., “A brief survey of self-organization in wireless sensor networks: Research Articles” *Wirel. Commun. Mob. Comput.*, 7(7):823 – 834, September, 2007.
- [48] Zhao, Shijun and Liu, Sijia and Feng, Ye., “Study on self-organization method for single target tracking in binary wireless sensor networks”, *Modelling, Identification Control (ICMIC), 2012 Proceedings of International Conference on* , pp:164-169, June, 2012.
- [49] Biswas, P.K. and Phoha, S., “Self-organizing sensor networks for integrated target surveillance”, *Computers, IEEE Transactions on*, 55(8):1033-1047, August, 2006.
- [50] Degesys, J. and Rose, I. and Patel, A. and Nagpal, R., “DESYNC: Self-Organizing Desynchronization and TDMA on Wireless Sensor Networks”, *Information Processing in Sensor Networks, 2007. IPSN 2007. 6th International Symposium on*, pp:11-20, April, 2007.
- [51] Nagpal, Radhika and Shrobe, Howard and Bachrach, Jonathan., “Organizing a global coordinate system from local information on an ad hoc sensor network”, *Proceedings of the 2nd international conference on Information processing in sensor networks*, pp:333-348, 2003.
- [52] Yu, C., Anderson, B. D. O., Dasgupta, S. and Fidan, B., “Control of a minimally persistent formation in the plane”, *SIAM Journal on Control and Optimization*, Special Issue on Control and Optimization in Cooperative Networks, Volume 48, Issue 1, pp. 206-233, February 2009.
- [53] Summers, T. H., Yu, C., Dasgupta, S., and Anderson, B. D.O., “Control of minimally persistent leader-remote-follower and coleader formations in the plane”, *IEEE Transactions on Automatic Control*, pp. 2778 - 2792, December 2011.
- [54] Xu, E., Ding, Z., and Dasgupta, S., “Target Tracking and Mobile Sensor Navi-

- gation in Wireless Sensor Networks”, *IEEE Transactions on Mobile Computing*, pp. 177 - 186, January, 2013.
- [55] Shames, I., Dasgupta, S., Fidan, B., and Anderson, B. D.O., “Circumnavigation from distance measurements under slow drift”, *IEEE Transactions on Automatic Control*, pp. 889 - 903, April 2012.
- [56] Khalil, Hassan K., ”Nonlinear Systems”, Third Edition, Prentice Hall PTR, 2002.
- [57] Steinhagen, P. and Lenstra, H.W., “Chebotarëv and his density theorem”, *Math. Intelligencer*, vol.18, pp. 26-37, 1996.
- [58] Alexeev, Boris and Cahill, Jameson and Mixon, Dustin G., “Full spark frames”, *Journal of Fourier Analysis and Applications*, vol.18, no.6, pp. 1167-1194, 2012.
- [59] Vaidyanathan, P. P., “Multirate Systems and Filter Banks”, 1993.
- [60] Lam, TY and Leung, KH., “On vanishing sums of roots of unity”, *Journal of algebra*, vol. 224, no. 1, pp. 91-109, 2000.